Momentum-resolved STEM: DPC, COM, inverse single- & multislice

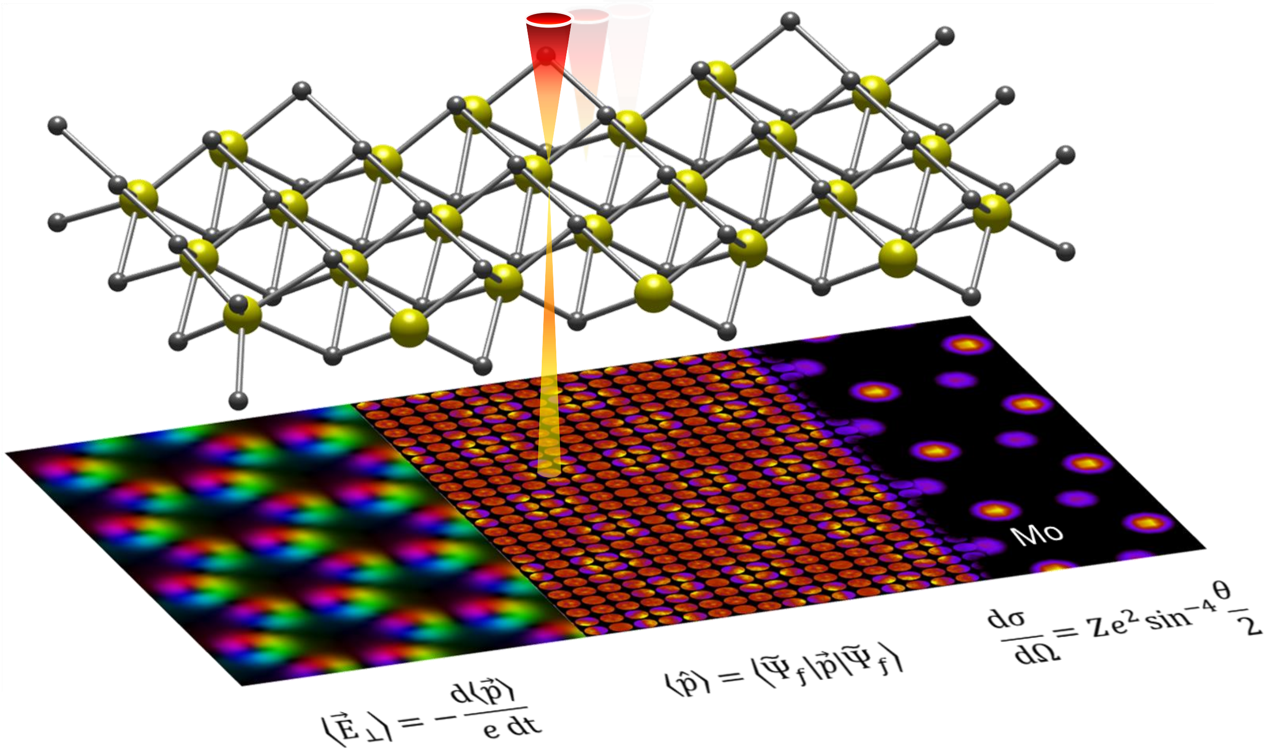

Knut Müller-Caspary

Ludwig-Maximilians-Universität Munich, Germany
Faculty for Chemistry and Pharmacy
Physical Chemistry
Email: k.mueller-caspary@cup.lmu.de

LMU
LUDWIG-
MAXIMILIANS-
UNIVERSITÄT
MÜNCHEN

Quantitative Electron Microscopy 2025

11^{th} – 23^{th} May 2025 6^{th} Edition

Port-Barcarès

Review and News of Quantitative TEM techniques

Outline

STEM, DPC, COM, phases and momentum transfer

Electric fields in thin specimen: Ehrenfest theorem

Approaches for polarisation-induced field mapping

Practice hint 1 – 5, focus, coherence

Gradient – based (single & multislice) ptychography

Introduction to the inverse problem

Minimizing the loss function: a single-scattering example

Inverse multislice: concept, coherence, TDS, parametrisation

Outline

STEM, DPC, COM, phases and momentum transfer

Gradient – based (single & multislice) ptychography

Electric fields in thin specimen: Ehrenfest theorem

Introduction to the inverse problem

Approaches for polarisation-induced field mapping

Minimizing the loss function: a single-scattering example

Practice hint 1 – 5, focus, coherence

Inverse multislice: concept, coherence, TDS, parametrisation

STEM concept

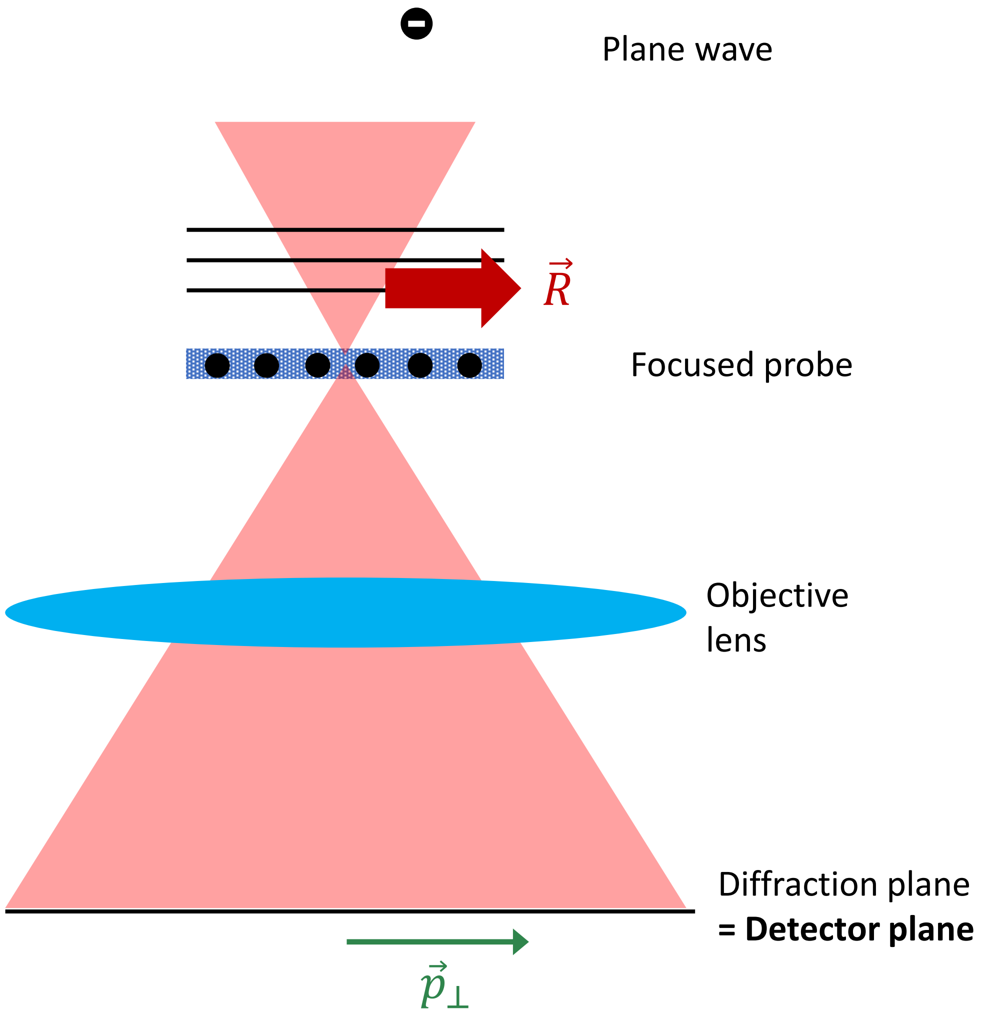

STEM

Information on **both**

- position (**real space**, specimen plane)
- direction (**reciprocal space**, detector plane)

collected **sequantially** in real space

STEM concept

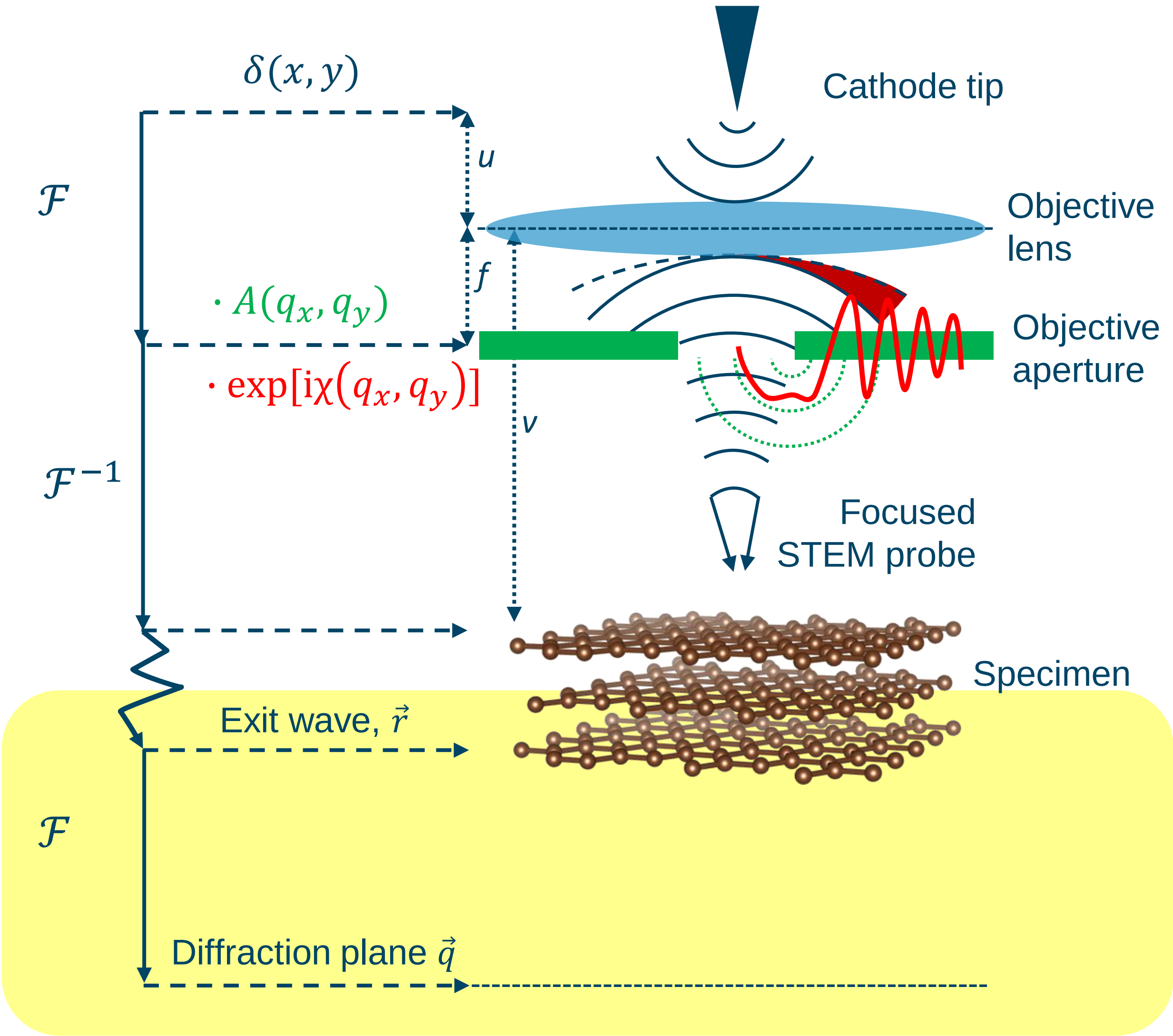

- The wave functions in real and reciprocal space represent exactly **the same quantity**
- Real and momentum space representation are thus **formally equivalent**.
- **What is the difference in practice?**

$\Psi(\vec{r})$

Change representation

$$\hat{\Psi}(\vec{p}) = \mathcal{F}[\Psi(\vec{r})](\vec{p})$$

with $\vec{p} = h \cdot \vec{q}$

Phase and momentum

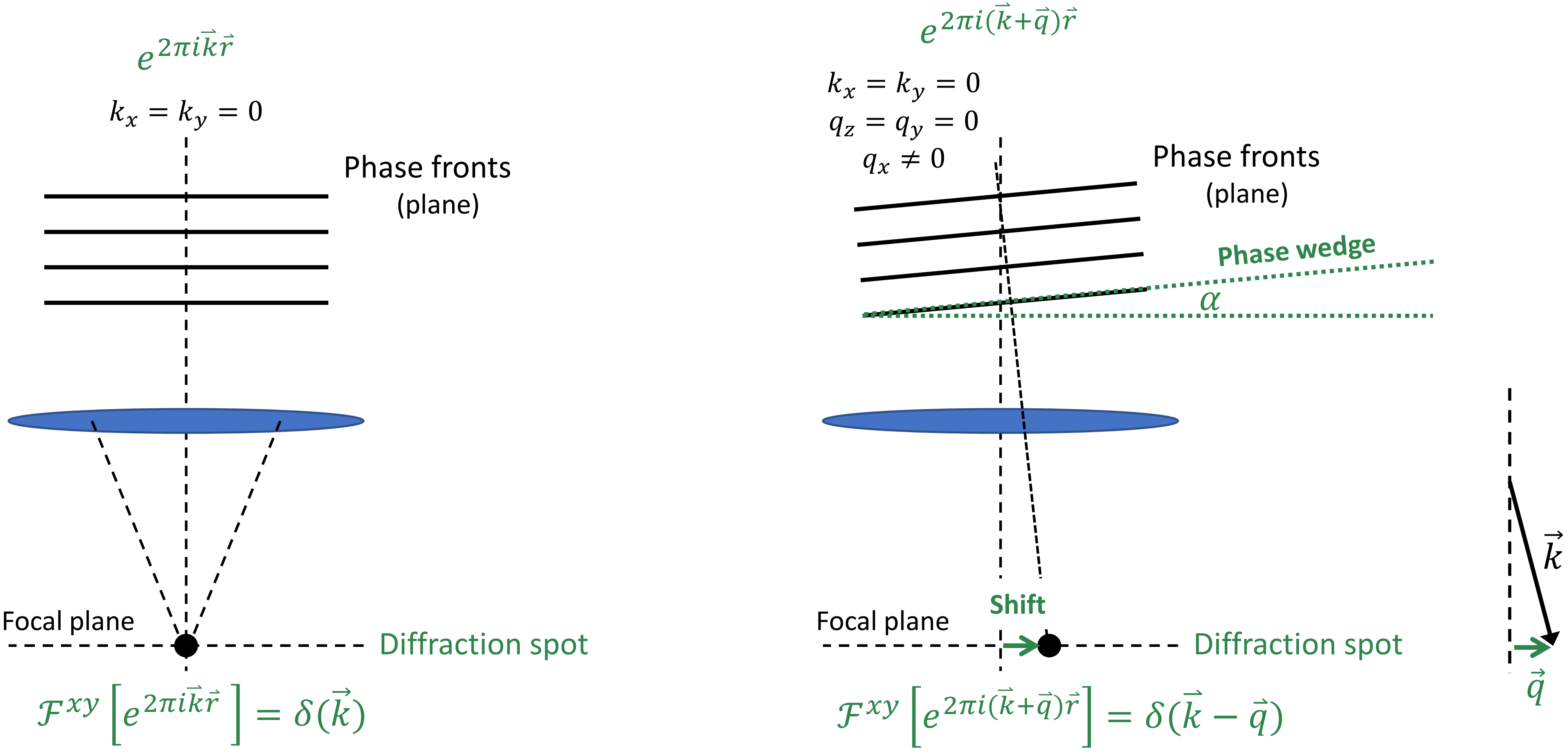

- A **phase wedge in real space** causes a **shift in diffraction space**
- The wave can be assigned a **lateral momentum** $\vec{p} = h \cdot \vec{q}$

Physical origins of phase modulations and momentum transfers

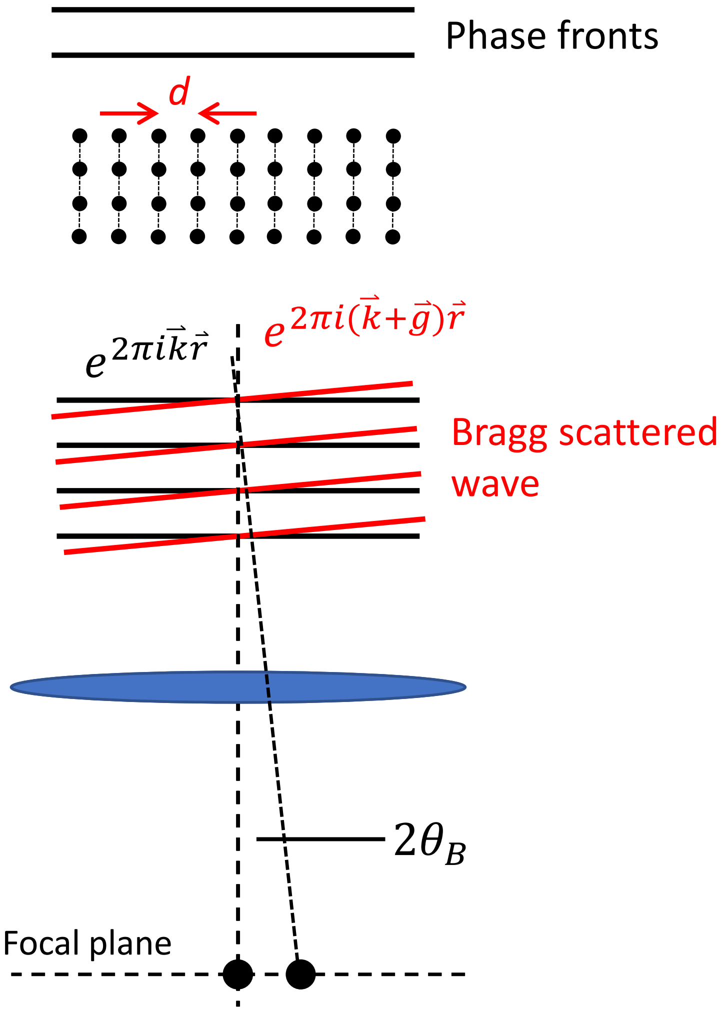

$|\vec{q}| = 1/d$

Measurement of movement of Bragg reflections: **Strain**

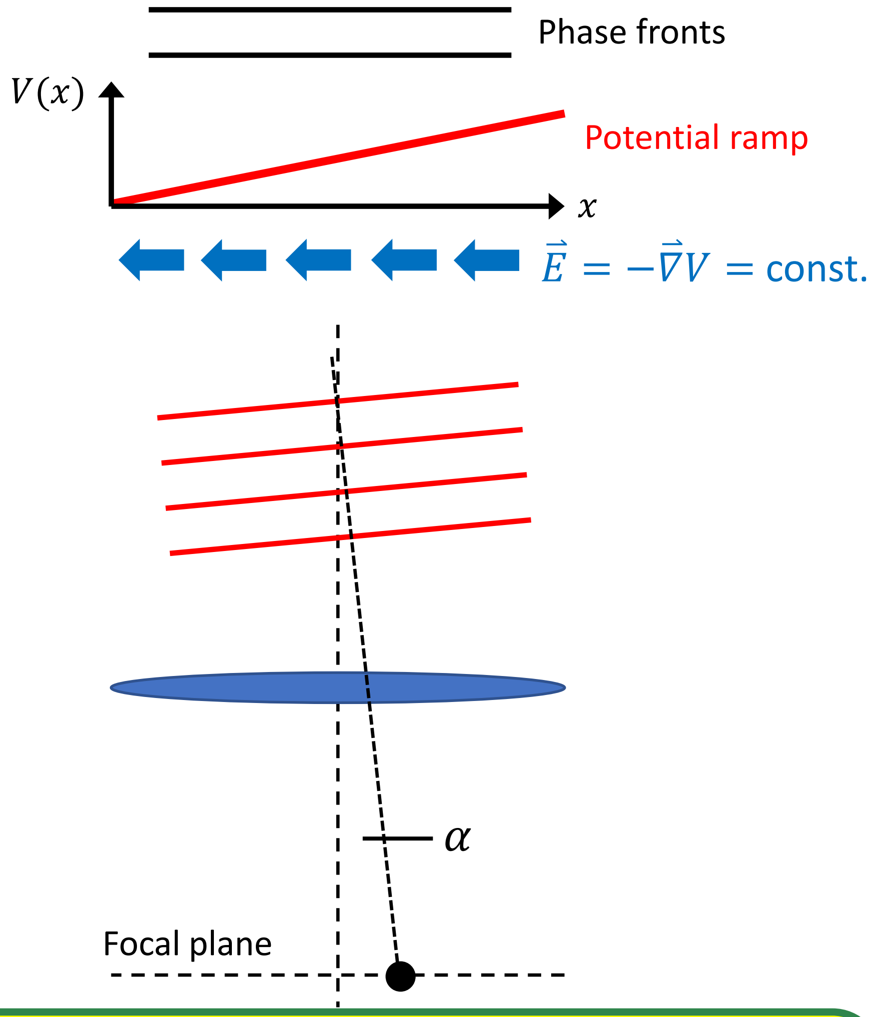

$$E = -\frac{h}{\lambda} \cdot \frac{v}{e \cdot t} \sin\alpha$$

Measurement of position of undiffracted beam/whole diffraction pattern: **Electric field**

Quantum mechanical considerations

Consider scattering by an atom:

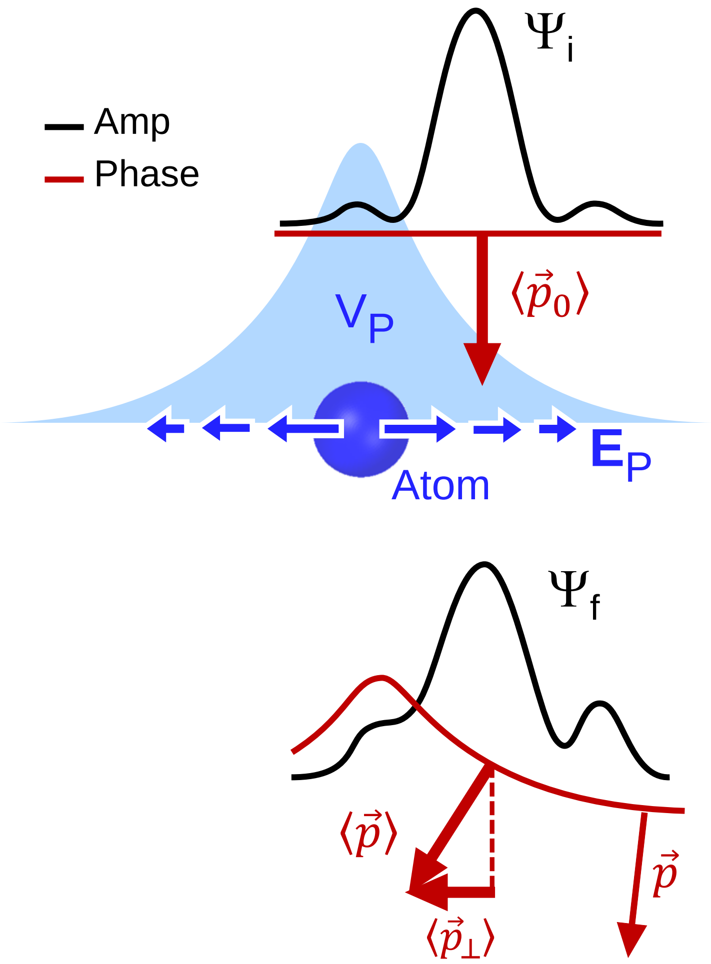

STEM probe wave function

Specimen exit wave function

Question 1:

- Can we measure the average beam deflection (momentum transfer) $\langle \vec{p}_\perp \rangle$ accurately?

Question 1a:

- Why should we do so?

→ Momentum transfer caused by field $\vec{E}$

→ Hope: recover $\vec{E}$ from $\langle \vec{p}_\perp \rangle$

Question 2:

- How are $\vec{E}$ and $\langle \vec{p}_\perp \rangle$ related physically and mathematically?

Quantum mechanical considerations: Momentum transfer

Two possibilities to calculate the expectation value of $\vec{p}$

1. Real space

$$\langle \vec{p}_\perp \rangle = \left\langle \Psi_f(\vec{r}_\perp) \left| \frac{\hbar}{i} \vec{\nabla} \right| \Psi_f(\vec{r}_\perp) \right\rangle$$

In $\vec{r}$ representation, $\vec{\nabla}$ acts on $\Psi_f(\vec{r}_\perp)$

→ **Wave fct unknown!**

2. Momentum space (equivalent!)

$$\langle \vec{p}_\perp \rangle = \langle \Psi_f(\vec{p}_\perp) | \vec{p}_\perp | \Psi_f(\vec{p}_\perp) \rangle$$
$$= \iint \vec{p}_\perp \, I(\vec{p}_\perp) \, d^2\vec{p}_\perp$$

→ **1st moment of diffracted intensity**

→ **Mathematically: „Centre of mass“**

- The **first moment of the diffracted intensity** equals the **expectation value of the momentum.**
- This is also referred to as **COM – imaging.**

MoS_2 example

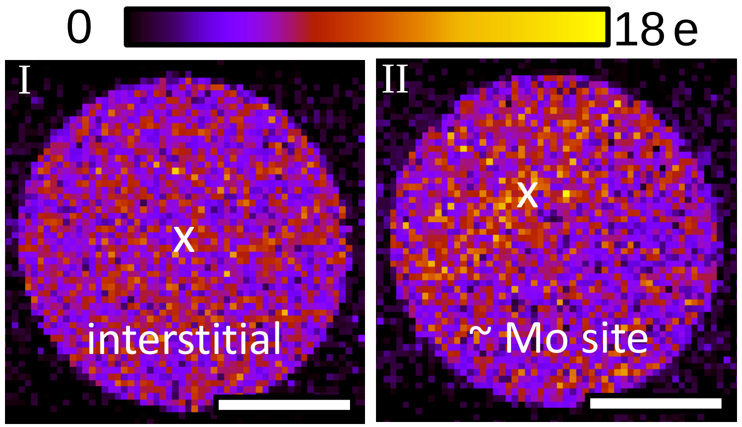

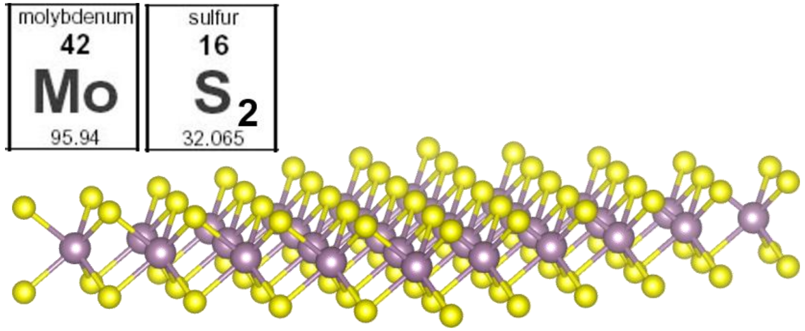

Waddel & Chapman, Optik **54**, 83 (1979)
Müller et al., Nat. Commun. **5**, 5653 (2014)
Müller-Caspary et al., Physical Review B 98, 121408(R) (2018)

Quantum mechanical considerations: Momentum transfer

Two possibilities to calculate the expectation value of $\vec{p}$

1. Real space

$$\langle \vec{p}_\perp \rangle = \left\langle \Psi_f(\vec{r}_\perp) \left| \frac{\hbar}{i} \vec{\nabla} \right| \Psi_f(\vec{r}_\perp) \right\rangle$$

In $\vec{r}$ representation, $\vec{\nabla}$ acts on $\Psi_f(\vec{r}_\perp)$

→ **Wave fct unknown!**

2. Momentum space (equivalent!)

$$\langle \vec{p}_\perp \rangle = \langle \Psi_f(\vec{p}_\perp) | \vec{p}_\perp | \Psi_f(\vec{p}_\perp) \rangle$$

$$= \iint \vec{p}_\perp \, I(\vec{p}_\perp) \, d^2\vec{p}_\perp$$

→ **1st moment of diffracted intensity**

→ **Mathematically: „Centre of mass"**

- The **first moment of the diffracted intensity** equals the **expectation value of the momentum.**
- This is also referred to as **COM – imaging.**

MoS_2 example

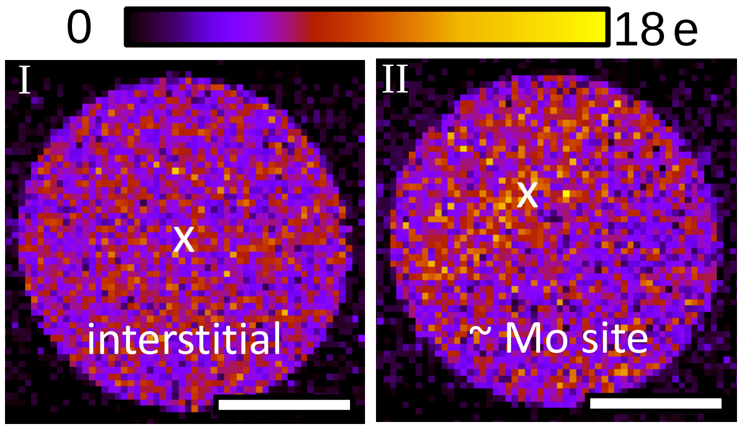

Each scan point yields a 2D vector

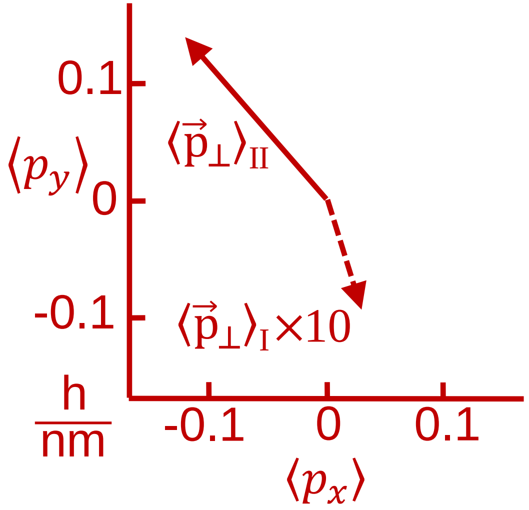

Waddel & Chapman, Optik **54**, 83 (1979)
Müller et al., Nat. Commun. **5**, 5653 (2014)
Müller-Caspary et al., Physical Review B 98, 121408(R) (2018)

Position-sensitive experimental setups: DPC

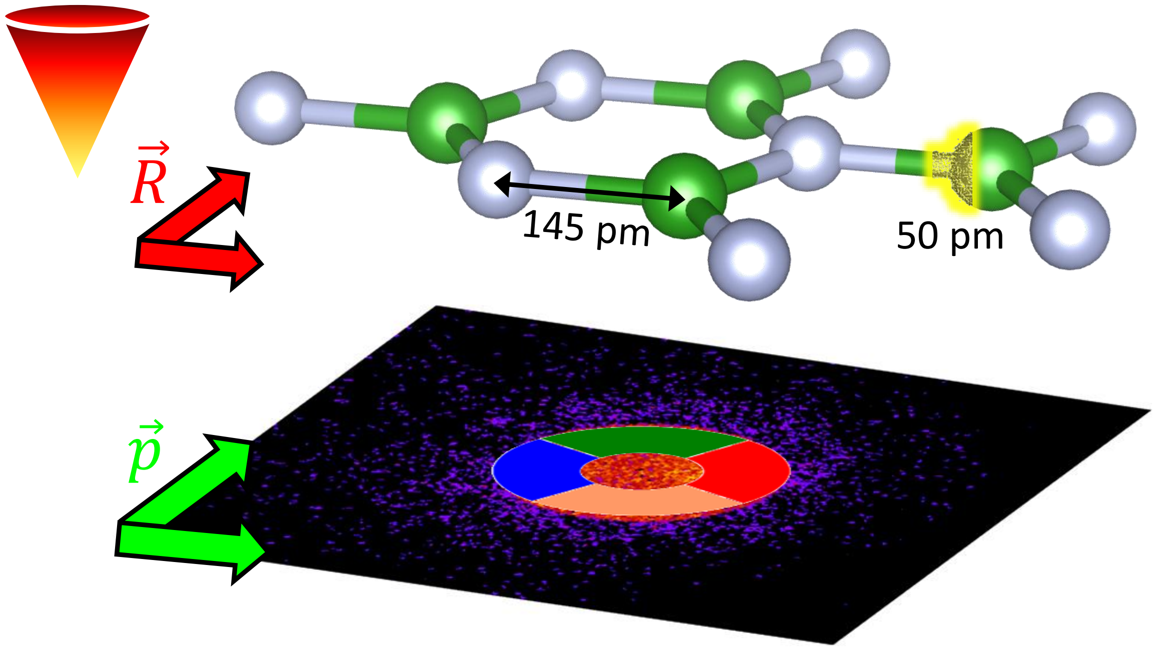

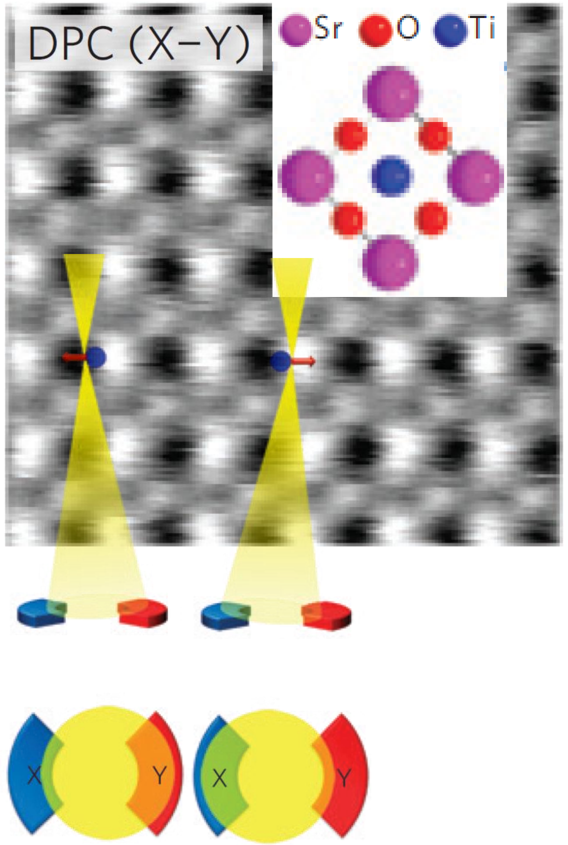

Position sensitivity by segmented ring detectors:
Differential Phase Contrast (DPC)

NATURE PHYSICS | VOL 8 | AUGUST 2012

Differential phase-contrast microscopy at atomic resolution

Naoya Shibata[1,2]★, Scott D. Findlay[3], Yuji Kohno[4], Hidetaka Sawada[4], Yukihito Kondo[4] and Yuichi Ikuhara[1,5]

Aberration-corrected STEM: Look inside atoms

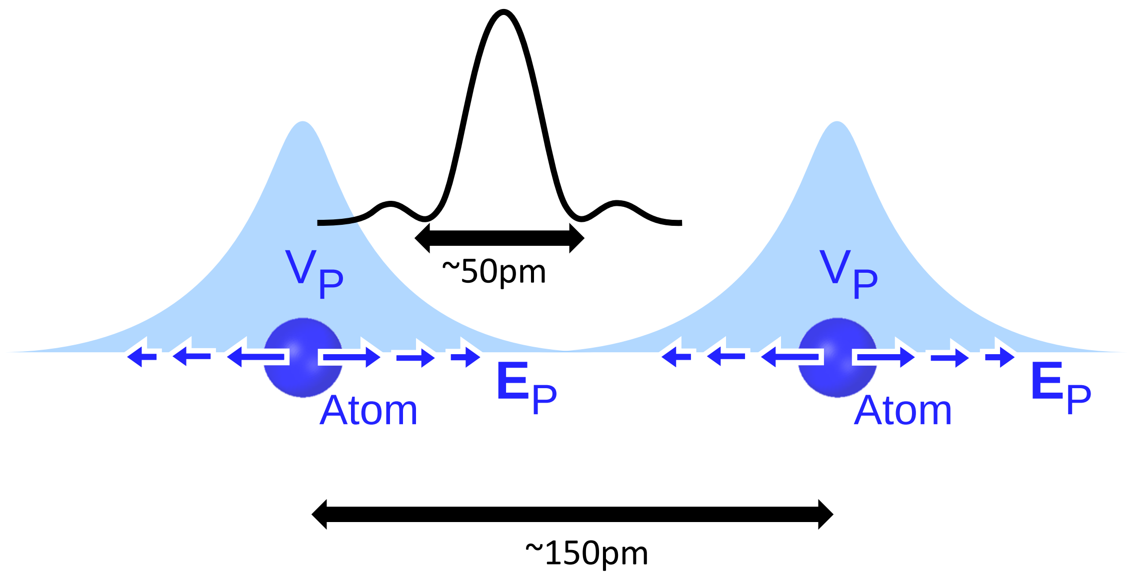

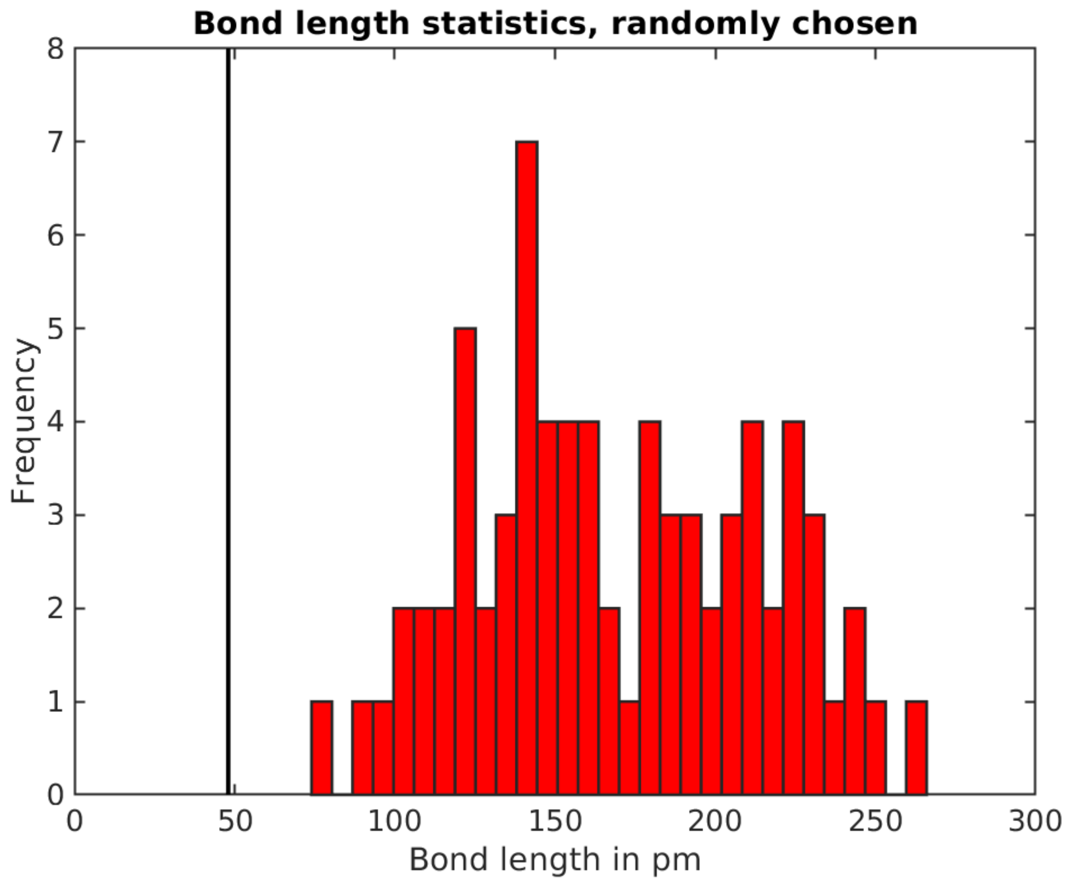

DPC: Historical snapshots

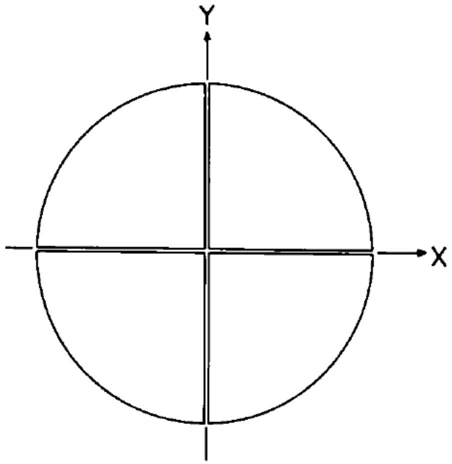

Fig. 5. Scheme of a STEM split detector.

Ultramicroscopy 2 (1977) 251–267

NONSTANDARD IMAGING METHODS IN ELECTRON MICROSCOPY

H. ROSE

→ Suggestion of a split quadrant detector

→ Difference signals (A-D) & (B-C) characteristic for disc position

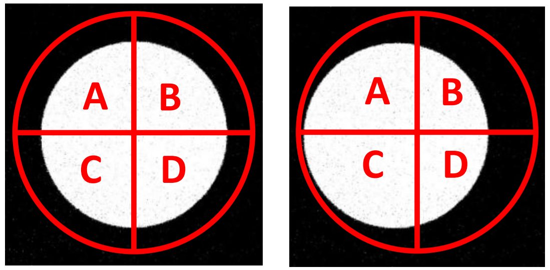

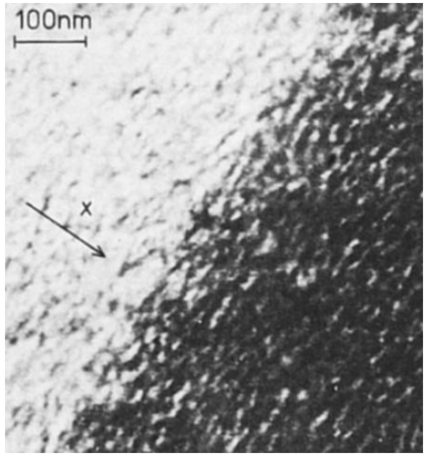

Ultramicroscopy 3 (1978) 203–214

THE DIRECT DETERMINATION OF MAGNETIC DOMAIN WALL PROFILES BY DIFFERENTIAL PHASE CONTRAST ELECTRON MICROSCOPY

J.N. CHAPMAN, P.E. BATSON, E.M. WADDELL and R.P. FERRIER

→ Magnetic domain walls in permalloy experimentally observed by DPC

DPC: Historical snapshots

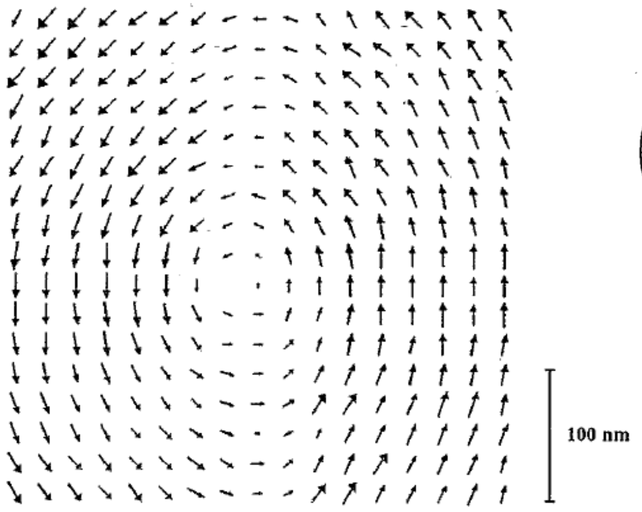

FIG. 7. Vector map of the vortex shown boxed in Fig. 5.

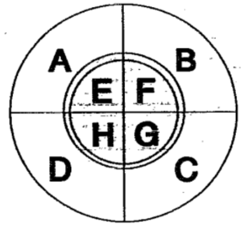

J. Appl. Phys. **73**, 2447 (1993)

Investigation of the micromagnetic structure of crosstie walls in permalloy

R. Ploessl, J. N. Chapman, A. M. Thompson, J. Zweck, and H. Hoffmann

→ Vortex structure of magnetisation in permalloy

Ultramicroscopy 67 (1997) 153–162

TEM imaging and evalution of magnetic structures in Co/Cu multilayers

Josef Zweck*, Tanja Zimmermann, Thomas Schuhrke

→ Contributions to understanding of GMR

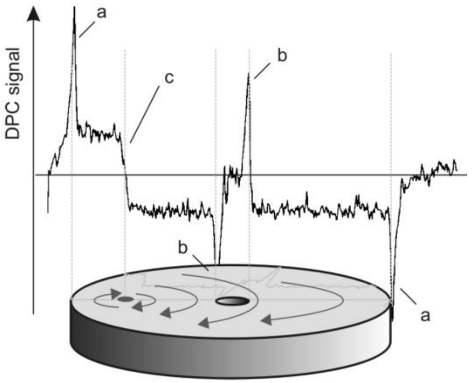

~ 200nm

PRL **95**, 237205 (2005) PHYSICAL REVIEW LETTERS week ending 2 DECEMBER 2005

Shifting and Pinning of a Magnetic Vortex Core in a Permalloy Dot by a Magnetic Field

Thomas Uhlig,* M. Rahm, Christian Dietrich, Rainer Höllinger, Martin Heumann, Dieter Weiss, and Josef Zweck†

→ Manipulation and live visualisation of magnetic vortices

DPC: Historical snapshots

ELSEVIER
Ultramicroscopy
Volume 228, September 2021, 113342

The differential phase contrast uncertainty relation: Connection between electron dose and field resolution

Simon Pöllath, Felix Schwarzhuber, Josef Zweck

$$\boxed{\Delta\langle p_x\rangle \cdot \Delta x \geq \frac{h}{2} \cdot \frac{1}{\sqrt{N_e}}} \qquad (29)$$

ELSEVIER
Ultramicroscopy
Volume 160, January 2016, Pages 265-280

Phase contrast STEM for thin samples: Integrated differential phase contrast

Ivan Lazić, Eric G.T. Bosch, Sorin Lazar

→ Physics of DPC image formation
→ Contrast of light atoms („iDPC“)

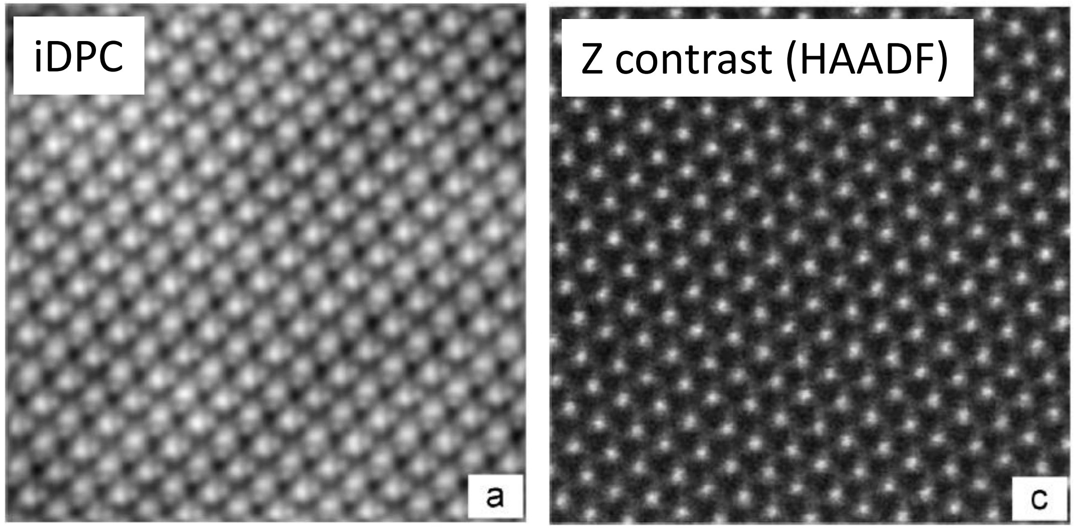

Capabilities and limitations of DPC

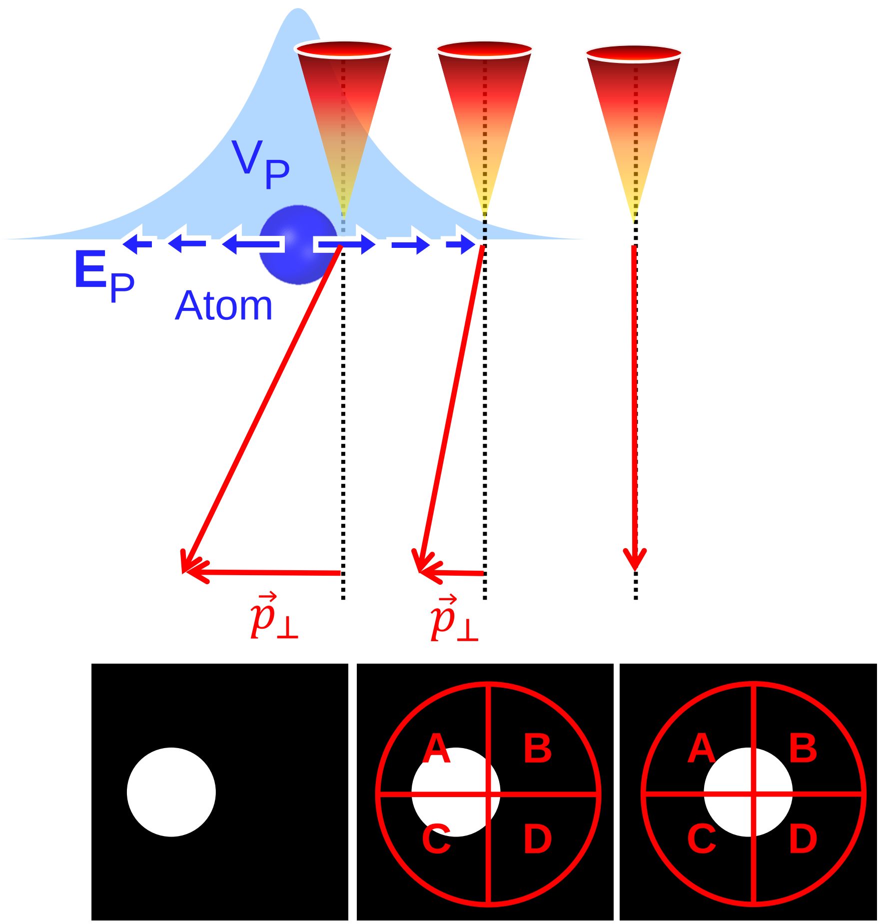

Diffraction pattern (000)

Dekkers & de Lang, Optik **41**, 452 (1974)
H. Rose, Ultramicroscopy **2**, 251(1977)

Capabilities and limitations of DPC

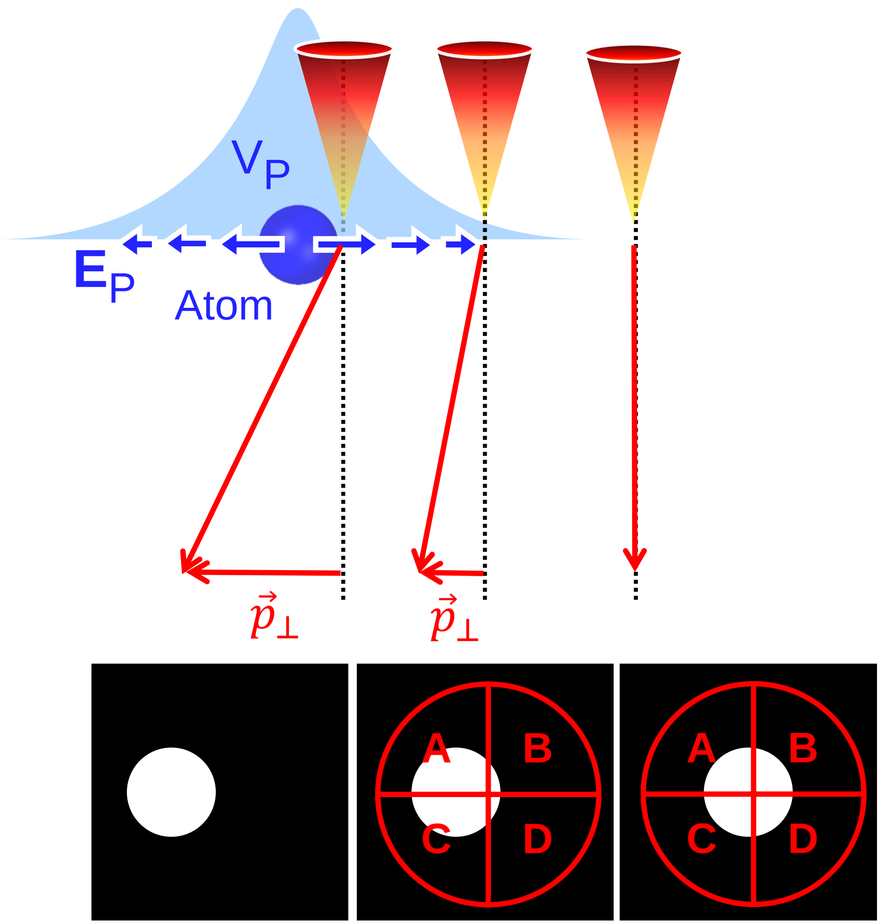

Diffraction pattern (000)

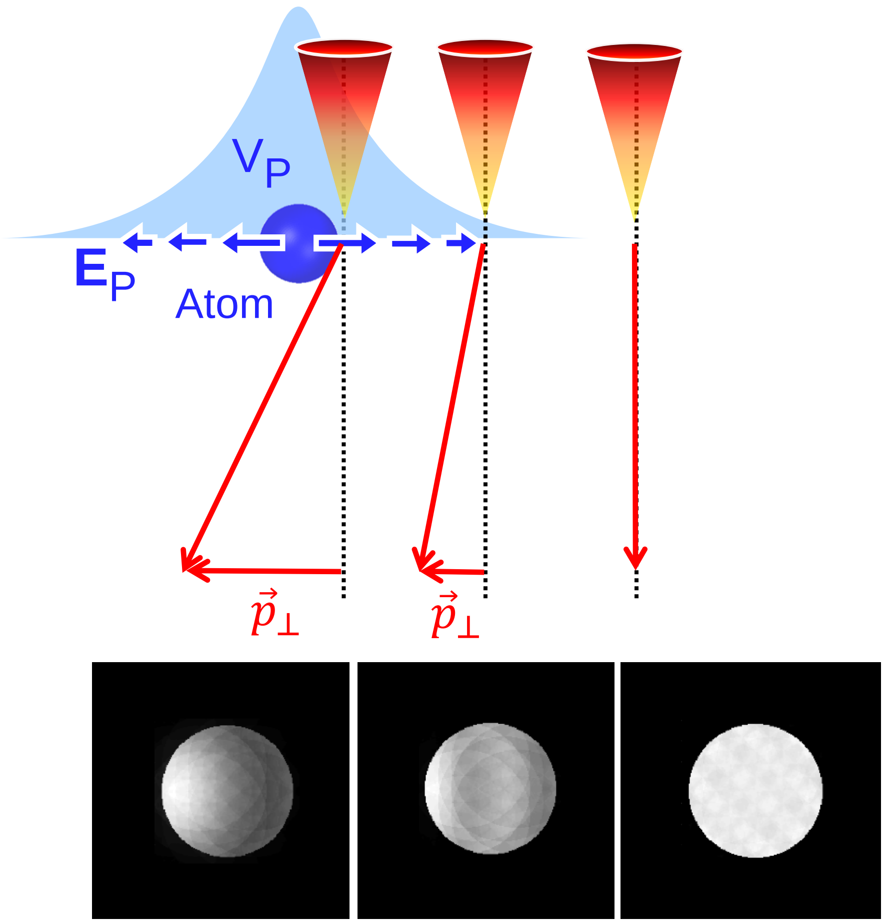

Diffraction pattern (000)

Dekkers & de Lang, Optik **41**, 452 (1974)
H. Rose, Ultramicroscopy **2**, 251(1977)

Capabilities and limitations of DPC

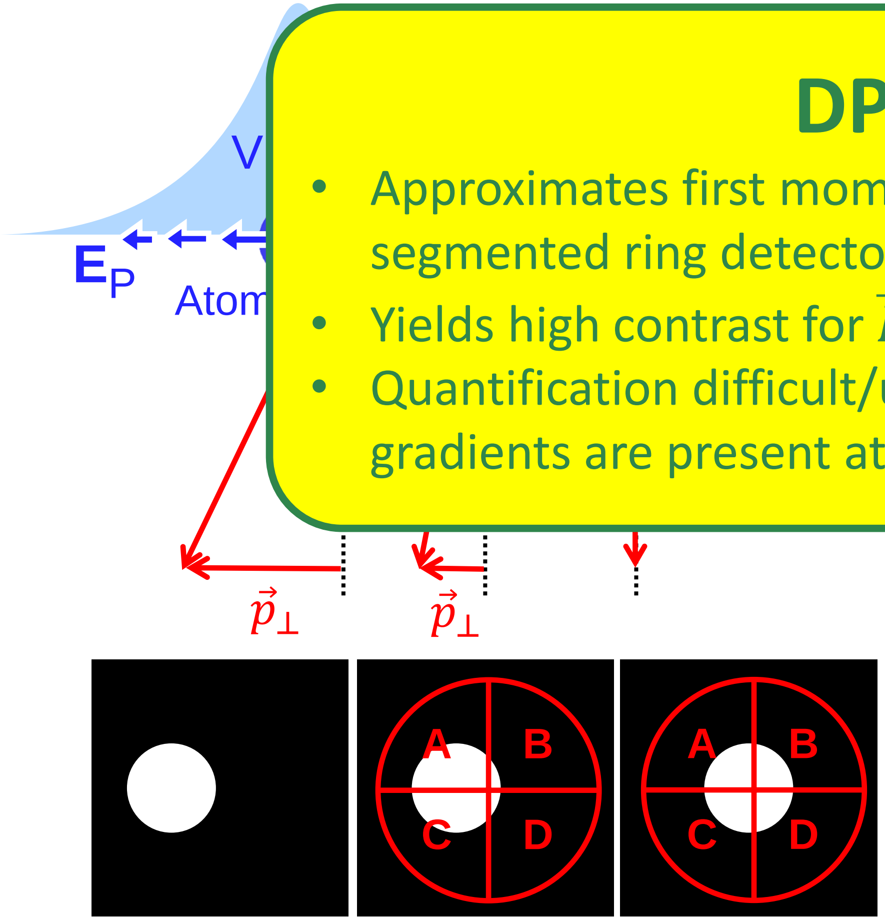

Diffraction pattern (000)

DPC

- Approximates first moment/COM imaging via segmented ring detectors
- Yields high contrast for $\vec{E}, \vec{B}$ and light elements
- Quantification difficult/usually fails when field gradients are present at the scale of the probe

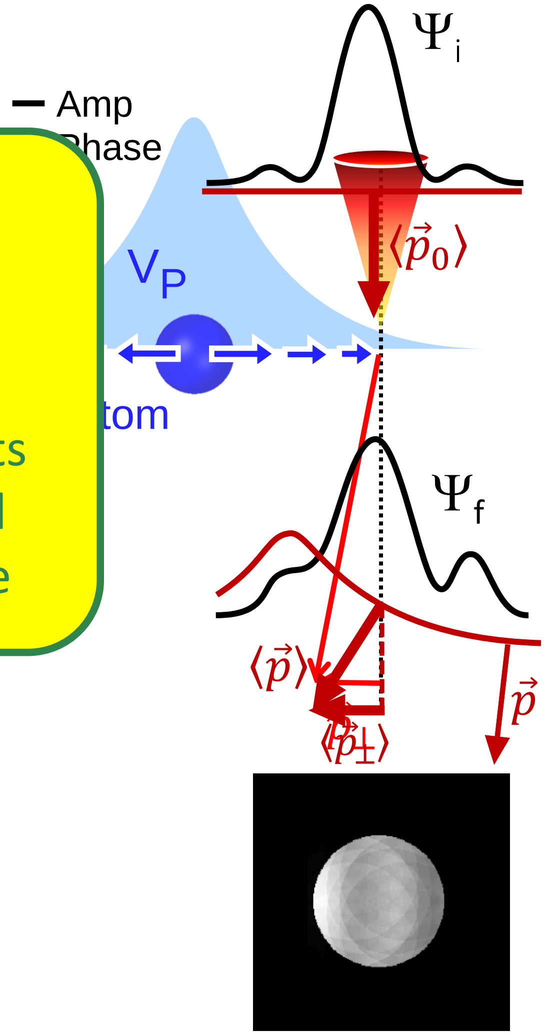

Diffraction pattern (000)

Dekkers & de Lang, Optik **41**, 452 (1974)
H. Rose, Ultramicroscopy **2**, 251(1977)

STEM with full momentum resolution

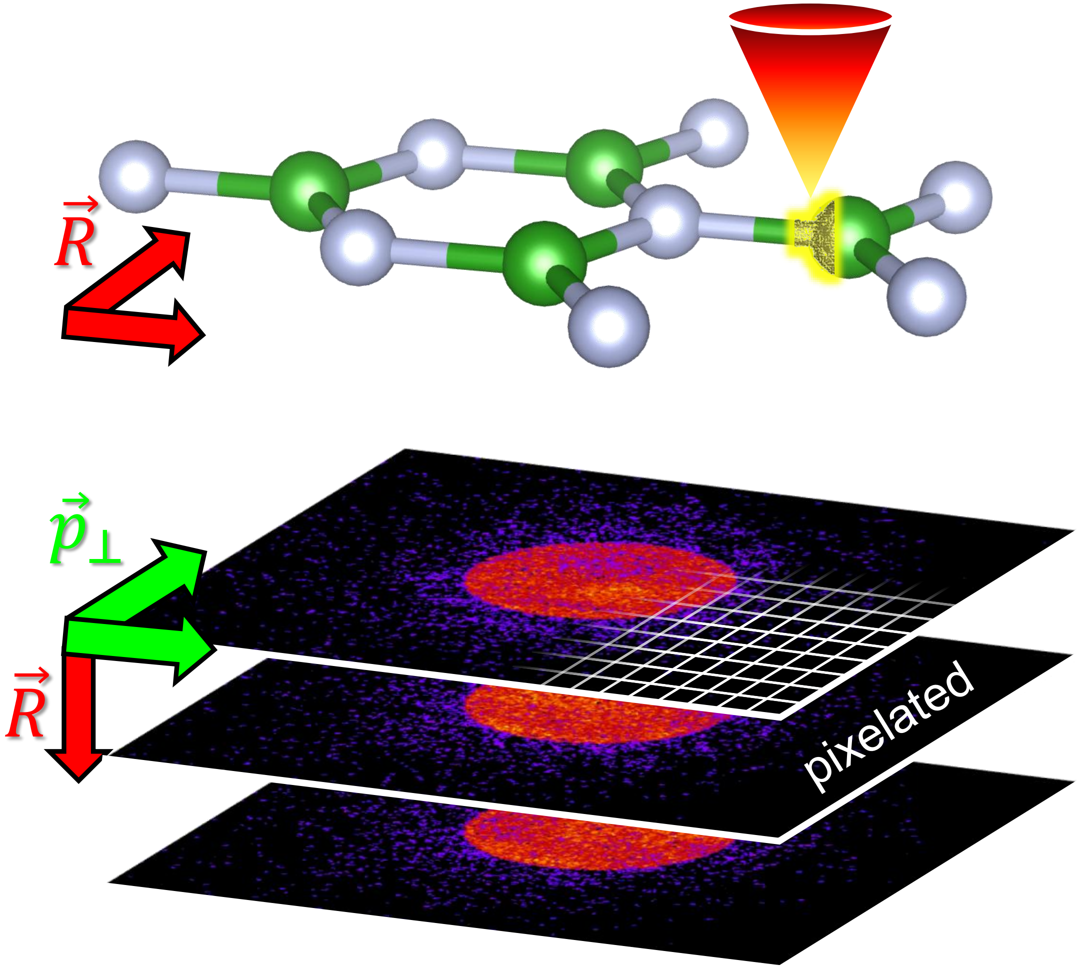

4-dimensional data set

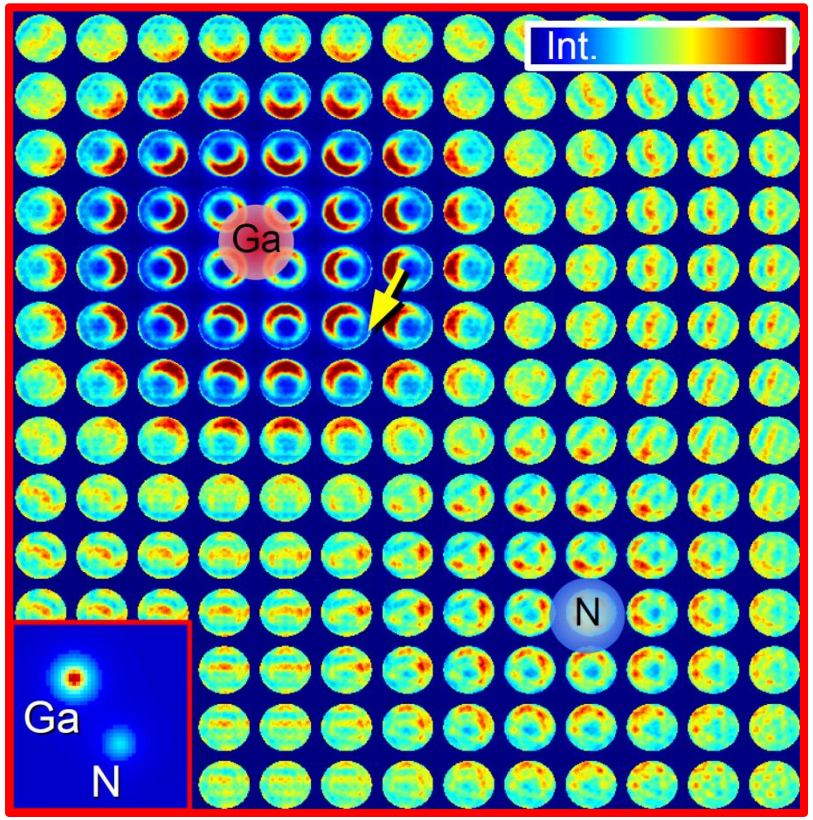

Full diffraction pattern at each scan position

Ultrafast cameras

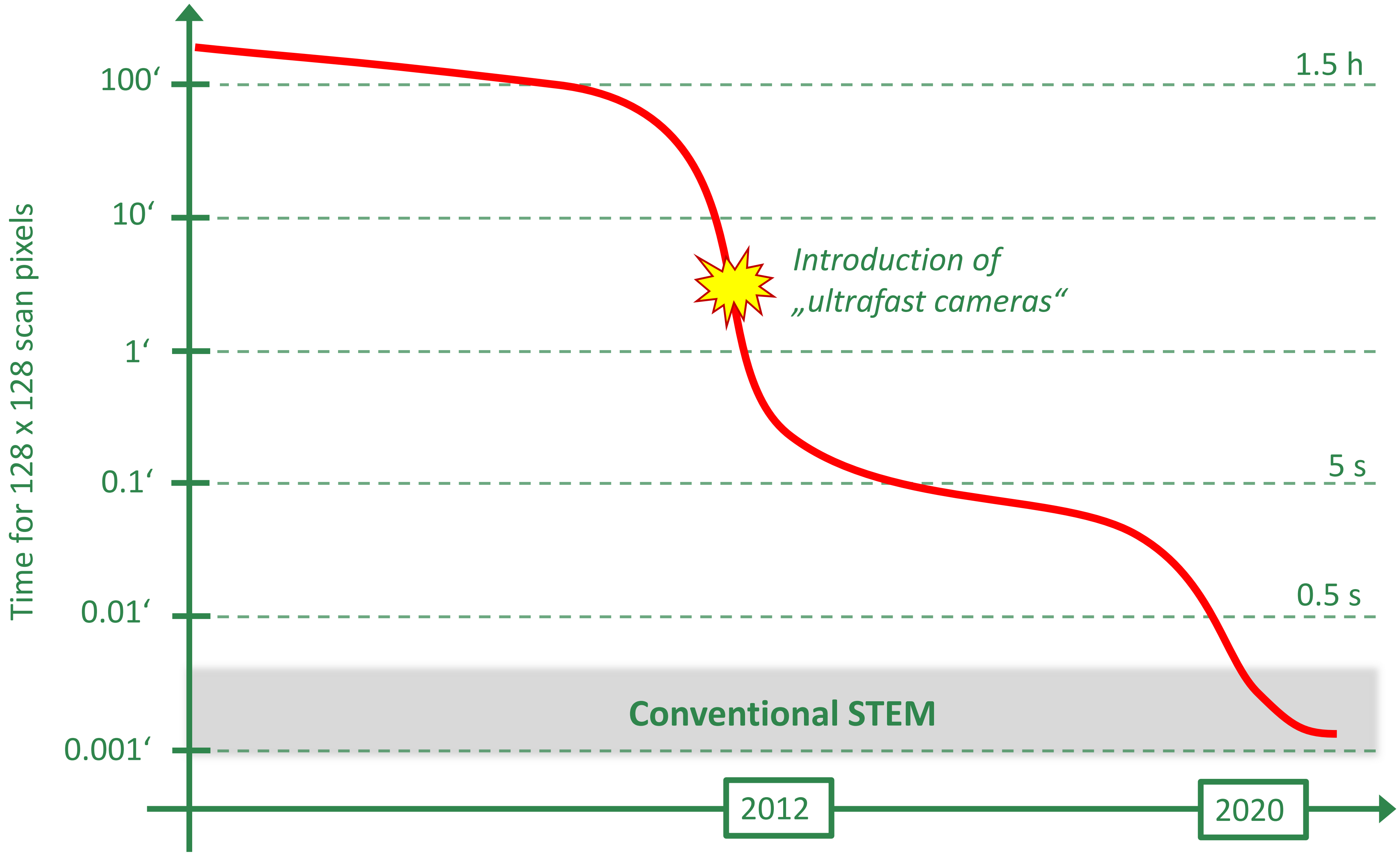

< ms range

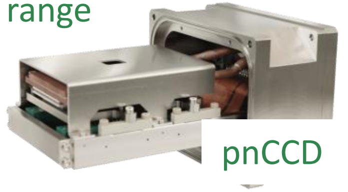

pnCCD

ps range (!)

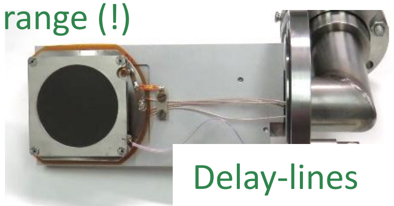

Delay-lines

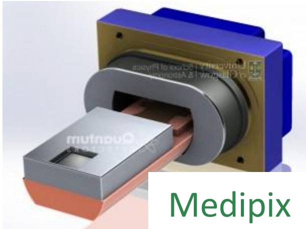

Medipix

K2

EMPAD

Tate et al, M&M **22**, 237 (2016)
Plackett et al., J. Instr. **8**, C01038 (2013)
H. Ryll et al., J. Instrum. **11**, P04006 (2016)
Müller-Caspary et al., Appl. Phys. Lett. **101**, 212110 (2012)
Müller-Caspary et al., Appl. Phys. Lett. **107**, 072110 (2015)

Ultrafast cameras

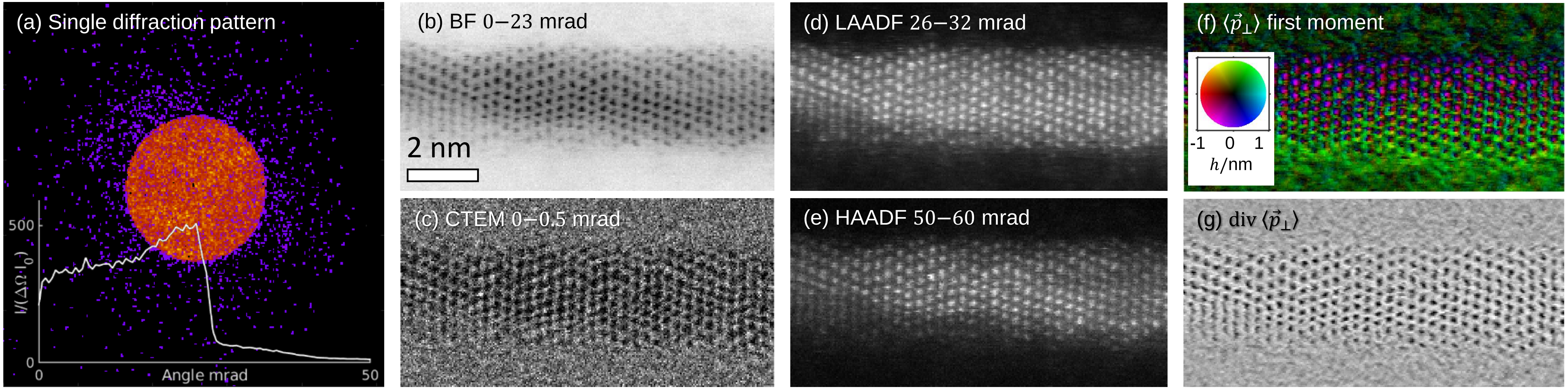

Momentum-resolved STEM: Allows versatile characterisation in addition to position-sensitivity

Tate et al, M&M **22**, 237 (2016)
Plackett et al., J. Instr. **8**, C01038 (2013)
H. Ryll et al., J. Instrum. **11**, P04006 (2016)
Müller-Caspary et al., Appl. Phys. Lett. **101**, 212110 (2012)
Müller-Caspary et al., Appl. Phys. Lett. **107**, 072110 (2015)

Approximating first moment with segmented detectors: Transfer function?

Differential Phase Contrast (DPC)

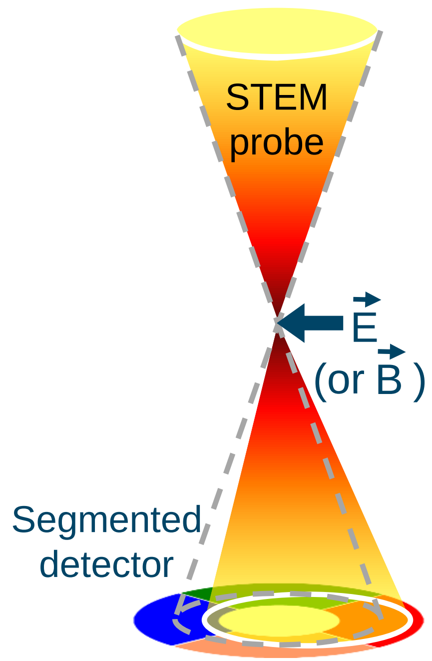

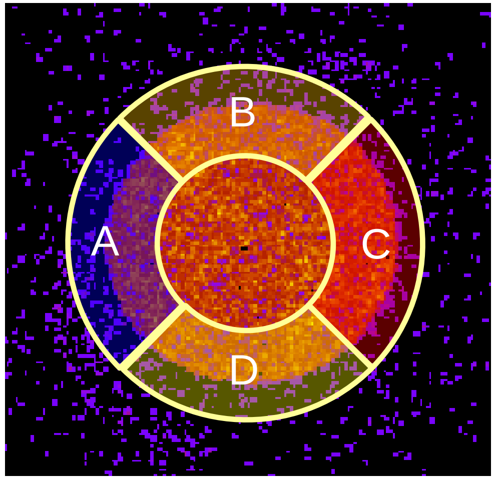

- Opposite segment differences approximate $\langle\hat{p}\rangle$:

$$\langle\hat{p}\rangle_{seg} \sim \begin{pmatrix} C-A \\ D-B \end{pmatrix}$$

- Correction for transfer function (Fourier space):

$$\mathcal{F}\{\langle\hat{p}\rangle_{seg}^{corr}\} = \frac{TF_{\text{first moment}}}{TF_{\text{segment Det.}}} \cdot \mathcal{F}\{\langle\hat{p}\rangle_{seg}\}$$

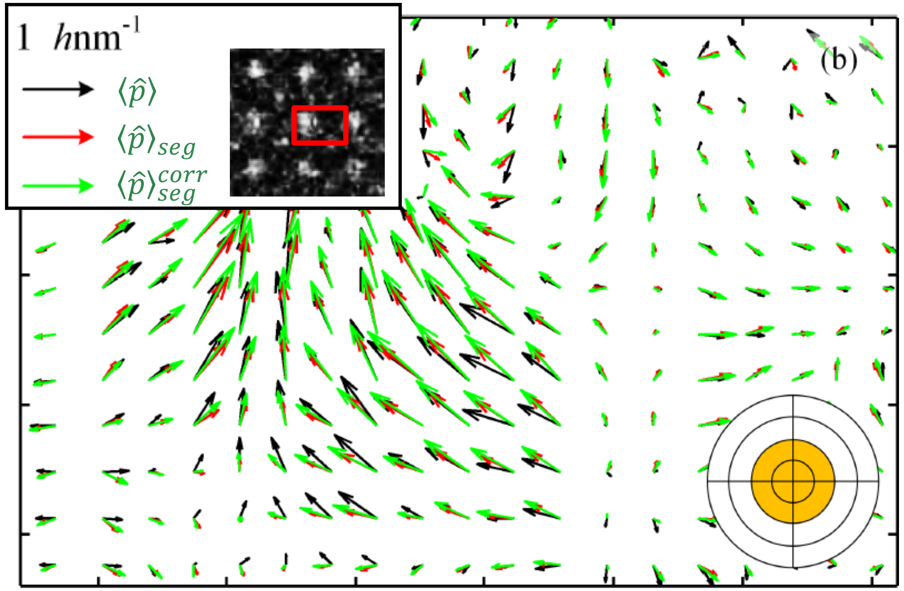

- **Segmented DPC yields first moments approximately**
- **Difficult to quantify, difficult to correct by TF**

Müller-Caspary et al., Ultramicroscopy **203**, 95 (2019)

Outline

STEM, DPC, COM, phases and momentum transfer

Electric fields in thin specimen: Ehrenfest theorem

Approaches for polarisation-induced field mapping

Practice hint 1 – 5, focus, coherence

Gradient – based (single & multislice) ptychography

Introduction to the inverse problem

Minimizing the loss function: a single-scattering example

Inverse multislice: concept, coherence, TDS, parametrisation

From momentum transfer to electric field

The **Ehrenfest theorem** states for a quantum mechanical operator $\hat{o}$:

$$\frac{d\langle\hat{o}\rangle}{dt} = \frac{i}{\hbar}\langle[\hat{H},\hat{o}]\rangle + \left\langle\frac{\partial\hat{o}}{\partial t}\right\rangle$$

with the Hamilton Operator

$$\hat{H} = \frac{\hat{p}_\perp^2}{2m_e} - e\hat{V}(\vec{r}) \quad .$$

We have $\hat{o} = \hat{p}_\perp$ and assume the **static case**, thus

$$\left\langle\frac{\partial\hat{o}}{\partial t}\right\rangle = 0 \quad .$$

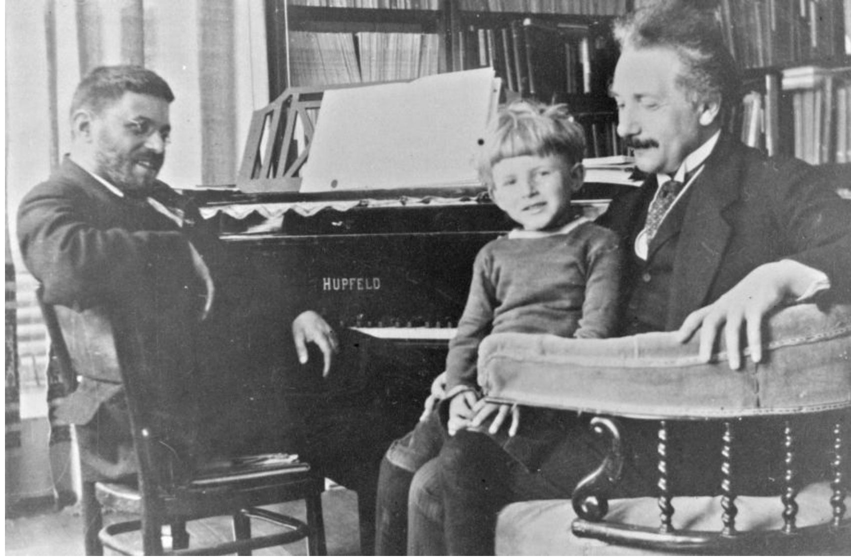

Bemerkung über die angenäherte Gültigkeit der klassischen Mechanik innerhalb der Quantenmechanik.

Von $\boxed{\textbf{P. Ehrenfest}}$ in Leiden, Holland.

(Eingegangen am 5. September 1927.)

$$\frac{dP}{dt} = \int dx\,\Psi\Psi^*\left(-\frac{\partial V}{\partial x}\right)$$

From momentum transfer to electric field

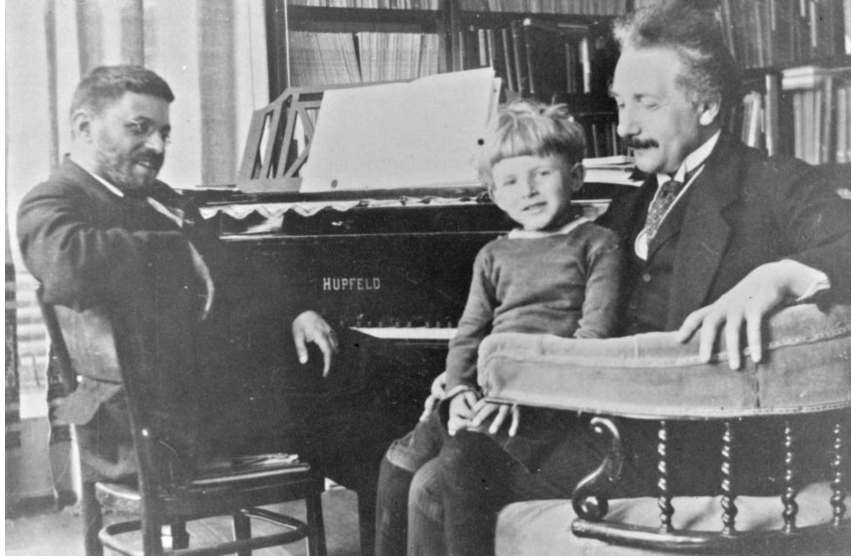

The **Ehrenfest theorem** states for a quantum mechanical operator $\hat{o}$:

$$\frac{d\langle\hat{o}\rangle}{dt} = \frac{i}{\hbar}\langle[\hat{H},\hat{o}]\rangle + \left\langle\frac{\partial\hat{o}}{\partial t}\right\rangle$$

with the Hamilton Operator

$$\hat{H} = \frac{\hat{p}_\perp^2}{2m_e} - e\hat{V}(\vec{r}) \quad .$$

We have $\hat{o} = \hat{p}_\perp$ and assume the **static case**, thus

$$\left\langle\frac{\partial\hat{o}}{\partial t}\right\rangle = 0 \quad .$$

From the commutator $\left[\hat{H},\hat{o}\right]$ we have to evaluate the expression

$$[\hat{p}_\perp^2,\hat{p}_\perp] = [\hat{p}_\perp\hat{p}_\perp,\hat{p}_\perp] = \hat{p}_\perp[\hat{p}_\perp,\hat{p}_\perp] + [\hat{p}_\perp,\hat{p}_\perp]\hat{p}_\perp = 0 \quad .$$

What remains is the potential part (care: $\vec{\nabla}_\perp$ acts on unwritten wave function, too):

$$\left[-e\hat{V}(\vec{r}),\frac{\hbar}{i}\vec{\nabla}_\perp\right] = -e\frac{\hbar}{i}\left(\hat{V}(\vec{r})\vec{\nabla}_\perp - \vec{\nabla}_\perp\hat{V}(\vec{r}) - \hat{V}(\vec{r})\vec{\nabla}_\perp\right) = e\frac{\hbar}{i}\vec{\nabla}_\perp\hat{V}(\vec{r}) = -e\frac{\hbar}{i}\vec{E}_\perp$$

Bemerkung über die angenäherte Gültigkeit der klassischen Mechanik innerhalb der Quantenmechanik.

Von $\boxed{\text{P. Ehrenfest}}$ in Leiden, Holland.

(Eingegangen am 5. September 1927.)

$$\frac{dP}{dt} = \int dx\,\Psi\Psi^*\left(-\frac{\partial V}{\partial x}\right)$$

From momentum transfer to electric field

From

$$\left\langle \frac{\partial \hat{o}}{\partial t} \right\rangle = 0, \quad [\hat{p}_\perp^2, \hat{p}_\perp] = 0, \quad \left[-e\hat{V}(\vec{r}), \frac{\hbar}{i} \vec{\nabla}_\perp \right] = -e \frac{\hbar}{i} \vec{E}_\perp$$

we arrive at

$$\frac{d\langle \hat{p}_\perp \rangle}{dt} = -e \langle \vec{E}_\perp \rangle \quad .$$

An electron with velocity v travels a distance dz during time interval dt, thus

$$d\langle \hat{p}_\perp \rangle = \frac{-e}{v} \langle \vec{E}_\perp \rangle \, dz \quad .$$

This can be integrated to yield

$$\boxed{\langle \hat{p}_\perp \rangle = \frac{-e}{v} \int \langle \vec{E}_\perp \rangle \, dz = \frac{-e}{v} \iiint \vec{E}_\perp(\vec{r}) \cdot I(\vec{r}) \, dx \, dy \, dz}$$

The **expectation value of the momentum** equals the integral over the product of **electric field and intensity** in the **whole interaction volume.** This expression is **exact.**

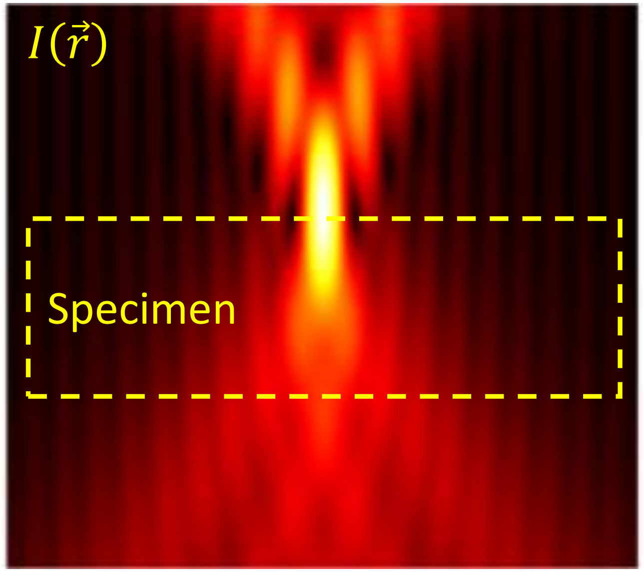

From momentum transfer to electric field

Correct result:

$$\langle \hat{p}_\perp \rangle = \frac{-e}{v} \int \langle \vec{E}_\perp \rangle \, dz = \frac{-e}{v} \iiint \vec{E}_\perp(\vec{r}) \cdot I(\vec{r}) \, dx \, dy \, dz$$

Problem:

$I(\vec{r})$ varies strongly in the specimen due to propagation and (multiple) scattering.

Solution:

Approximate $I(\vec{r})$ to be the intensity of the STEM probe in the whole specimen.

→ For thin specimen $I(\vec{r}) \approx I(\vec{r}_\perp) = I(x,y)$

→ Perform z Integration of $\vec{E}_\perp(\vec{r})$:

$$\langle \hat{p}_\perp \rangle = \frac{-e}{v} \iiint \vec{E}_\perp(\vec{r}) \, dz \quad \cdot I(x,y) \, dx \, dy$$

$$= \frac{-e}{v} \iint \vec{E}_\perp^P(x,y) \cdot I(x,y) \, dx \, dy$$

Projected electric field [V]:

$$\vec{E}_\perp^P(x,y) := \int \vec{E}_\perp(\vec{r}) \, dz$$

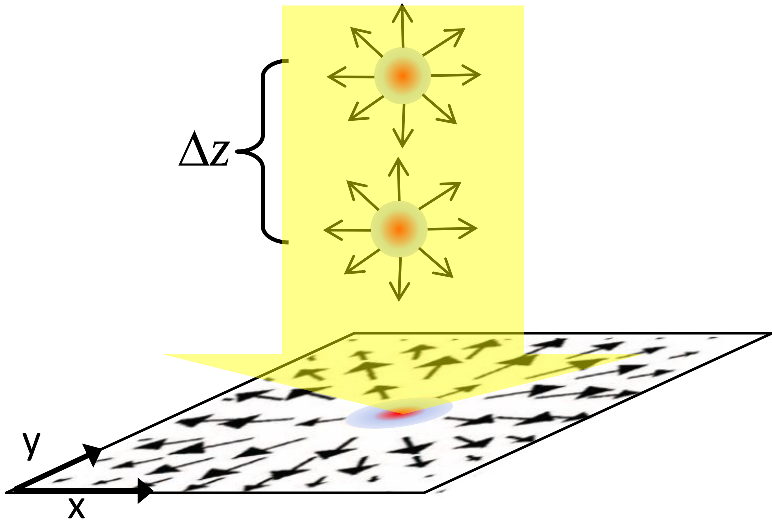

From momentum transfer to electric field

Thin specimen:

$$\langle \hat{p}_\perp \rangle = \frac{-e}{v} \iint \vec{E}_\perp^P(x,y) \cdot I(x,y)\, dx\, dy$$

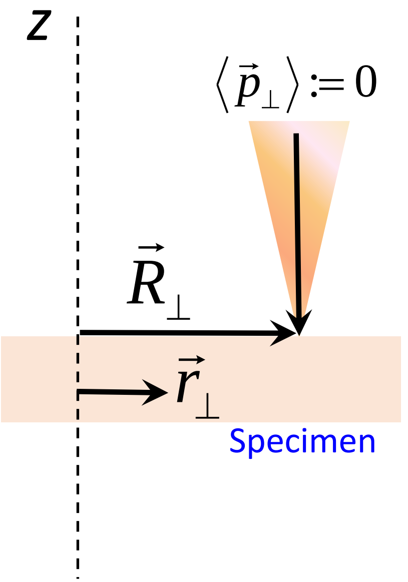

Now we introduce the scan coordinate $\vec{R}$:

$I(x,y)$ equals a probe centered on the optical axis $I^c(x,y)$, which is shifted to $\vec{R} = (X,Y)$:

$$I(x,y) = I^c(x-X, y-Y)$$

Thus:

$$\langle \hat{p}_\perp(\vec{R}) \rangle = \frac{-e}{v} \iint \vec{E}_\perp^P(x,y) \cdot I^c(x-X, y-Y) dx\, dy$$

Or:

$$\langle \hat{\boldsymbol{p}}_\perp(\vec{\boldsymbol{R}}) \rangle = \frac{-\boldsymbol{e}}{\boldsymbol{v}} \left[\boldsymbol{I^c} \star \vec{\boldsymbol{E}}_\perp^{\boldsymbol{P}} \right]$$

The average momentum transfer in a thin specimen equals the cross-correlation ($\star$) of the intensity of the STEM probe and the projected electric field.

Examples

The early days (2014)

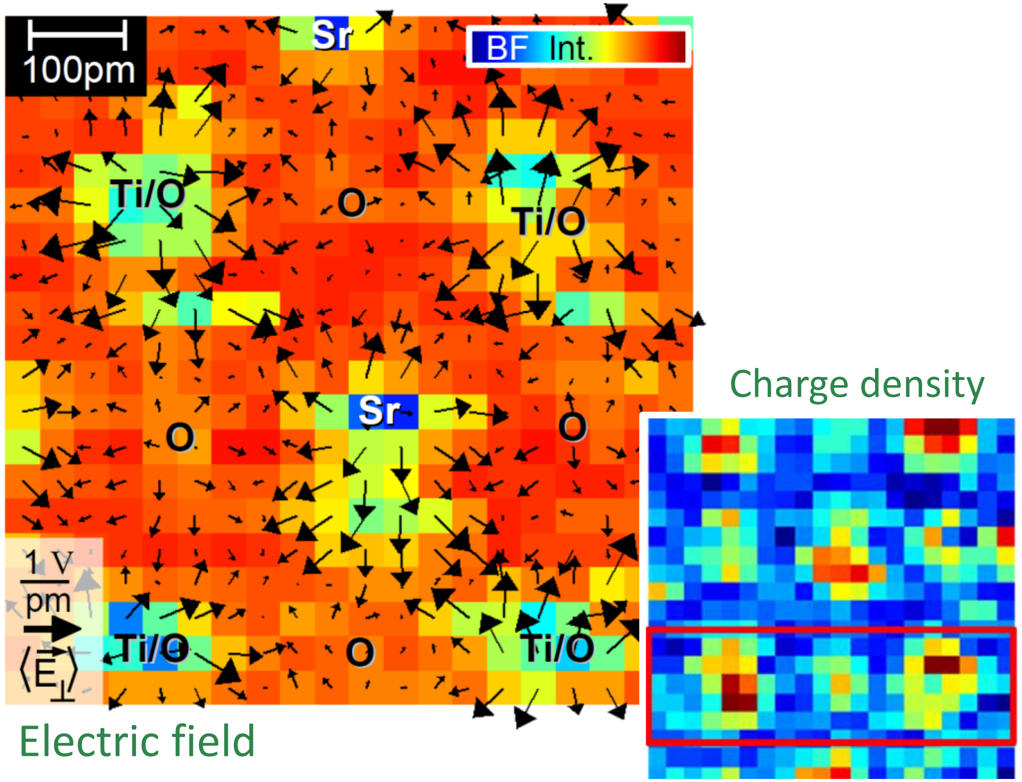

Electric field

Charge density

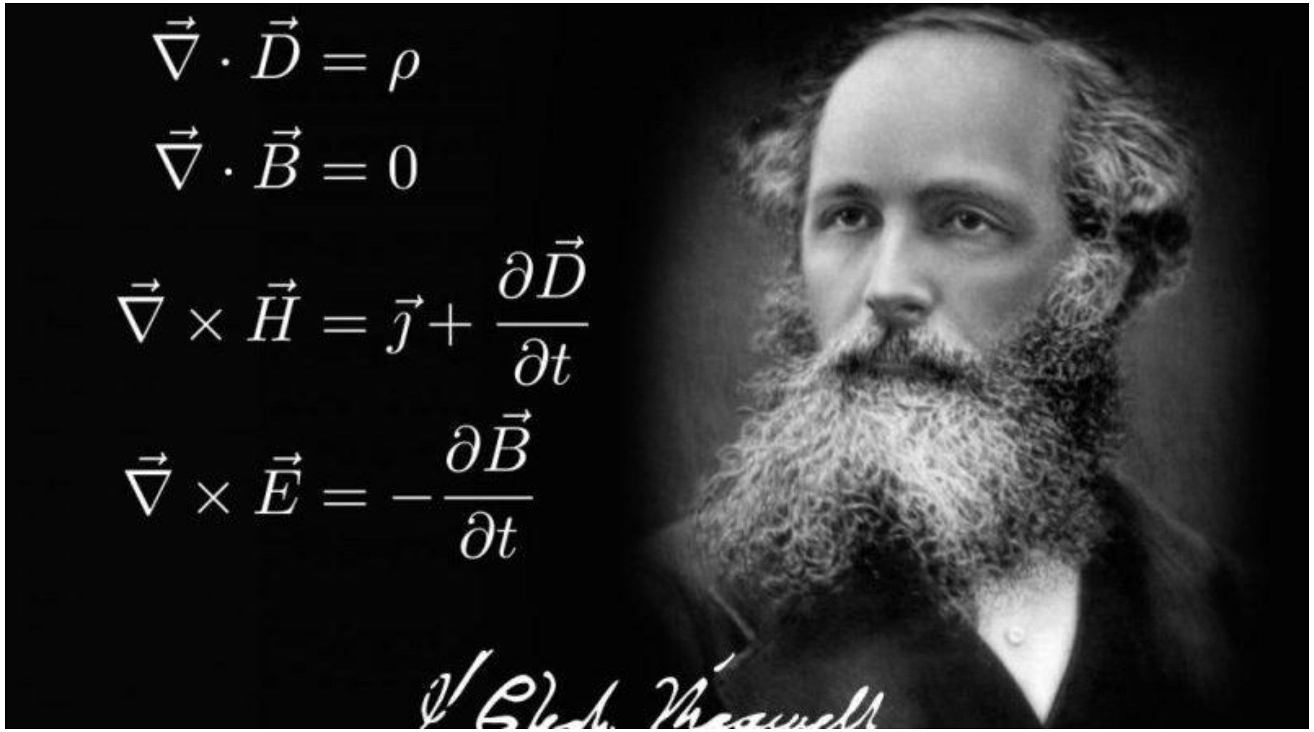

Data taken by
Armand Béché

The **charge density** can be calculated from the **measured electric field** by the **divergence** operator

$$\varrho(\vec{R}) = -\frac{v\varepsilon_0}{e} \operatorname{div} \langle \hat{p}_\perp(\vec{R}) \rangle$$

Examples

The early days (2014)

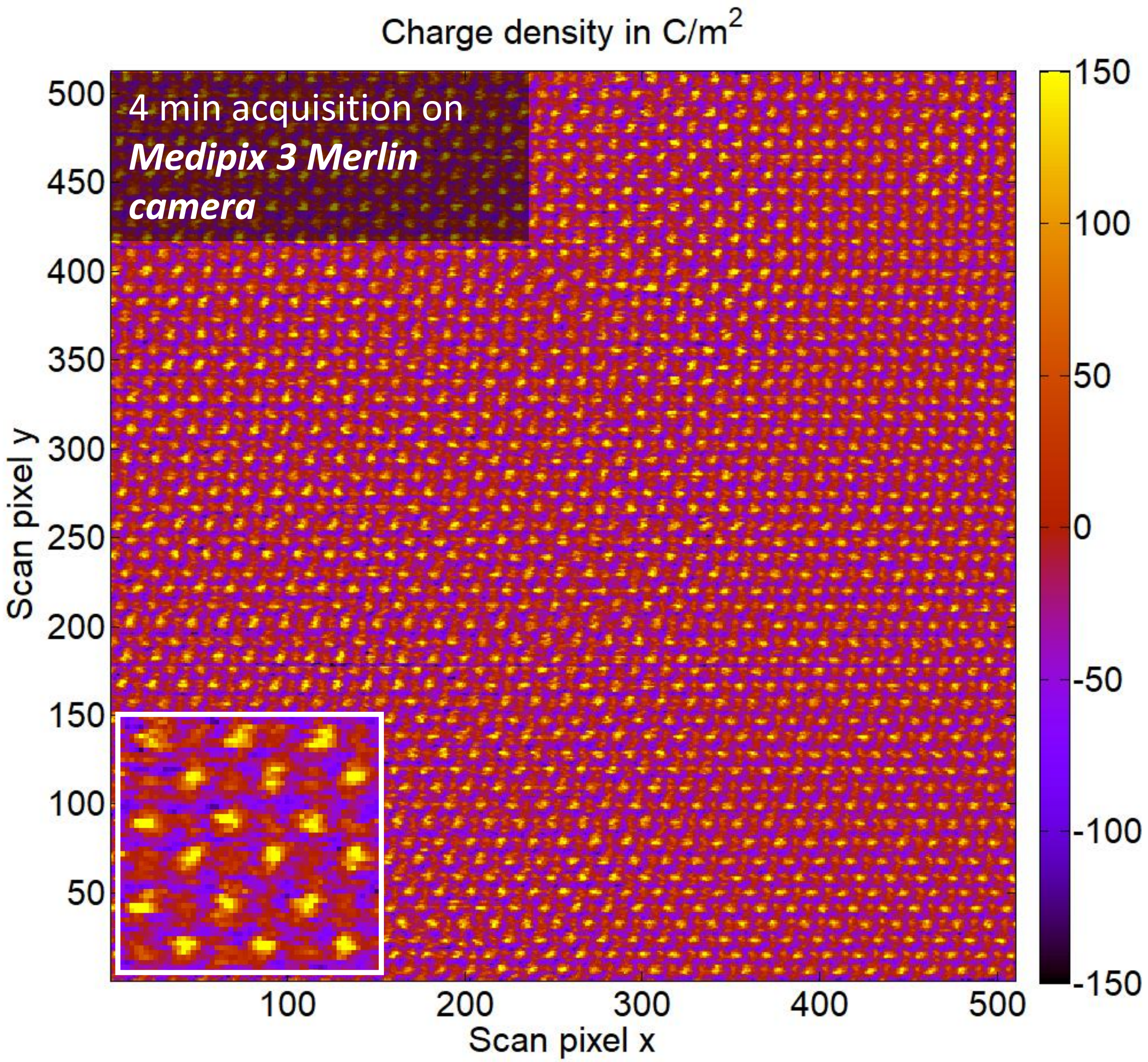

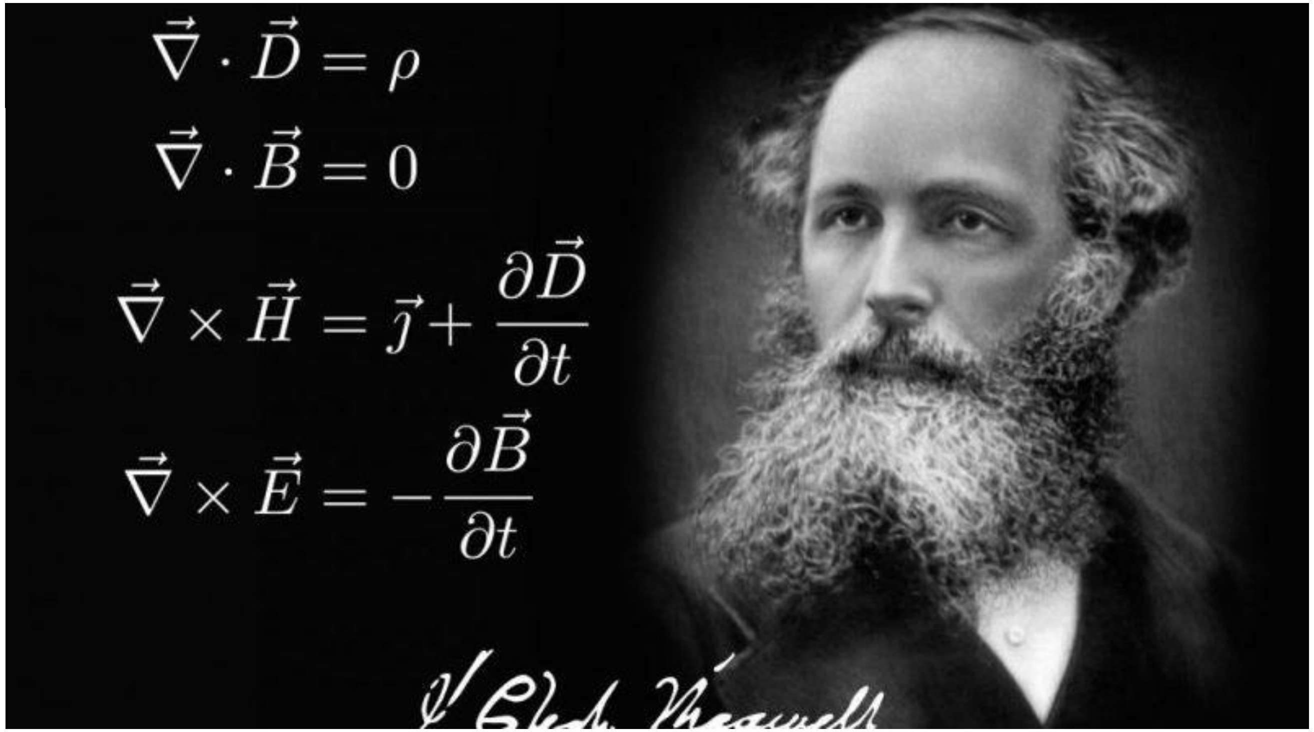

The **charge density** can be calculated from the **measured electric field** by the **divergence** operator

$$\varrho(\vec{R}) = -\frac{v\varepsilon_0}{e}\,\mathrm{div}\,\langle\hat{p}_\perp(\vec{R})\rangle$$

Calculating the electrostatic potential

Starting point: Electric field given by

$$\vec{E}(\vec{r}) = -\vec{\nabla}V(\vec{r})$$

Fourier Transform of both sides:

$$\mathcal{F}[\vec{E}](\vec{q}) = -\mathcal{F}[\vec{\nabla}V](\vec{q}) = -\iint \underbrace{\left(\vec{\nabla}V(\vec{r})\right)}_{u'} \underbrace{e^{-2\pi i\vec{q}\vec{r}}}_{v} d^2r$$

$$u'v = (uv)' - uv'$$

Calculating the electrostatic potential

Starting point: Electric field given by

$$\vec{E}(\vec{r}) = -\vec{\nabla} V(\vec{r})$$

Fourier Transform of both sides:

$$\mathcal{F}[\vec{E}](\vec{q}) = -\mathcal{F}[\vec{\nabla} V](\vec{q}) = -\iint \underbrace{\left(\vec{\nabla} V(\vec{r})\right)}_{u'} \underbrace{e^{-2\pi i \vec{q}\vec{r}}}_{v} \, d^2 r \qquad u'v = (uv)' - uv'$$

Inserting product rule:

$$\mathcal{F}[\vec{E}](\vec{q}) = -\vec{\nabla}_{\vec{r}} \iint V(\vec{r}) \cdot e^{-2\pi i \vec{q}\vec{r}} \, d^2 r + 2\pi i \vec{q} \iint V(\vec{r}) \cdot e^{-2\pi i \vec{q}\vec{r}} \, d^2 r$$

red: $\mathcal{F}[V](\vec{q})$

$$\Leftrightarrow \mathcal{F}[\vec{E}](\vec{q}) = -\vec{\nabla}_{\vec{r}} \, \mathcal{F}[V](\vec{q}) + 2\pi i \vec{q} \, \mathcal{F}[V](\vec{q})$$

Calculating the electrostatic potential

Starting point: Electric field given by

$$\vec{E}(\vec{r}) = -\vec{\nabla}V(\vec{r})$$

Fourier Transform of both sides:

$$\mathcal{F}[\vec{E}](\vec{q}) = -\mathcal{F}[\vec{\nabla}V](\vec{q}) = -\iint \underbrace{\left(\vec{\nabla}V(\vec{r})\right)}_{u'} \underbrace{e^{-2\pi i\vec{q}\vec{r}}}_{v} \, d^2r \qquad u'v = (uv)' - uv'$$

Inserting product rule:

$$\mathcal{F}[\vec{E}](\vec{q}) = -\vec{\nabla}_{\vec{r}} \iint V(\vec{r}) \cdot e^{-2\pi i\vec{q}\vec{r}} \, d^2r + 2\pi i\vec{q} \iint V(\vec{r}) \cdot e^{-2\pi i\vec{q}\vec{r}} \, d^2r$$

red: $\mathcal{F}[V](\vec{q})$

$$\Leftrightarrow \mathcal{F}[\vec{E}](\vec{q}) = -\vec{\nabla}_{\vec{r}}\, \mathcal{F}[V](\vec{q}) + 2\pi i\vec{q}\, \mathcal{F}[V](\vec{q})$$

Solving for $\mathcal{F}[V](\vec{q})$:

$$\frac{\vec{q}}{2\pi i q^2} \cdot \mathcal{F}[\vec{E}](\vec{q}) = \mathcal{F}[V](\vec{q})$$

Inverse Fourier Transform:

$$\boxed{V(\vec{r}) = \mathcal{F}^{-1}\left\{\frac{\vec{q}}{2\pi i q^2} \cdot \mathcal{F}[\vec{E}](\vec{q})\right\}(\vec{r})}$$

1. Fourier transform $\vec{E}$ component-wise
2. Multiply by reciprocal space coordinate essentially
3. Inverse Fourier-transform result.

First moment STEM
Data-driven summary: BL WSe_2

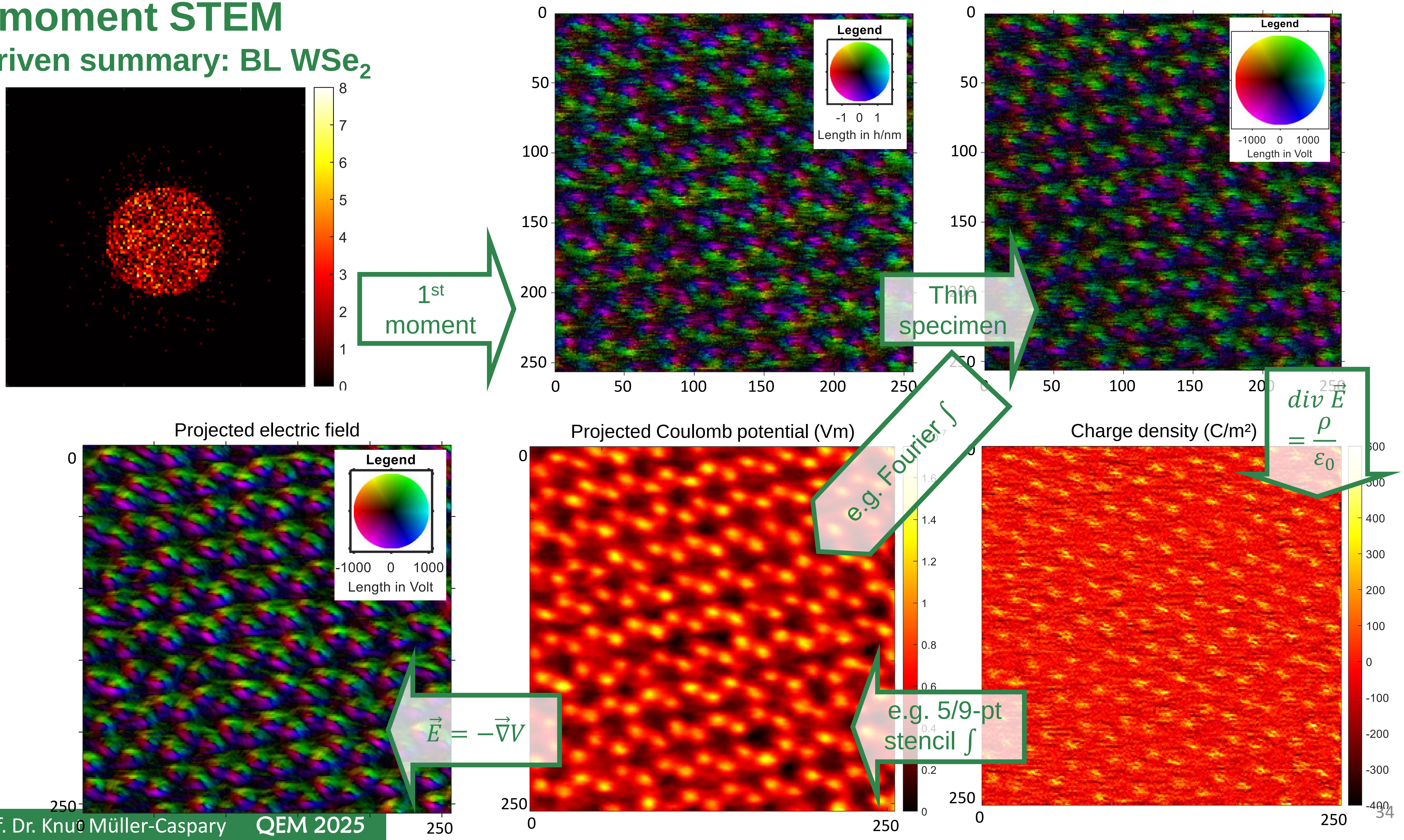

Outline

STEM, DPC, COM, phases and momentum transfer

Gradient – based (single & multislice) ptychography

Electric fields in thin specimen: Ehrenfest theorem

Introduction to the inverse problem

Approaches for polarisation-induced field mapping

Minimizing the loss function: a single-scattering example

Practice hint 1 – 5, focus, coherence

Inverse multislice: concept, coherence, TDS, parametrisation

Motivation

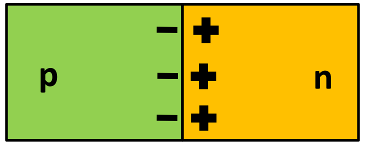

Electric field at pn-Jct.

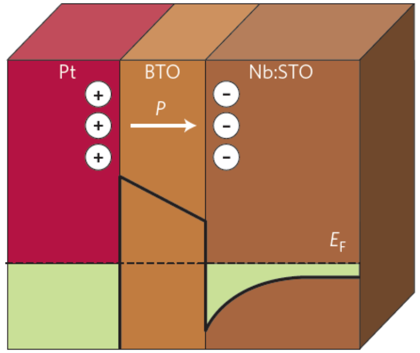

Ferroelectric Tunnel Jct.

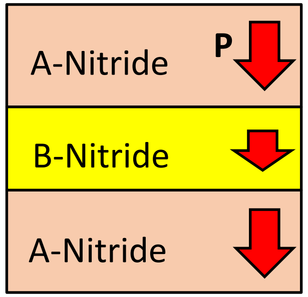

Polarisation in nitride heterostructures

Measurement of polarisation-induced electric fields

So far: Approximation for thin specimen ($< 5\ nm$) only.

Question:
Can one measure meso-scale electric field in thick specimens?

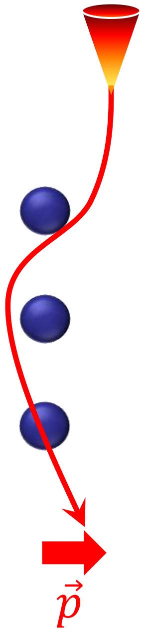

Problem:
Dynamical scattering such that

$$\cancel{\langle \hat{p}_\perp(\vec{R}) \rangle = \frac{-e\,t}{v}\left[I^c \star \vec{E}^P_\perp\right]}$$

Measurement of polarisation-induced electric fields

So far: Approximation for thin specimen ($< 5\ nm$) only.

Question:
Can one measure meso-scale electric field in thick specimens?

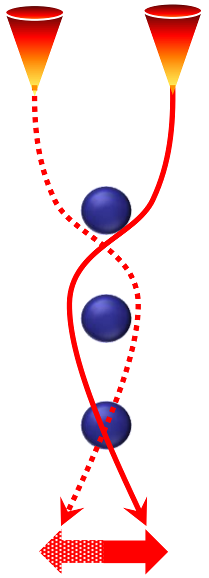

However:
Inversion symmetry → no net momentum transfer around an atomic column.

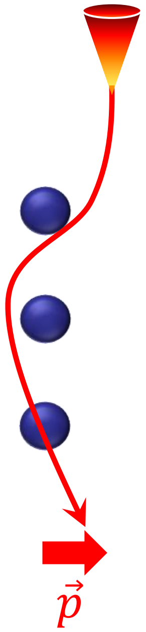

Problem:
Dynamical scattering such that

$$\cancel{\langle \hat{p}_\perp(\vec{R}) \rangle = [I^c \star \vec{E}_\perp^P]}$$

Measurement of polarisation-induced electric fields

So far: Approximation for thin specimen ($< 5\ nm$) only.

Question:
Can one measure meso-scale electric field in thick specimens?

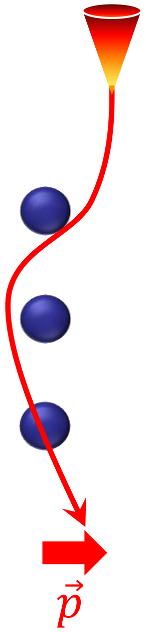

Problem:
Dynamical scattering such that

$$\cancel{\langle \hat{p}_\perp(\vec{R}) \rangle = -\frac{e}{v}\left[I^c \star \vec{E}_\perp^P\right]}$$

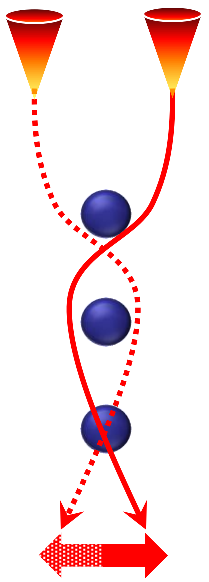

However:
Inversion symmetry → no net momentum transfer around an atomic column.

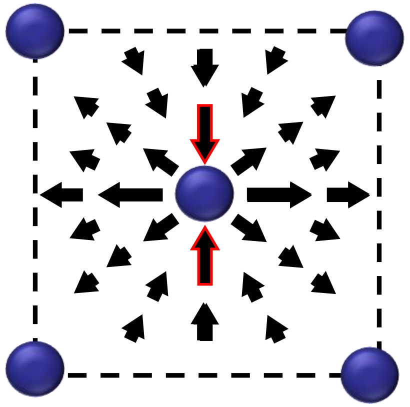

Unit cell average:
(Hopefully) vanishes at all thicknesses

Measurement of polarisation-induced electric fields

So far: Approximation for thin specimen ($< 5\ nm$) only.

Question:
Can one measure meso-scale electric field in thick specimens?

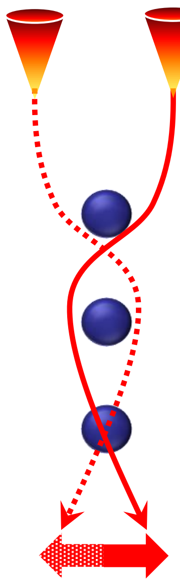

However:
Inversion symmetry → no net momentum transfer around an atomic column.

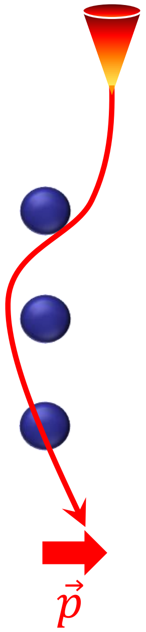

Problem:
Dynamical scattering such that

$$\cancel{\langle \hat{p}_\perp(\vec{R})\rangle = \frac{-e}{v}\left[I^c \star \vec{E}_\perp^P\right]}$$

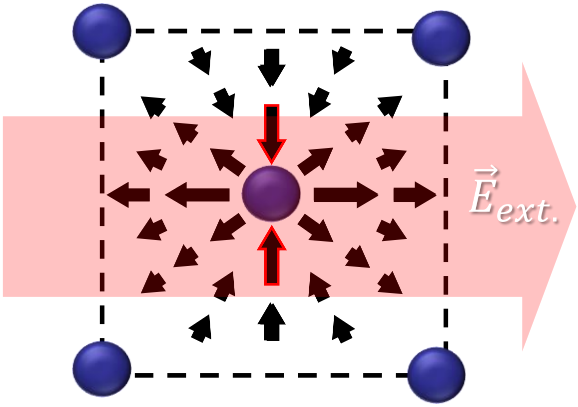

Unit cell average:
(Hopefully) vanishes at all thicknesses

If not:
Due to a **long-range external field $\vec{E}_{ext.}$**

Measurement of polarisation-induced electric fields

Write electric field as a sum of constant external and varying part causing dynamical scattering:

$$\vec{E}_\perp\,(x,y,z) = \vec{E}_{ext} + \vec{E}_{dyn}(x,y,z)\ .$$

Average momentum transfer:

$$\langle \hat{p}_\perp(\vec{R}) \rangle = -\frac{e}{v} \cdot \vec{E}_{ext.} \cdot t + \langle \hat{p}_\perp(\vec{R}) \rangle_{dyn}$$

Above: **Correct result**

$$\langle \hat{p}_\perp \rangle = \frac{-e}{v} \iiint \vec{E}_\perp(\vec{r}) \cdot I(\vec{r})\, dx\, dy\, dz$$

Measurement of polarisation-induced electric fields

Above: **Correct result**

$$\langle \hat{p}_\perp \rangle = \frac{-e}{v} \iiint \vec{E}_\perp(\vec{r}) \cdot I(\vec{r})\, dx\, dy\, dz$$

Write electric field as a sum of constant external and varying part causing dynamical scattering:

$$\vec{E}_\perp\,(x, y, z) = \vec{E}_{ext} + \vec{E}_{dyn}(x, y, z)\ \ .$$

Average momentum transfer:

$$\langle \hat{p}_\perp(\vec{R}) \rangle = -\frac{e}{v} \cdot \vec{E}_{ext.} \cdot t + \langle \hat{p}_\perp(\vec{R}) \rangle_{dyn}$$

Unit cell average: minimize impact of $\langle \hat{p}_\perp(\vec{R}) \rangle_{dyn}$:

$$\left[\langle \hat{p}_\perp(\vec{R}) \rangle\right]_{UC} = -\frac{e}{v} \cdot \vec{E}_{ext.} \cdot t + \vec{\delta}(t)$$

$\vec{\delta}(t)$: Systematic error due to violation of inversion symmetry

... which is usually present in the materials of interest ...

Measurement of polarisation-induced electric fields

Above: **Correct result**

$$\langle \hat{p}_\perp \rangle = \frac{-e}{v} \iiint \vec{E}_\perp(\vec{r}) \cdot I(\vec{r})\, dx\, dy\, dz$$

Write electric field as a sum of constant external and varying part causing dynamical scattering:

$$\vec{E}_\perp\,(x, y, z) = \vec{E}_{ext} + \vec{E}_{dyn}(x, y, z)\ .$$

Average momentum transfer:

$$\langle \hat{p}_\perp(\vec{R}) \rangle = -\frac{e}{v} \cdot \vec{E}_{ext.} \cdot t + \langle \hat{p}_\perp(\vec{R}) \rangle_{dyn}$$

Unit cell average: minimize impact of $\langle \hat{p}_\perp(\vec{R}) \rangle_{dyn}$:

$$[\langle \hat{p}_\perp(\vec{R}) \rangle]_{UC} = -\frac{e}{v} \cdot \vec{E}_{ext.} \cdot t + \vec{\delta}(t)$$

$\vec{\delta}(t)$: Systematic error due to violation of inversion symmetry

... which is usually present in the materials of interest ...

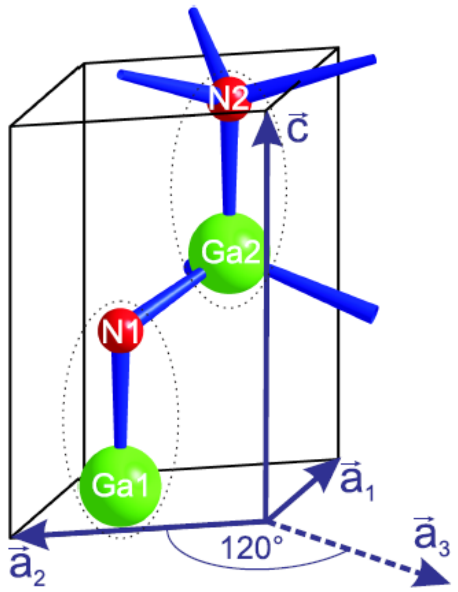

Piezo-/spontaneous polarisation in GaN

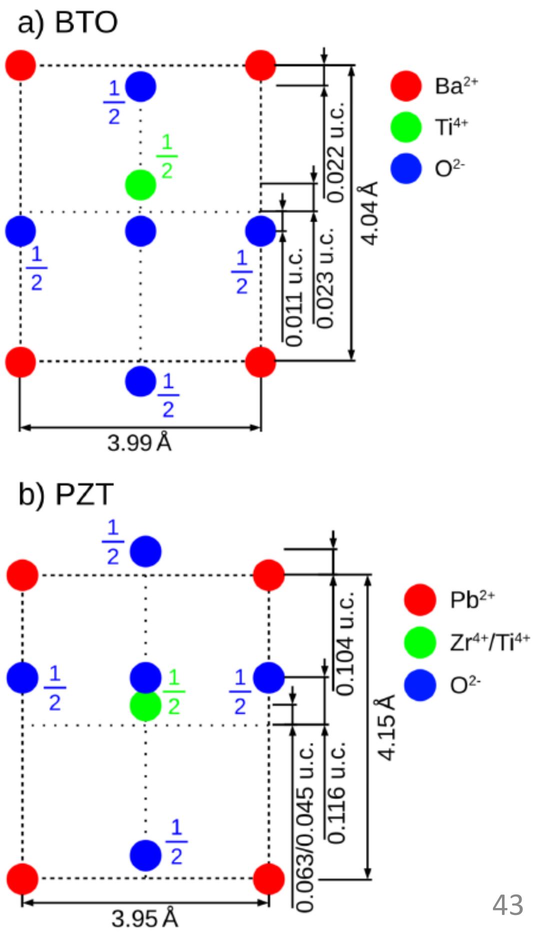

Ferroelectricity in perovskites

Measurement of polarisation-induced electric fields: GaN

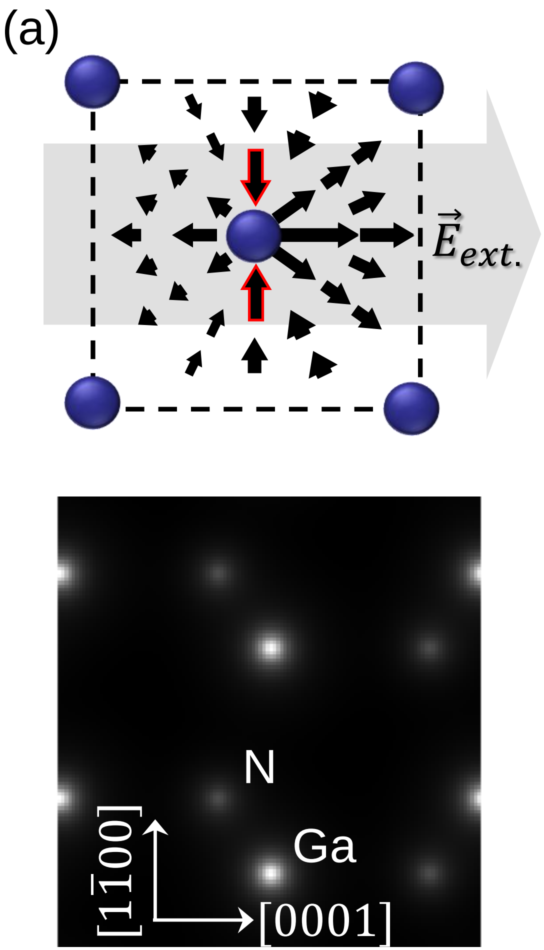

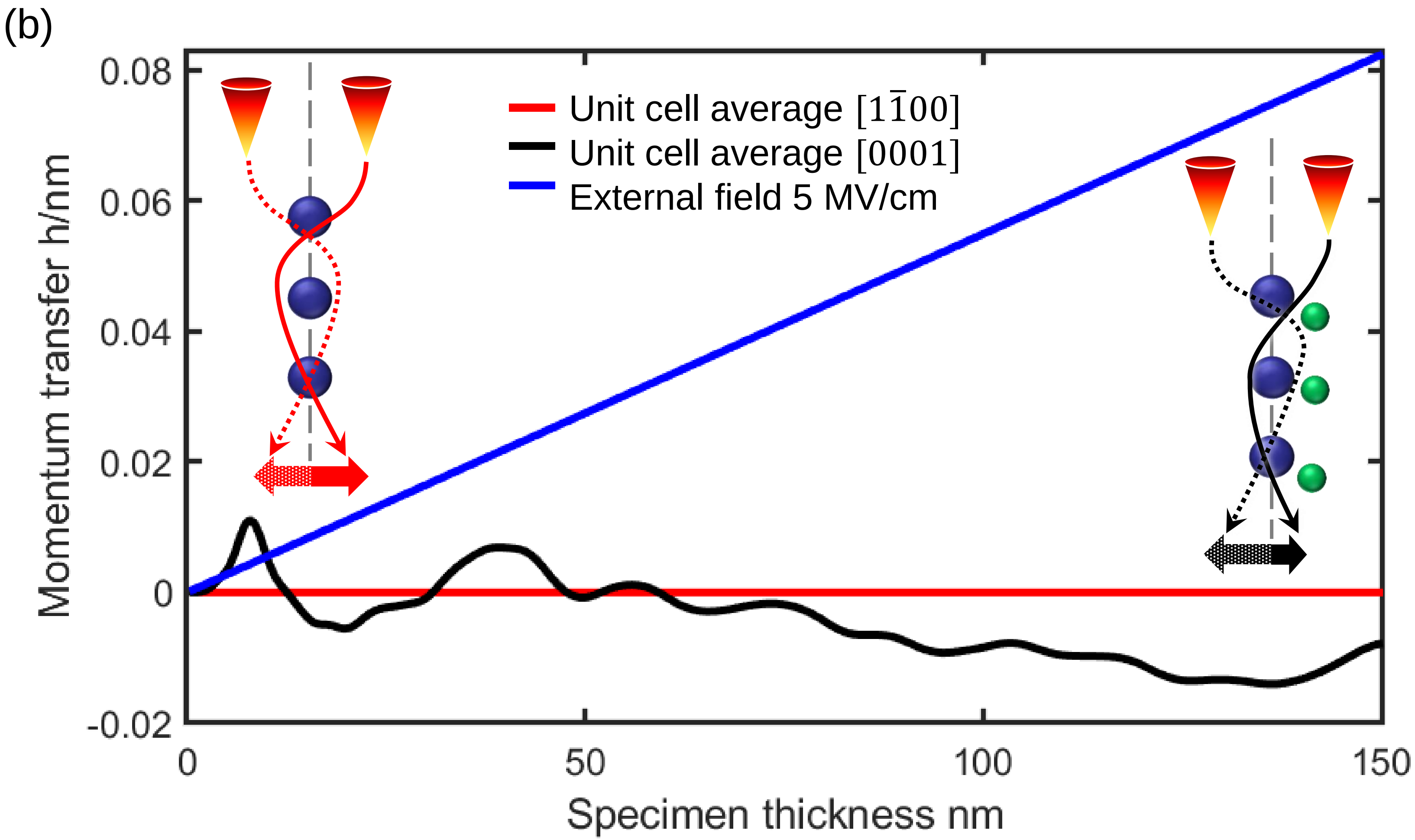

Measurement of polarisation-induced electric fields

AlN/GaN nanodiscs

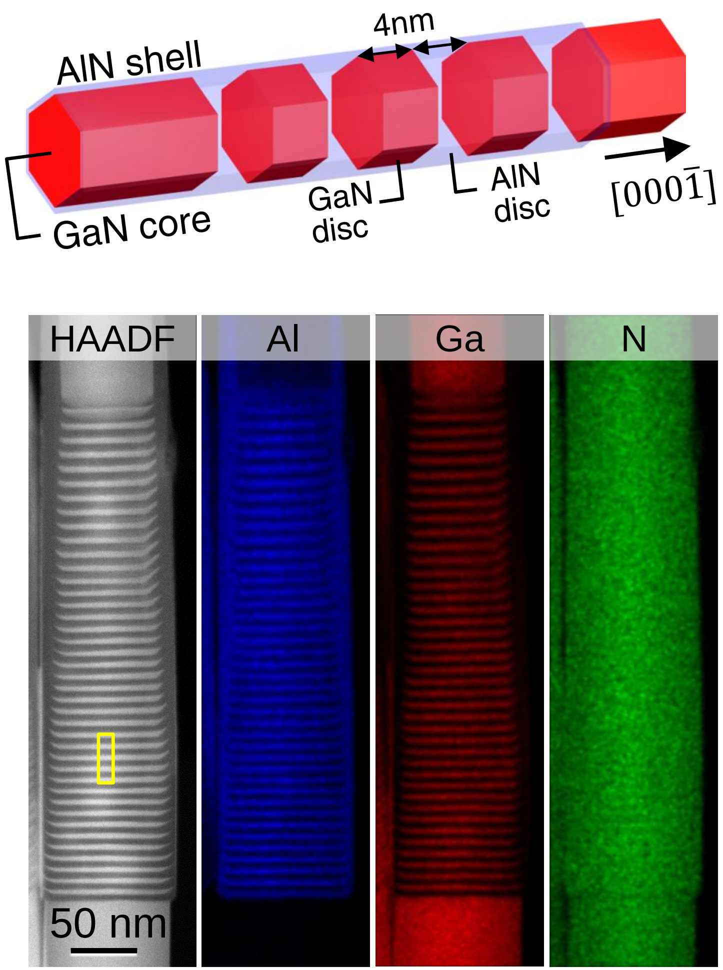

STEM probe

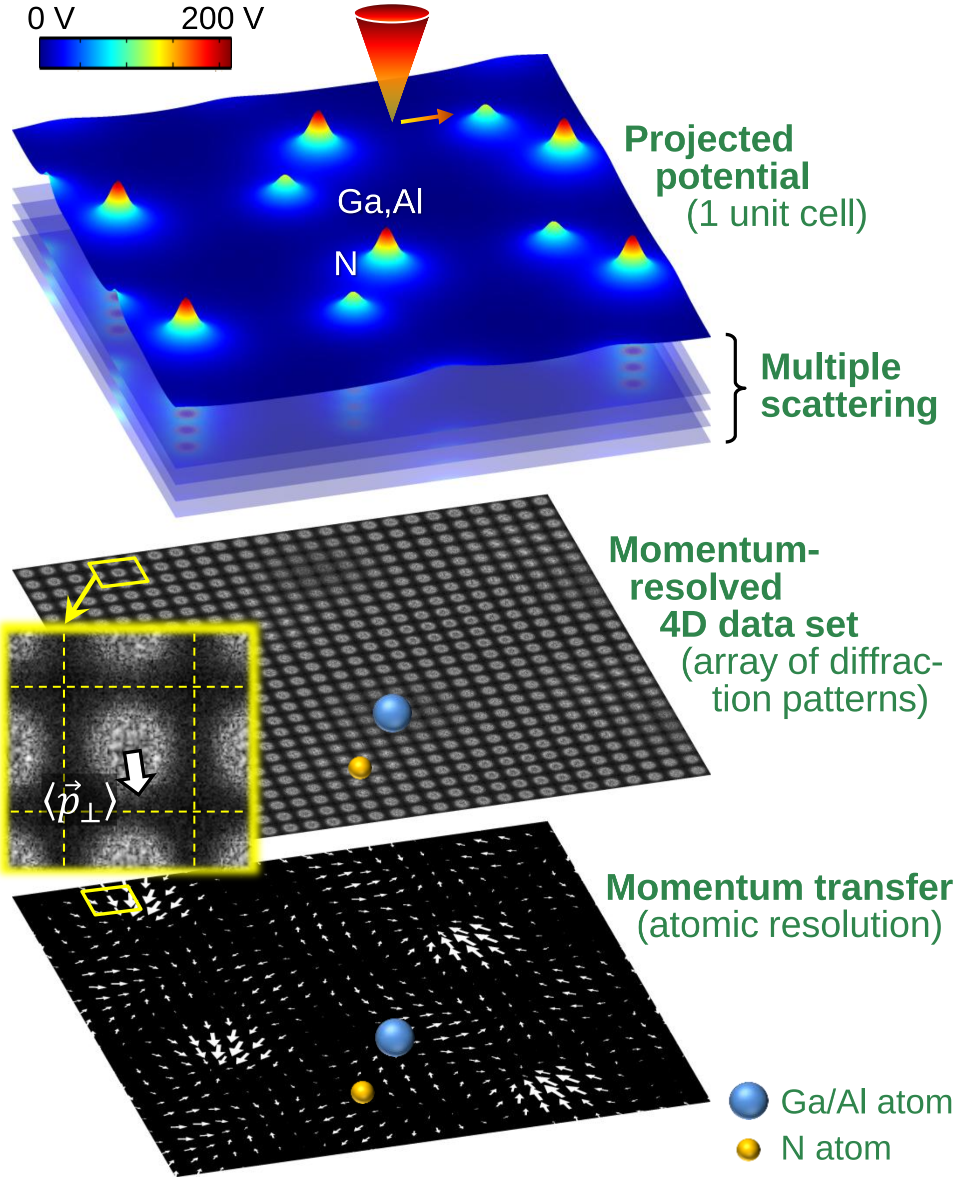

J. Müßner *et al.*, ACS nano **11** (2017) 8758
K. Müller-Caspary et al., PRL **122**, 106102 (2019)

Measurement of polarisation-induced electric fields

AlN/GaN nanodiscs

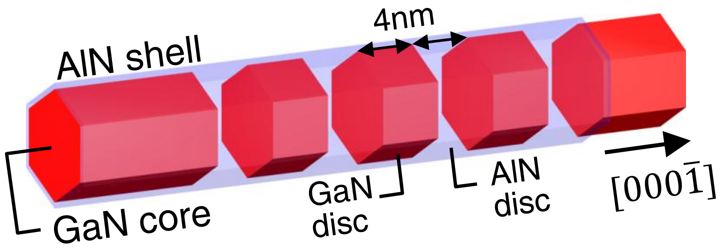

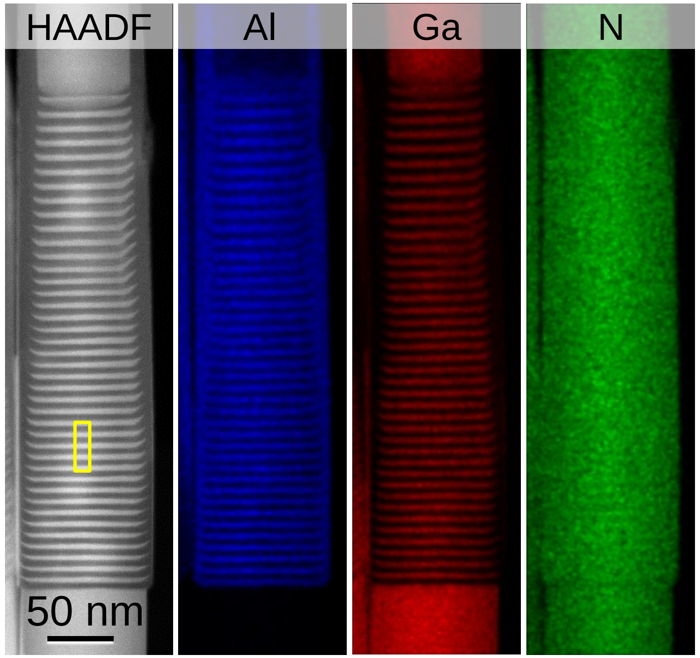

STEM probe

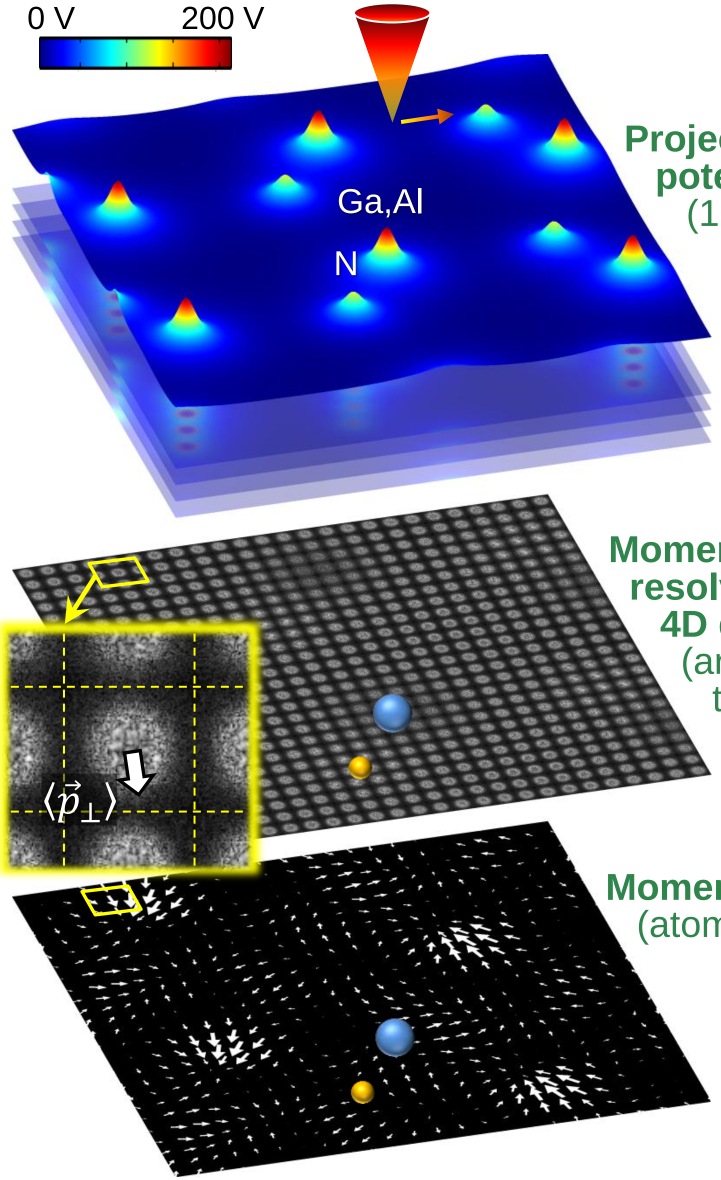

Projected potential (1 unit cell)

Multiple scattering

Momentum-resolved 4D data set (array of diffraction patterns)

Momentum transfer (atomic resolution)

Ga/Al atom

N atom

Background

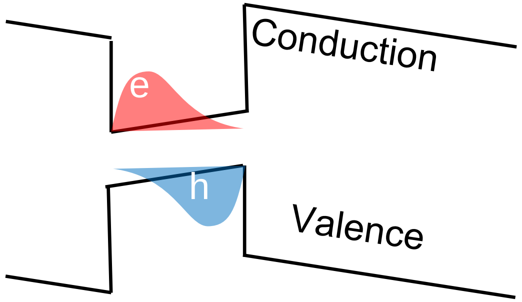

- Polarisation-induced electric fields
- Quantum-confined Stark effect

Coop:
M. Eickhoff
A. Rosenauer
Bremen

J. Müßner *et al.*, ACS nano **11** (2017) 8758
K. Müller-Caspary et al., PRL **122**, 106102 (2019)

Measurement of polarisation-induced electric fields

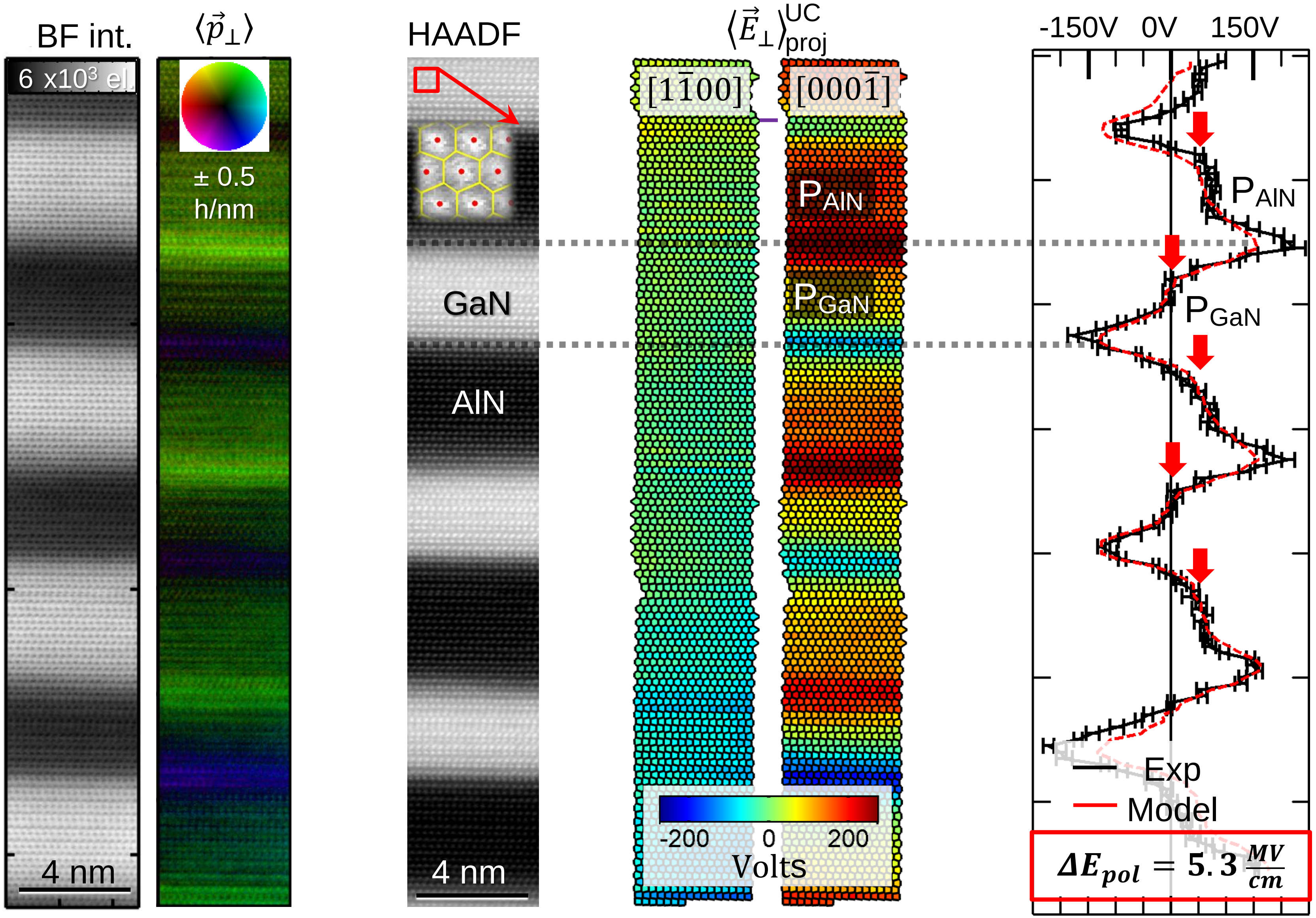

$$\Delta E_{pol} = 5.3\,\frac{MV}{cm}$$

- Polarisation-induced electric fields at unit-cell resolution
- 5 – 6 MV/cm measured

K. Müller-Caspary et al., PRL **122**, 106102 (2019)

Measurement of polarisation-induced electric fields

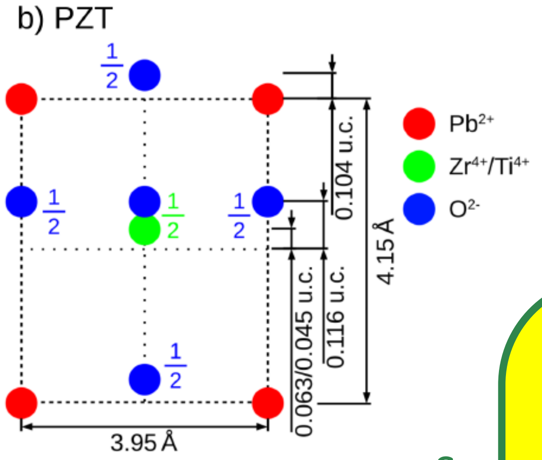

Sys

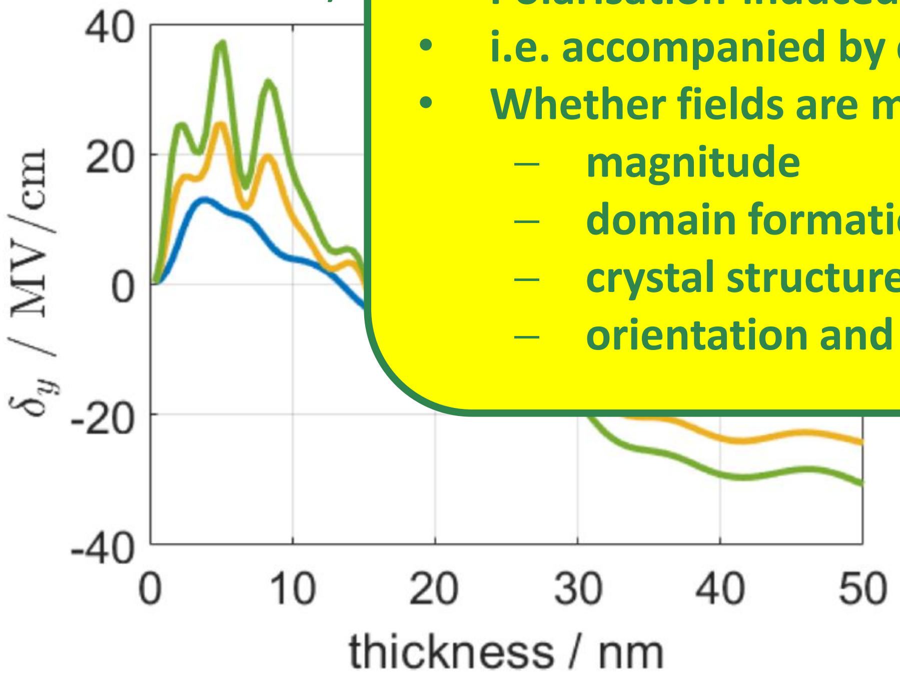

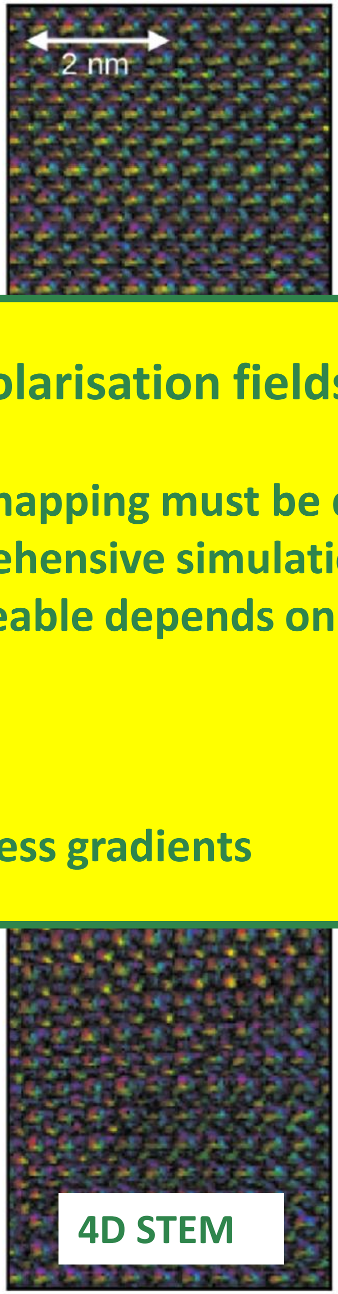

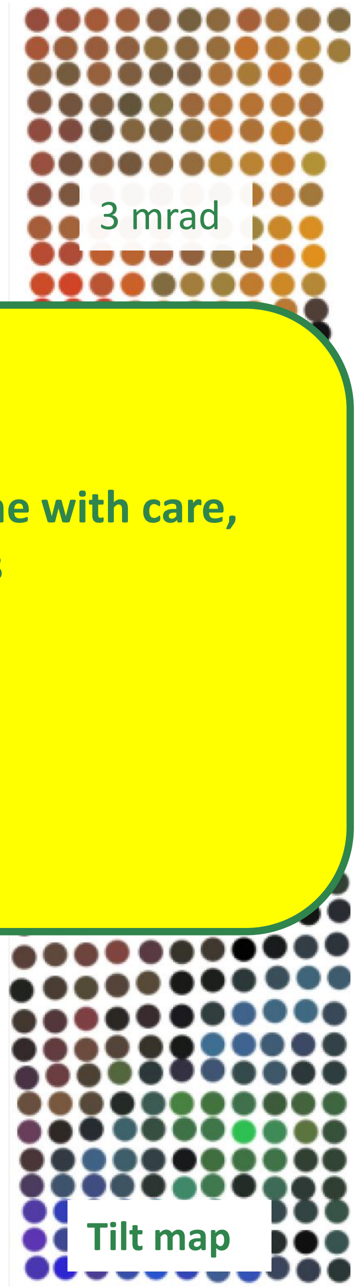

Summary polarisation fields

- Polarisation-induced field mapping must be done with care,
- i.e. accompanied by comprehensive simulations
- Whether fields are measureable depends on
  - magnitude
  - domain formation
  - crystal structure
  - orientation and thickness gradients

Achim Strauch et al, Microscopy and Microanalysis 29, **499** (2023)

Mauricio Cattaneo et al., Ultramicroscopy **267**, 114050 (2024)

Outline

STEM, DPC, COM, phases and momentum transfer

Gradient – based (single & multislice) ptychography

Electric fields in thin specimen: Ehrenfest theorem

Introduction to the inverse problem

Approaches for polarisation-induced field mapping

Minimizing the loss function: a single-scattering example

Practice hint 1 – 5, focus, coherence

Inverse multislice: concept, coherence, TDS, parametrisation

Practice hint 1: Relative rotation between scan and camera

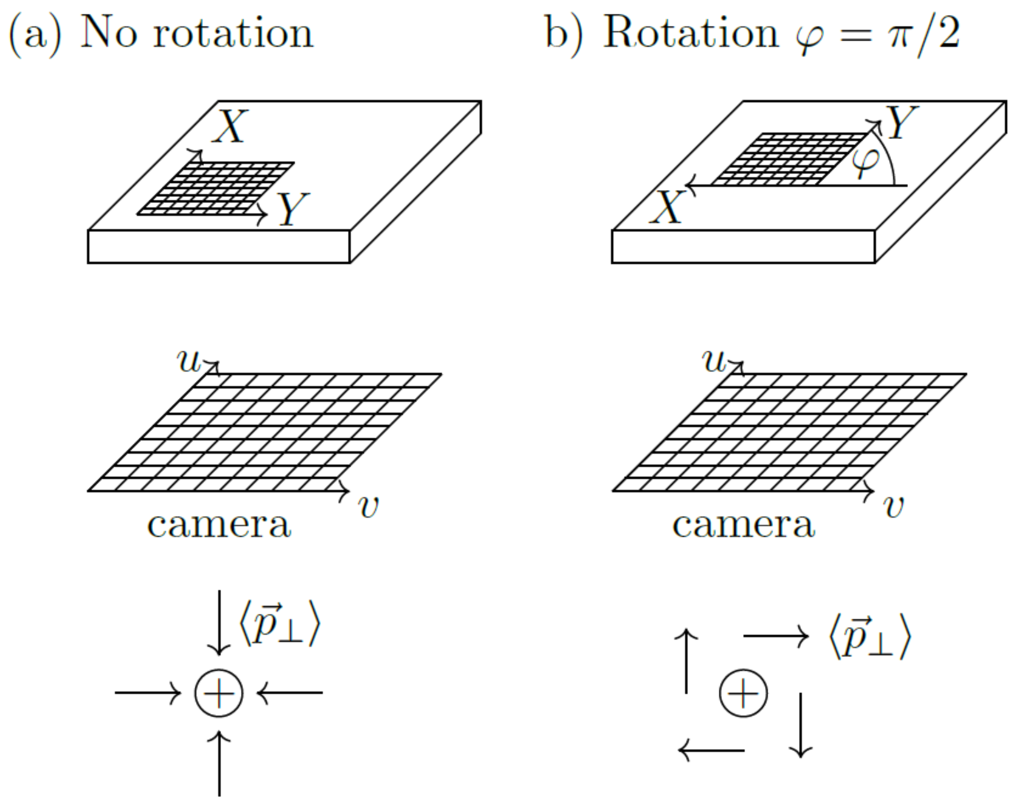

- *Usually*, the momentum vector field is registered in the coordinate system of the **scan.**
- Momentum vectors are *usually* determined in the coordinate system of the **camera.**
- In almost all cases both coordinate systems are **rotated** against each other.
- This can cause a **gradient** field to appear as a **curl** field

→ **Measure correct rotation and**
→ **Correct directions of measured momentum transfers**

Josef Zweck et al., Ultramicroscopy **250**, 113752 (2023)

Practice hint 2: Relative rotation between scan and camera

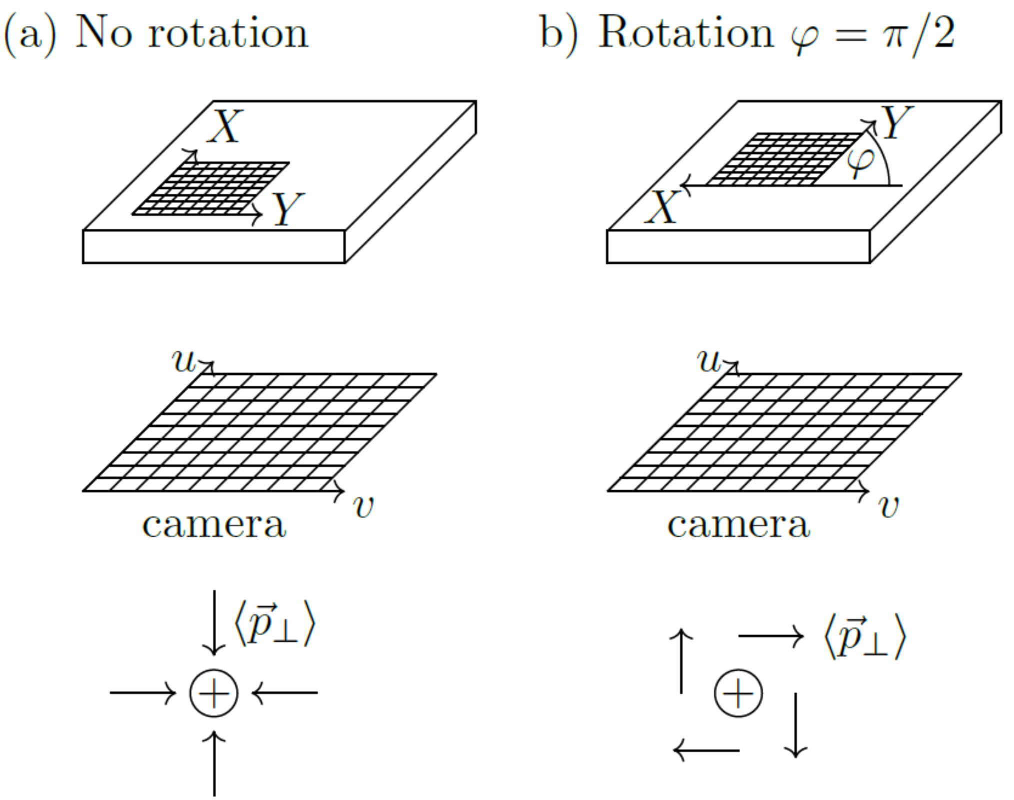

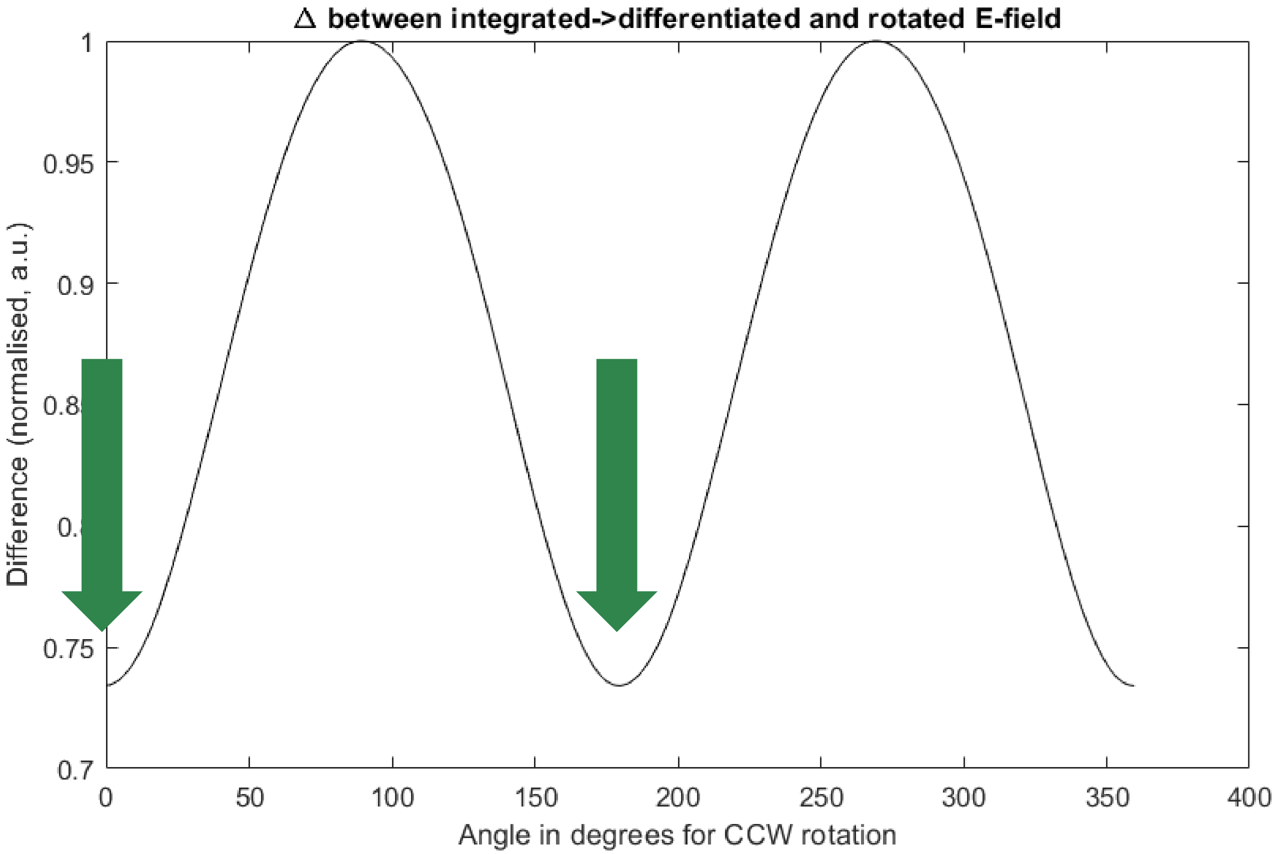

One method: Minimize

$$\vec{E}(\vec{r}) + \vec{\nabla}\left[\mathcal{F}^{-1}\left\{\frac{\vec{q}}{2\pi i q^2}\cdot\mathcal{F}[\vec{E}](\vec{q})\right\}(\vec{r})\right]$$

by varying the rotation of $\vec{E}$

Practice hint 3 & 4: Sampling in diffraction space and cutoff

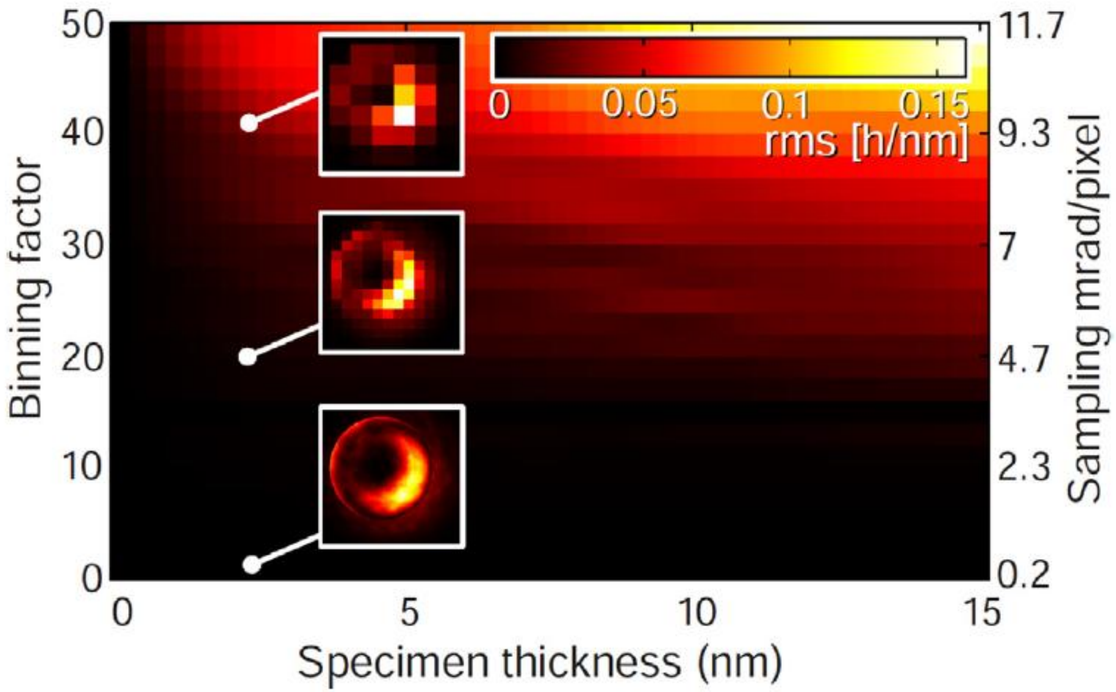

Sampling of the diffraction pattern

- can be **quite low** for pixelated STEM compared to the typical number of camera pixels
- negligible error for a **20 x 20 sampling** in the present study

Müller-Caspary & Krause et al., Ultramicroscopy **178**, 62 (2017)

Practice hint 3 & 4: Sampling in diffraction space and cutoff

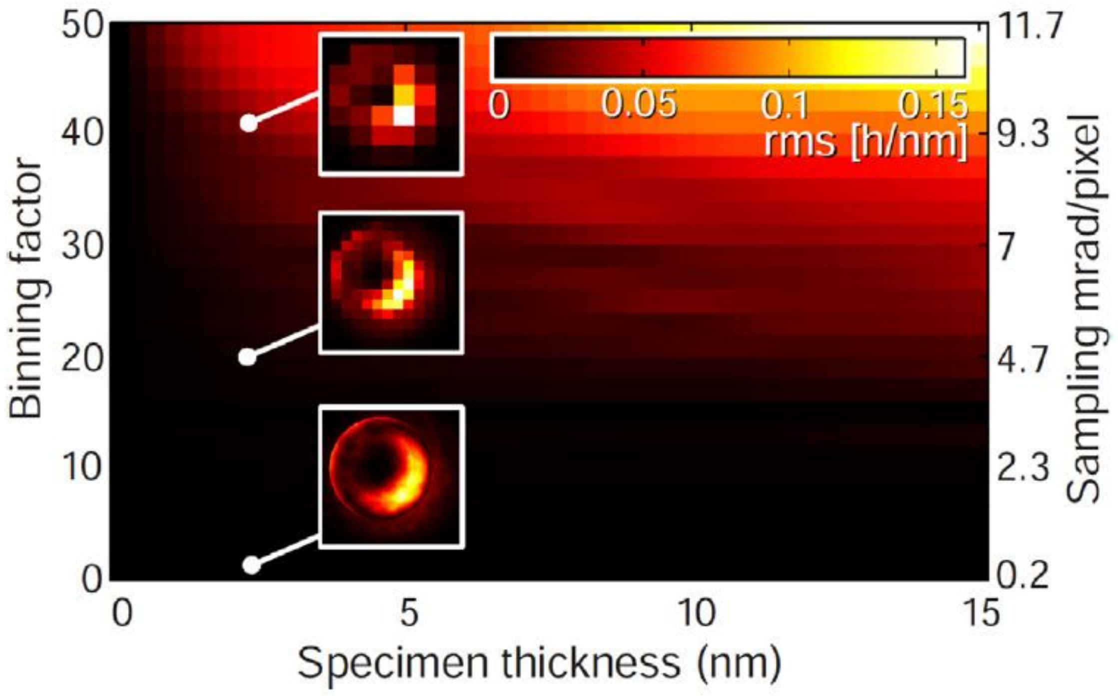

Sampling of the diffraction pattern

- can be **quite low** for pixelated STEM compared to the typical number of camera pixels
- negligible error for a **20 x 20 sampling** in the present study

In the strict sense:

- **Infinite** integration limits for first moment:

$$\langle \vec{p}_\perp(\vec{R}) \rangle = h \iint_{-\infty}^{\infty} \vec{q}_\perp I(\vec{q}_\perp, \vec{R}) \; d^2q$$

- **However:**
  - Detectors are finite
  - Cutoff depends on camera length

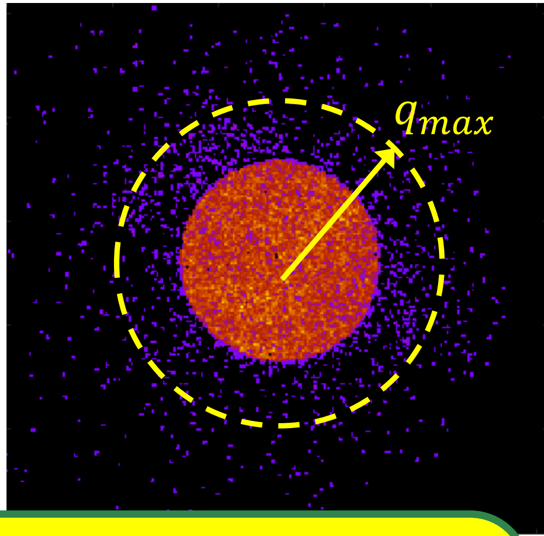

- No **general** rule for robust cutoff
- Should be checked such that $\langle \vec{p}_\perp(\vec{R}) \rangle$ **converges** when increasing q_{max}
- Rule of thumb: q_{max} in the range of **1.2 – 1.5 x Ronchigram radius**

Müller-Caspary & Krause et al., Ultramicroscopy **178**, 62 (2017)

Practice hint 5: Signal-dependent focus

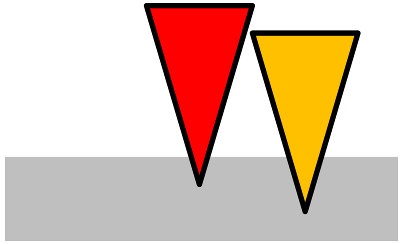

Specimen

Ring detector → fast → 1. Adjust to max. Z-contrast

Fast camera → slow → 2. Acquire $\vec{p}_\perp$-resolved STEM

Result **Result**

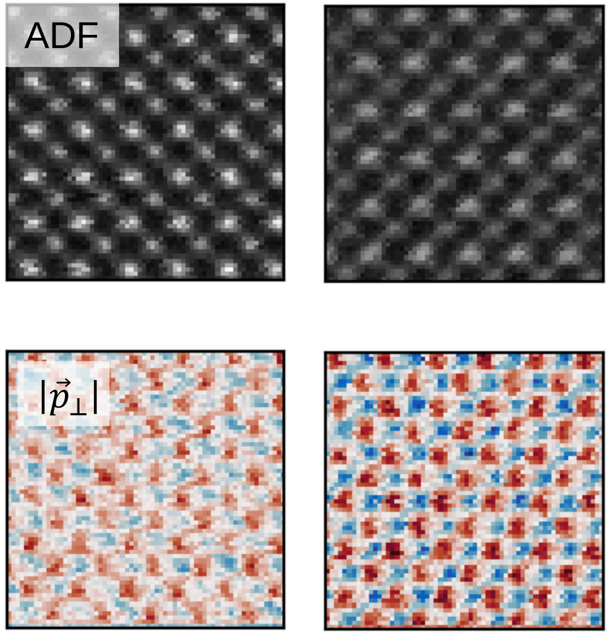

- The optimum focus is signal-dependent
- Angle dependence?
- <u>Consequence:</u> Pixelated detectors are not really universal
- → **Focal series momentum-resolved STEM ...**

Hoel Robert et al., Ultramicroscopy **233**,113425 (2022)

Focal series momentum-resolved STEM

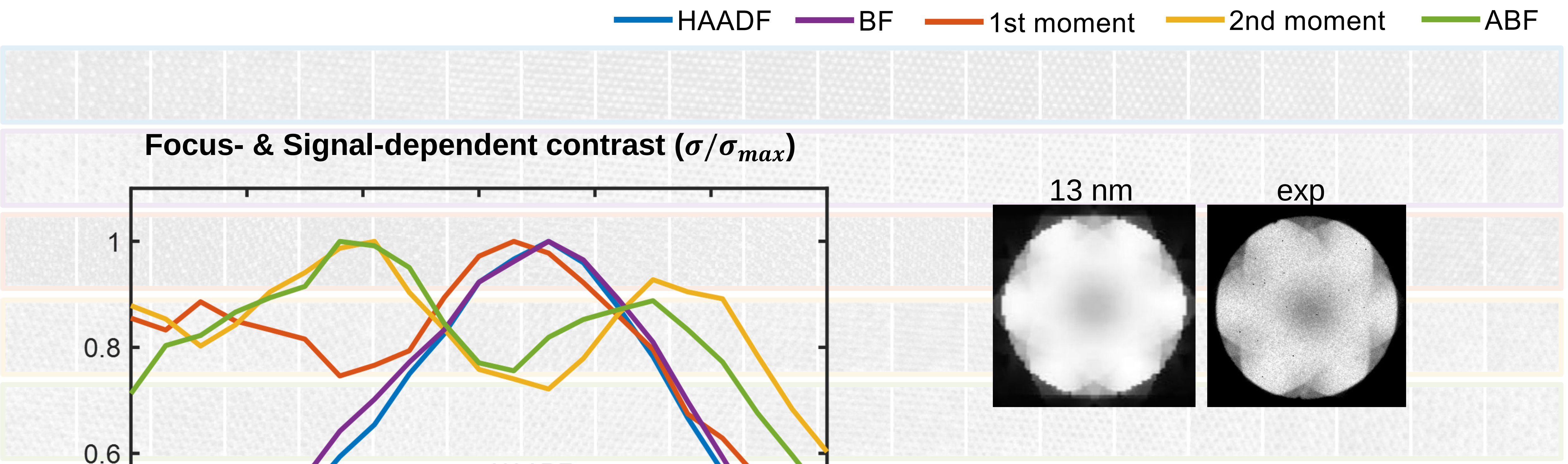

Focus- & Signal-dependent contrast (σ/σ_{max})

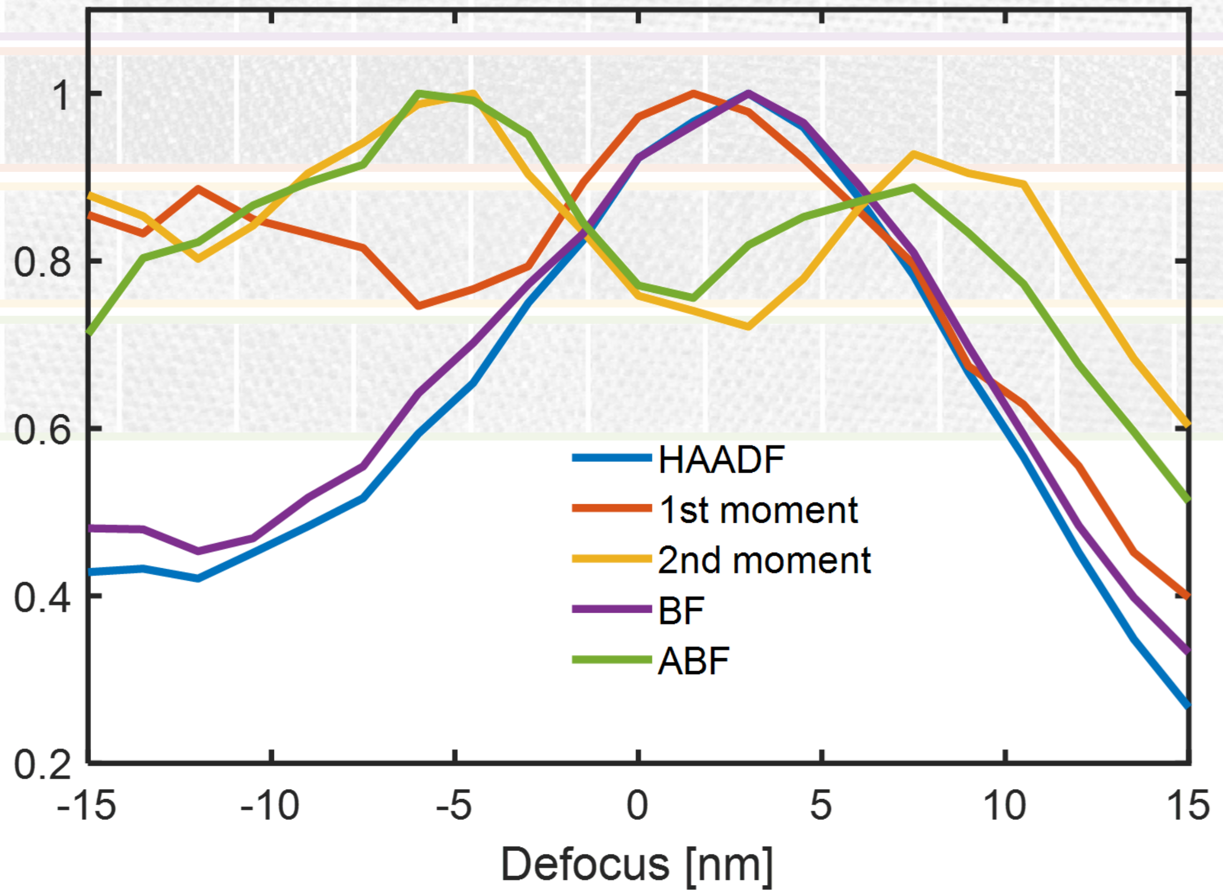

Conclusion

→ Sensitivity to surfaces

→ Momentum-resolved STEM is not fully „universal"...

Hoel Robert et al., Ultramicroscopy **233**,113425 (2022)

Focal series momentum-resolved STEM

And this effect can be much worse even!

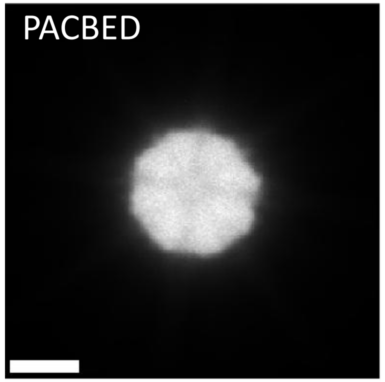

Medipix data, unfiltered

It is recommended to focus on the first moment before recording (not the HAADF), since both signals might have different optimum foci.

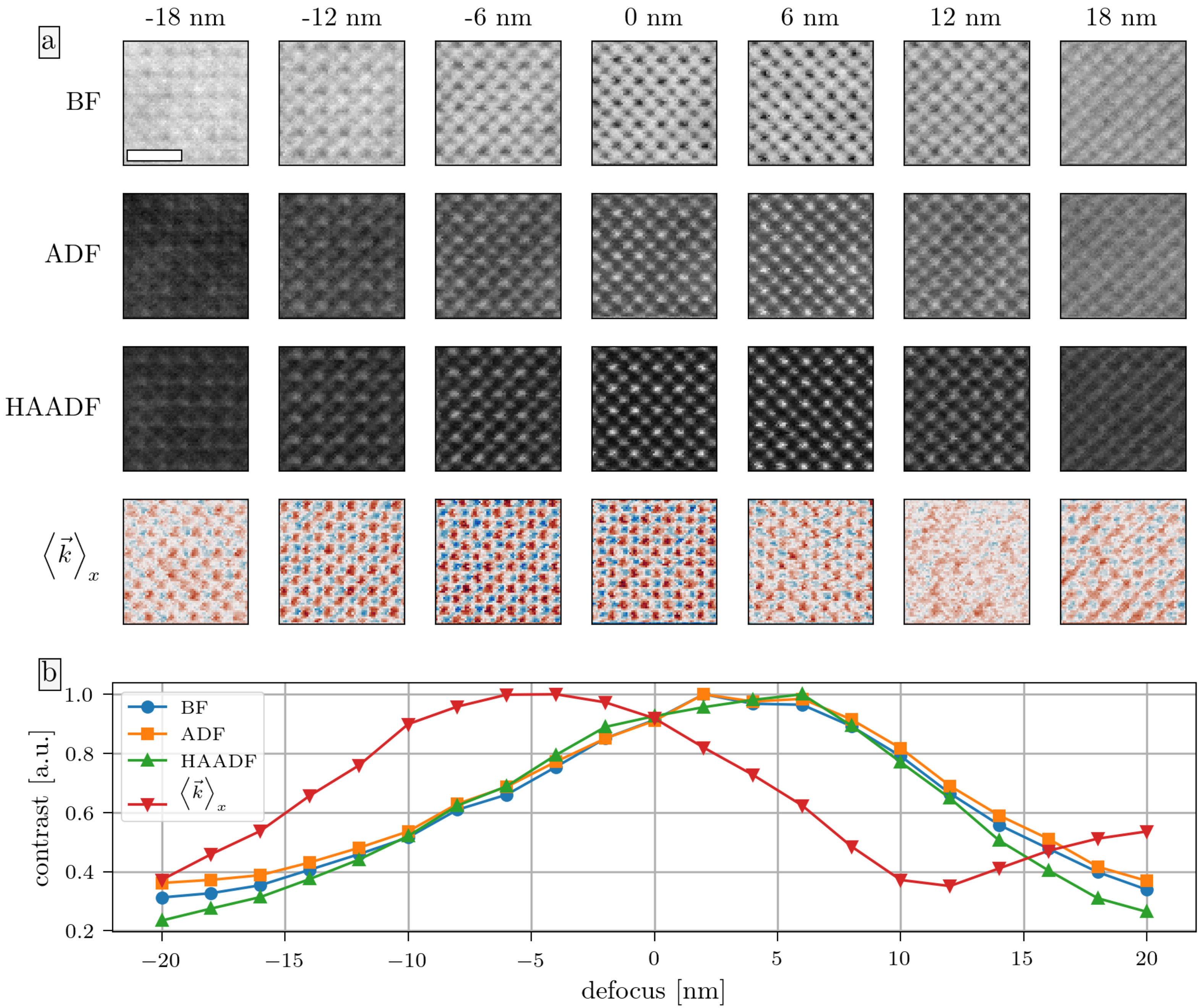

Coherence

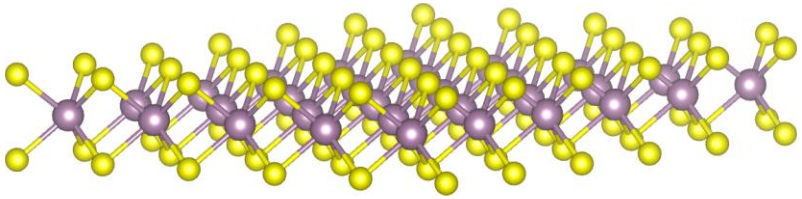

Monolayer MoS_2

$$\langle \vec{p}_\perp \rangle = \frac{-e}{v} \left(\vec{E}_P * I_0 \right) \left(\vec{R} \right)$$

Legend

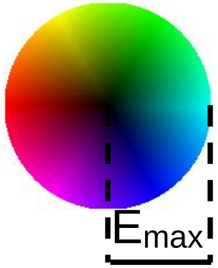

Experiment

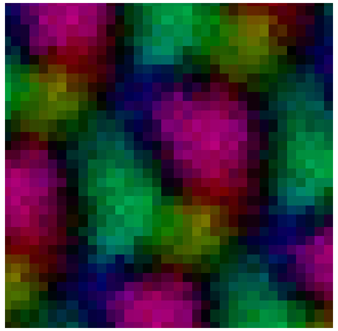

E_{max} = 100V

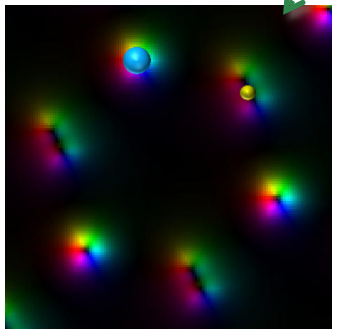

E_{max} = 2.5kV

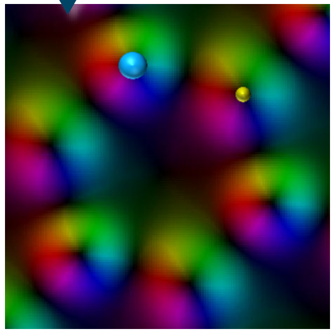

E_{max} = 300V

- Simulation does **not match at all**

Müller-Caspary et al., Physical Review B 98, 121408(R) (2018)

Coherence (spatial)

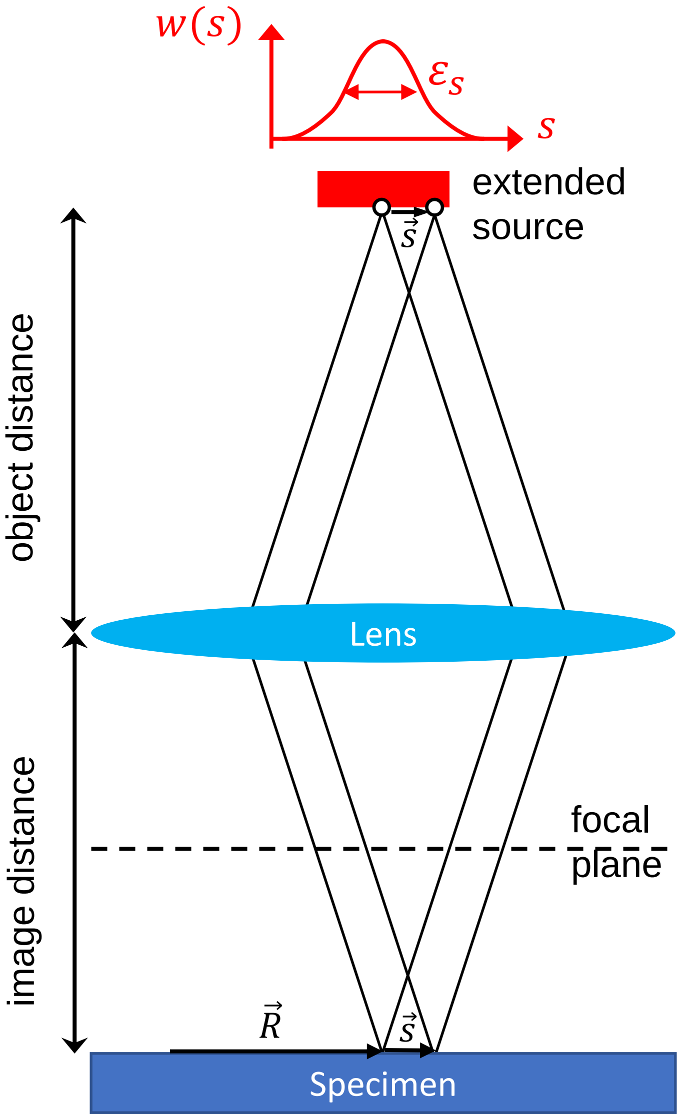

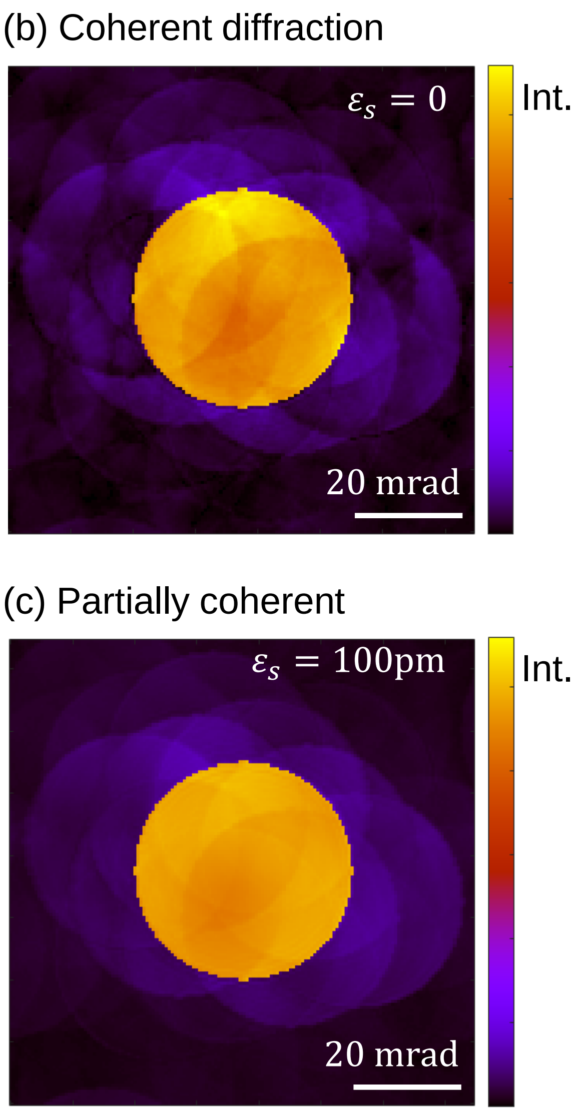

1. Intensity of diffraction pattern formed by source point $\vec{s}$ at nominal scan position $\vec{R}$:

$$\mathrm{w(s)} \cdot \mathrm{K}(\vec{p}, \vec{R} + \vec{s})$$

2. Recorded diffraction pattern: Incoherent summation over all source points:

$$\mathrm{K}(\vec{p}, \vec{R}) = \iint \mathrm{w(s)} \cdot \mathrm{K}(\vec{p}, \vec{R} + \vec{s})\, d^2\vec{s}$$

3. First moment of recorded diffraction pattern:

$$\langle \vec{p}(\vec{R}) \rangle = \iint \iint \mathrm{w(s)} \cdot \mathrm{K}(\vec{p}, \vec{R} + \vec{s})\, \vec{p}\;\, d^2\vec{s} d^2\vec{p}$$

$$= \iint \iint \mathrm{K}(\vec{p}, \vec{R} + \vec{s})\, \vec{p}\;\, d^2\vec{p}\, \mathrm{w(s)}\, d^2\vec{s}$$

$$= \langle \vec{p}(\vec{R} + \vec{s}) \rangle$$

$$= (\boldsymbol{w} \circ \langle \vec{\boldsymbol{p}} \rangle)(\vec{\boldsymbol{R}})$$

4. Measured electric field: $\vec{E}(\vec{R}) = [w \circ (\vec{E}^P \star I_0)](\vec{R})$

5. Measured charge density: $\varrho(\vec{R}) = [w \circ (\varrho^P \star I_0)](\vec{R})$

6. **... same for partial temporal coherence**

Müller-Caspary et al., Physical Review B 98, 121408(R) (2018)

Coherence (spatial)

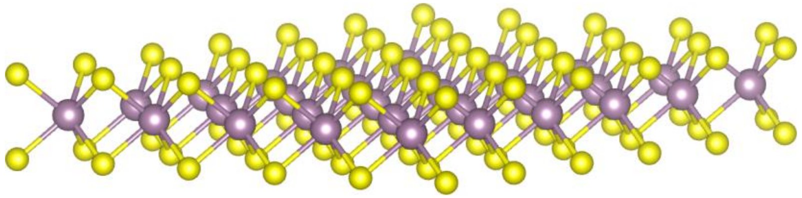

Monolayer MoS_2

$$\langle \vec{p}_\perp \rangle = \frac{-e}{v}\left(\vec{E}_P * I_0\right)\left(\vec{R}\right)$$

$$w \circ \left(\vec{E}_P * I_0\right)$$

Legend

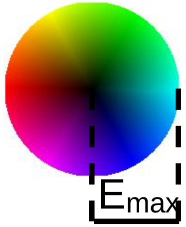

Experiment

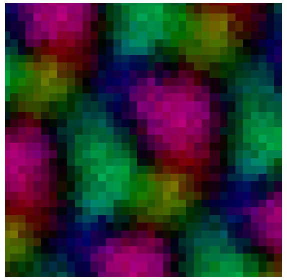

E_{max} = 100V

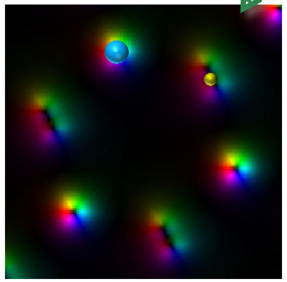

E_{max} = 2.5kV

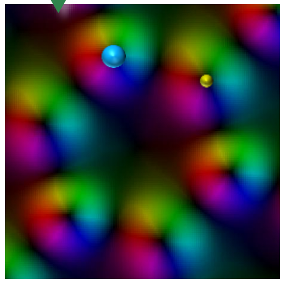

E_{max} = 300V

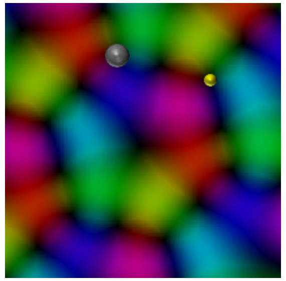

E_{max} = 100V

- Partial coherence has drastic effect on measured field and charge density

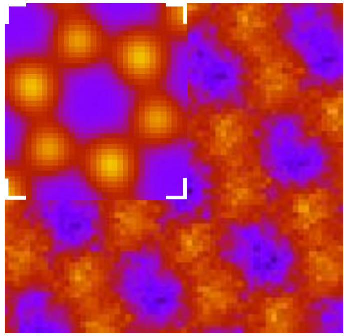

ML average

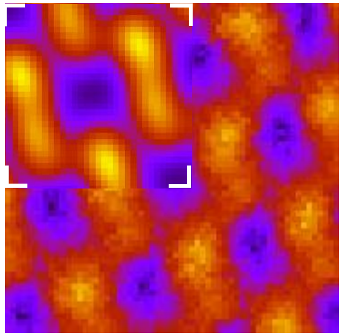

BL average

Müller-Caspary et al., Physical Review B 98, 121408(R) (2018)

Outline

STEM, DPC, COM, phases and momentum transfer

Gradient – based (single & multislice) ptychography

Electric fields in thin specimen: Ehrenfest theorem

Introduction to the inverse problem

Approaches for polarisation-induced field mapping

Minimizing the loss function: a single-scattering example

Practice hint 1 – 5, focus, coherence

Inverse multislice: concept, coherence, TDS, parametrisation

Inversion of multislice

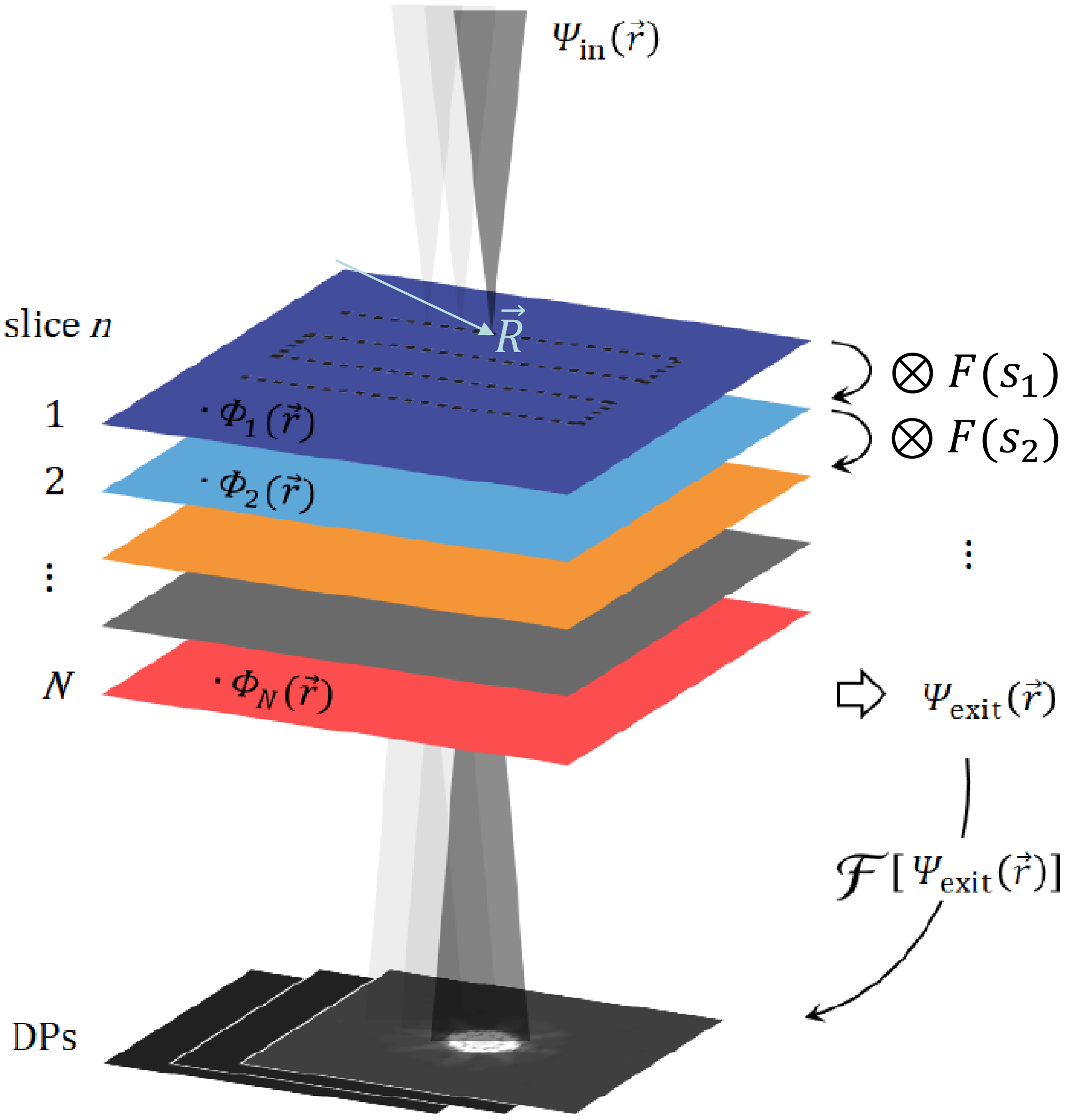

Forward multislice (coherent formulation)

$$\Psi_{\mathrm{exit}}(\vec{r},\vec{R}) = F\left(\tfrac{1}{2}s_N\right) \otimes \Phi_N(\vec{r}) \cdot F\left(\tfrac{1}{2}s_N\right) \otimes F\left(\tfrac{1}{2}s_{N-1}\right) \otimes \Phi_{N-1}(\vec{r}) \cdot F\left(\tfrac{1}{2}s_{N-1}\right) \otimes \cdots \otimes F\left(\tfrac{1}{2}s_1\right) \otimes \Phi_1(\vec{r}) \cdot F\left(\tfrac{1}{2}s_1\right) \otimes \Psi_{\mathrm{in}}(\vec{r},\vec{R})$$

„Phaseless inverse multiple scattering problem“

$$I(\vec{k},\vec{R}) = \left|\mathcal{F}_{\vec{r}}\left[\Psi(\vec{r},\vec{R})_{\mathrm{exit}}\right](\vec{k})\right|^2$$

Diffraction patterns

Inversion of multislice

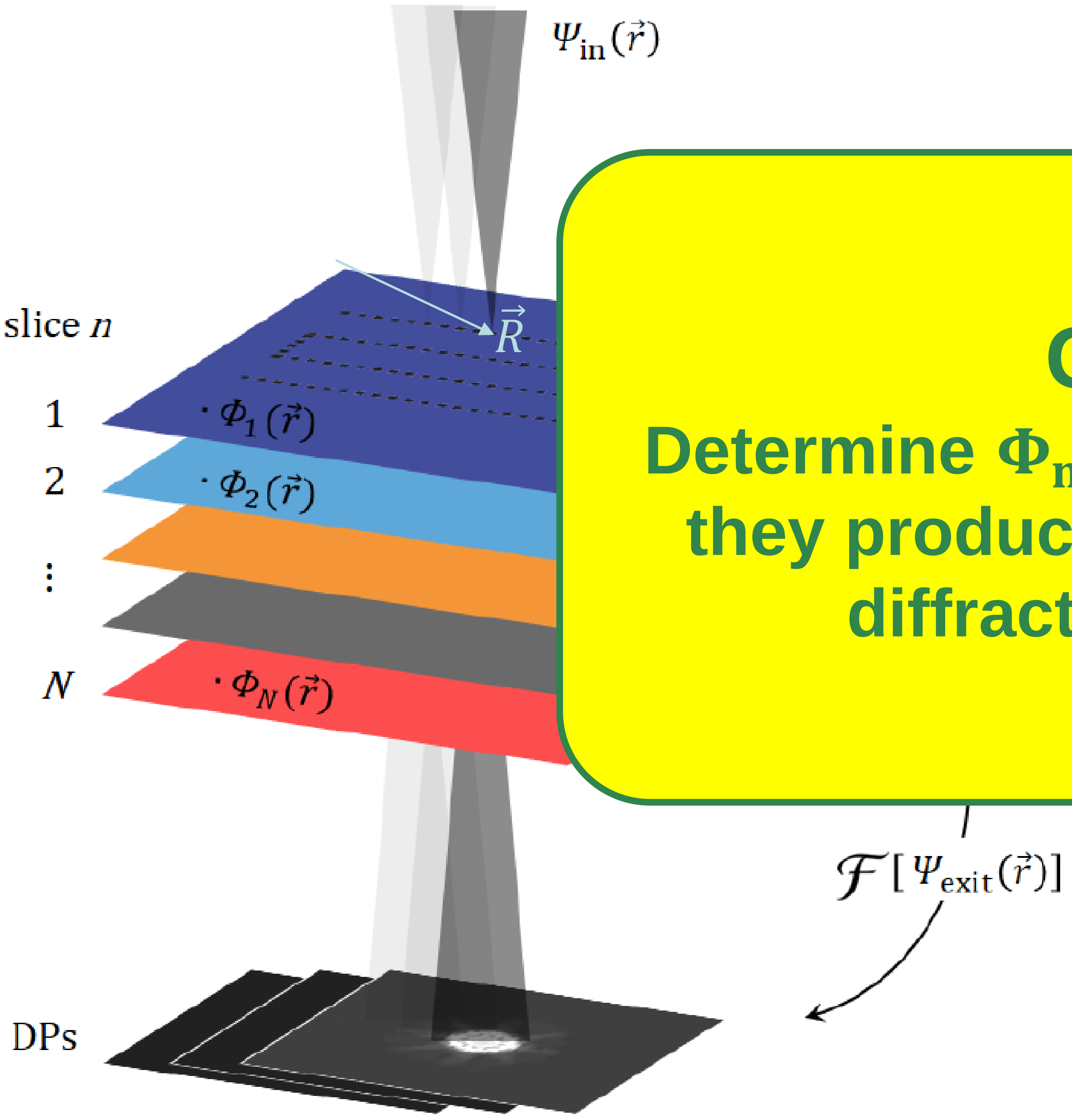

(coherent formulation)

$\otimes\, \Phi_N(\vec{r}) \cdot F\left(\tfrac{1}{2} s_N\right) \otimes$

$_{N-1}(\vec{r}) \cdot F\left(\tfrac{1}{2} s_{N-1}\right) \otimes$

$\cdot\, F\left(\tfrac{1}{2} s_1\right) \otimes \Psi_{\text{in}}(\vec{r}, \vec{R})$

Goal:

Determine Φ_n and Ψ_{in} such that they produce the same set of diffraction patterns

„Phaseless inverse multiple scattering problem“

$$I(\vec{k}, \vec{R}) = \left|\mathcal{F}_{\vec{r}}\left[\Psi(\vec{r}, \vec{R})_{\text{exit}}\right](\vec{k})\right|^2$$

Diffraction patterns

Some literature (incomplete!)

Candes, Emmanuel J. / Li, Xiaodong / Soltanolkotabi, Mahdi
Phase Retrieval via Wirtinger Flow: Theory and Algorithms
2015

IEEE Trans Inf Theory , Vol. 61, No. 4
p. 1985-2007

PRL 109, 245502 (2012) PHYSICAL REVIEW LETTERS week ending 14 DECEMBER 2012

Method for Retrieval of the Three-Dimensional Object Potential by Inversion of Dynamical Electron Scattering

Wouter Van den Broek* and Christoph T. Koch

PHYSICAL REVIEW B 87, 184108 (2013)

General framework for quantitative three-dimensional reconstruction from arbitrary detection geometries in TEM

Wouter Van den Broek* and Christoph T. Koch

Blind ptychography: uniqueness and ambiguities

Albert Fannjiang and Pengwen Chen

Published 26 February 2020 • © 2020 IOP Publishing Ltd

Inverse Problems, Volume 36, Number 4

Citation Albert Fannjiang and Pengwen Chen 2020 *Inverse Problems* **36** 045005

DOI 10.1088/1361-6420/ab6504

Reconstructing state mixtures from diffraction measurements

Pierre Thibault & Andreas Menzel

Nature **494**, 68–71 (2013) | Cite this article

Ultramicroscopy 109 (2009) 1256–1262

Contents lists available at ScienceDirect

Ultramicroscopy

journal homepage: www.elsevier.com/locate/ultramic

An improved ptychographical phase retrieval algorithm for diffractive imaging

Andrew M. Maiden*, John M. Rodenburg

Article | Open access | Published: 12 June 2020

Mixed-state electron ptychography enables sub-angstrom resolution imaging with picometer precision at low dose

Zhen Chen, Michal Odstrcil, Yi Jiang, Yimo Han, Ming-Hui Chiu, Lain-Jong Li & David A. Muller

Nature Communications **11**, Article number: 2994 (2020) | Cite this arti

arXiv > cs > arXiv:1912.01703

Search...

Help | A

Computer Science > Machine Learning

[Submitted on 3 Dec 2019]

PyTorch: An Imperative Style, High-Performance Deep Learning Library

Adam Paszke, Sam Gross, Francisco Massa, Adam Lerer, James Bradbury, Gregory Chanan, Trevor Killeen, Zeming Lin, Natalia Gimelshein, Luca Antiga, Alban Desmaison, Andreas Köpf, Edward Yang, Zach DeVito, Martin Raison, Alykhan Tejani, Sasank Chilamkurthy, Benoit Steiner, Lu Fang, Junjie Bai, Soumith Chintala

IEEE TRANSACTIONS ON COMPUTATIONAL IMAGING, VOL. 8, 2022

Inverse Multislice Ptychography by Layer-Wise Optimisation and Sparse Matrix Decomposition

Arya Bangun, Oleh Melnyk, Benjamin März, Benedikt Diederichs, Alexander Clausen, Dieter Weber, Frank Filbir, and Knut Müller-Caspary

Electron ptychography achieves atomic-resolution limits set by lattice vibrations

Zhen Chen[1*], Yi Jiang[2], Yu-Tsun Shao[1], Megan E. Holtz[3†], Michal Odstrčil[4‡], Manuel Guizar-Sicairos[4], Isabelle Hanke[5], Steffen Ganschow[5], Darrell G. Schlom[3,5,6], David A. Muller[1,6*]

PHYSICAL REVIEW B **110**, 064102 (2024)

Thermal vibrations in the inversion of dynamical electron scattering

Ziria Herdegen,[1] Benedikt Diederichs,[1,2] and Knut Müller-Caspary[1,*]

Exact inversion of partially coherent dynamical electron scattering for picometric structure retrieval

Benedikt Diederichs, Ziria Herdegen, Achim Strauch, Frank Filbir & Knut Müller-Caspary

Nature Communications **15**, Article number: 101 (2024) | Cite this article

Research Article | Vol. 26, No. 3 | 5 Feb 2018 | OPTICS EXPRESS 3108

Optics EXPRESS

Iterative least-squares solver for generalized maximum-likelihood ptychography

Michal Odstrčil,[1,*] Andreas Menzel,[1] and Manuel Guizar-Sicairos[1,2]

ELSEVIER

Ultramicroscopy

Volume 109, Issue 4, March 2009, Pages 338-343

ultramicroscopy

Probe retrieval in ptychographic coherent diffractive imaging

Pierre Thibault[a], Martin Dierolf[a b], Oliver Bunk[a], Andreas Menzel[a], Franz Pfeiffer[a b]

Research Article | Vol. 28, No. 19 / 14 September 2020 / *Optics Express* 28306

Optics EXPRESS

Overcoming information reduced data and experimentally uncertain parameters in ptychography with regularized optimization

Marcel Schloz,[1] Thomas Christopher Pekin,[1] Zhen Chen,[2] Wouter Van den Broek,[1,*] David Anthony Muller,[2,3] and Christoph Tobias Koch[1]

Appl Cryst JAC JOURNAL OF APPLIED CRYSTALLOGRAPHY

ISSN 1600-5767

PtychoShelves, a versatile high-level framework for high-performance analysis of ptychographic data[1]

Klaus Wakonig,[a,b*] Hans-Christian Stadler,[a] Michal Odstrčil,[a‡] Esther H. R. Tsai,[a§] Ana Diaz,[a] Mirko Holler,[a] Ivan Usov,[a] Jörg Raabe,[a] Andreas Menzel[a] and Manuel Guizar-Sicairos[a*]

Revision: Data fitting

Set of measurements

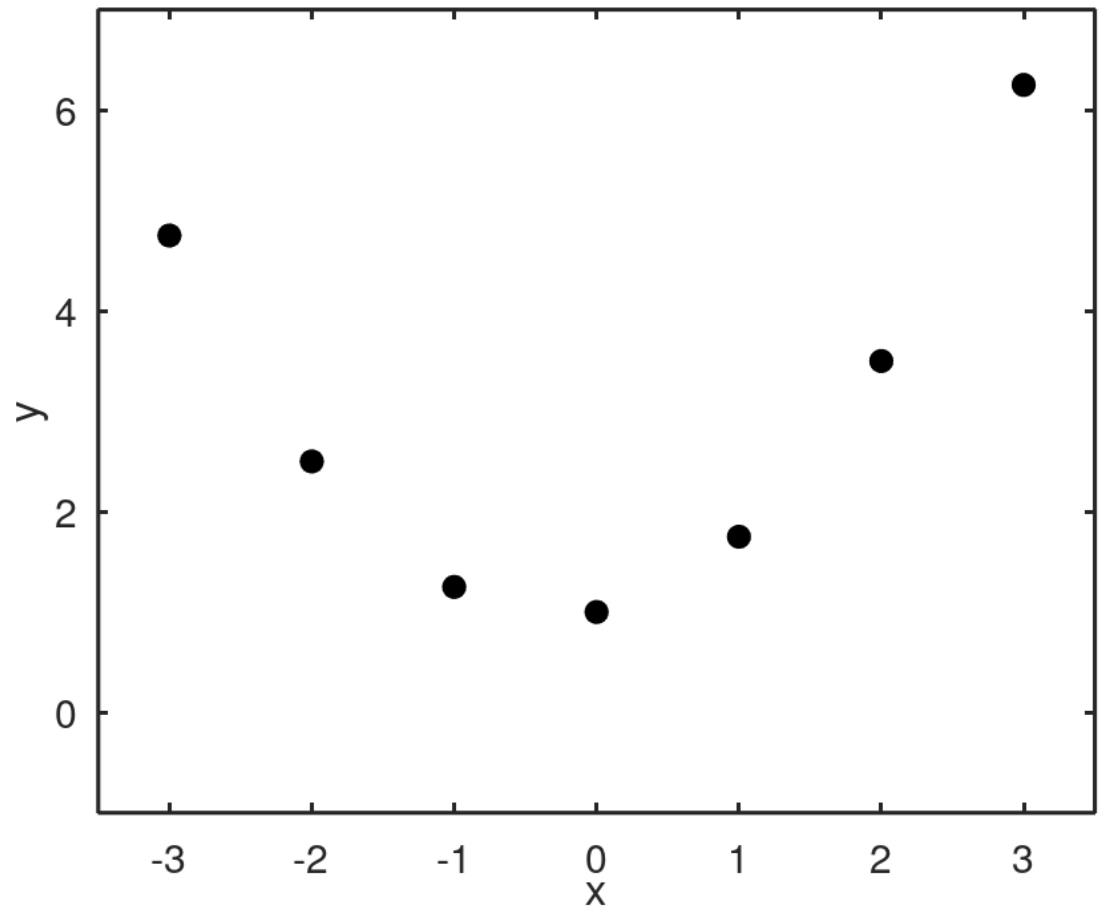

- We strive to express the experimental data (y_i, x_i) by a **model** $\boldsymbol{Y}(x)$
- Let us use a second order polynomial
$$Y(x_i) = ax_i^2 + bx_i + c$$
- Let the parameters $\{a, b, c\}$ be fully unknown

x_i	y_i
-3	4.75
-2	2.5
-1	1.25
0	1
1	1.75
2	3.5
3	6.25

Revision: Data fitting

Set of measurements

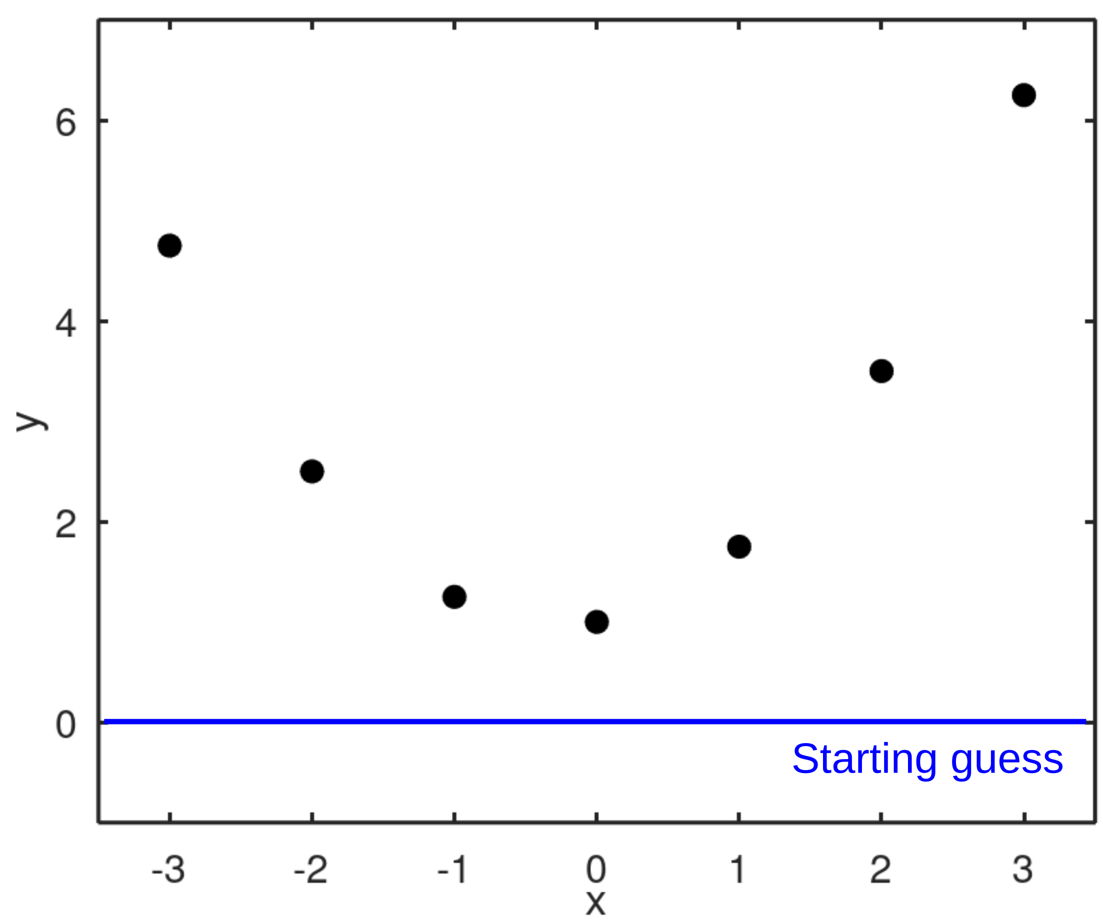

x_i	y_i
-3	4.75
-2	2.5
-1	1.25
0	1
1	1.75
2	3.5
3	6.25

- We strive to express the experimental data (y_i, x_i) by a **model** $\boldsymbol{Y}(x)$
- Let us use a second order polynomial
$$Y(x_i) = ax_i^2 + bx_i + c$$
- Let the parameters $\{a, b, c\}$ be fully unknown
- Concept:
  1. Start with a guess $\{a^{(0)}, b^{(0)}, c^{(0)}\}$
  2. Quantify the consistency with the experiment
  3. Update the parameters $\{a, b, c\}$
- Define **„Loss function“**, e.g. the $\boldsymbol{\mathcal{L}_2}$ **loss** as
$$\mathcal{L}_2 = \sum_{i=1}^{N} [Y(x_i) - y_i]^2 = \sum_{i=1}^{N} \left[ax_i^2 + bx_i + c - y_i\right]^2$$
- Example at starting condition with $a^{(0)} = b^{(0)} = c^{(0)} = 0$:
$$\mathcal{L}_2 = \sum_{i=1}^{7} y_i^2 = 85.75$$

Revision: Data fitting

x_i	y_i
-3	4.75
-2	2.5
-1	1.25
0	1
1	1.75
2	3.5
3	6.25

Set of measurements

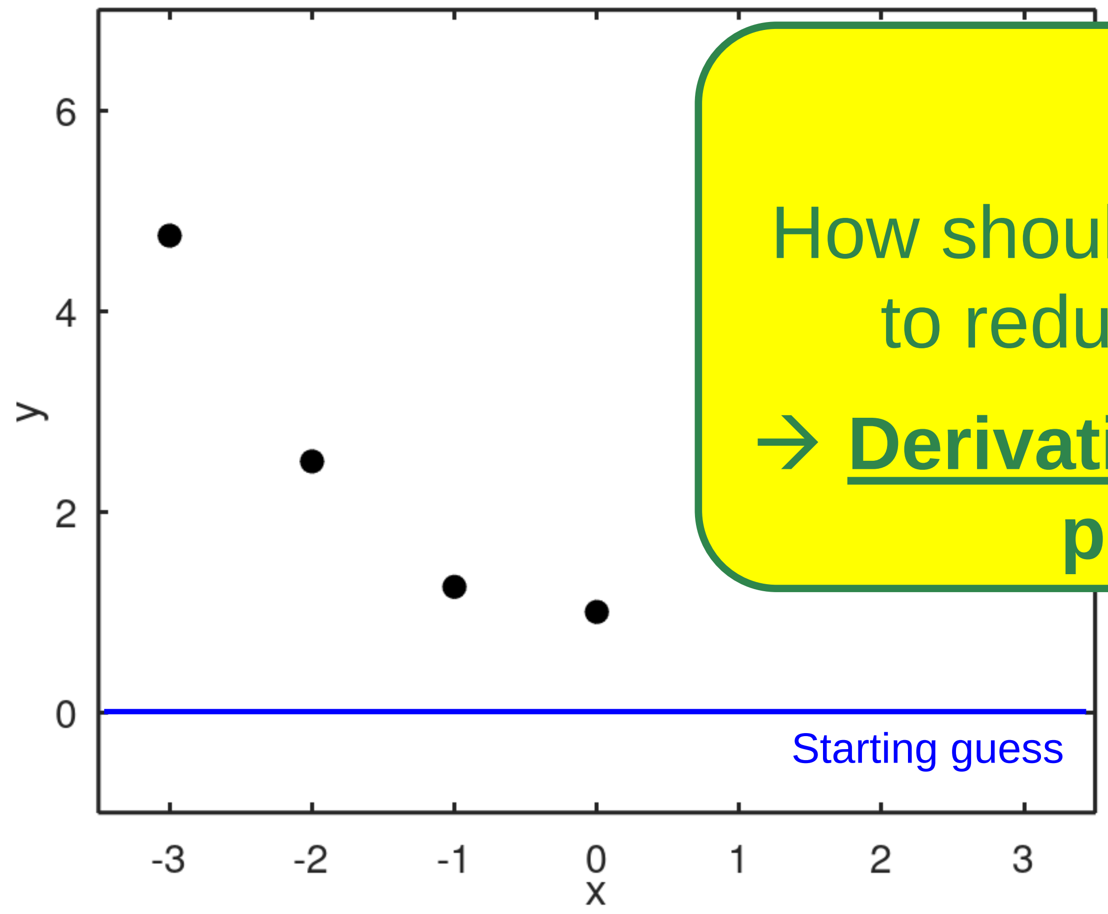

- We strive to express the experimental data (y_i, x_i) by a **model** $\boldsymbol{Y}(x)$
- Let us use a second order polynomial

Question

How should a,b,c be updated so as to reduce (change) the loss?

→ **<u>Derivatives</u> of loss w.r.t. all free parameters needed**

- Define **„Loss function“**, e.g. the **$\mathcal{L}_2$ loss** as

$$\mathcal{L}_2 = \sum_{i=1}^{N} [Y(x_i) - y_i]^2 = \sum_{i=1}^{N} \left[ax_i^2 + bx_i + c - y_i\right]^2$$

- Example at starting condition with $a^{(0)} = b^{(0)} = c^{(0)} = 0$:

$$\mathcal{L}_2 = \sum_{i=1}^{7} y_i^2 = 85.75$$

Revision: Data fitting

$$\mathcal{L}_2 = \sum_{i=1}^{N} \left[a x_i^2 + b x_i + c - y_i\right]^2$$

Set of measurements

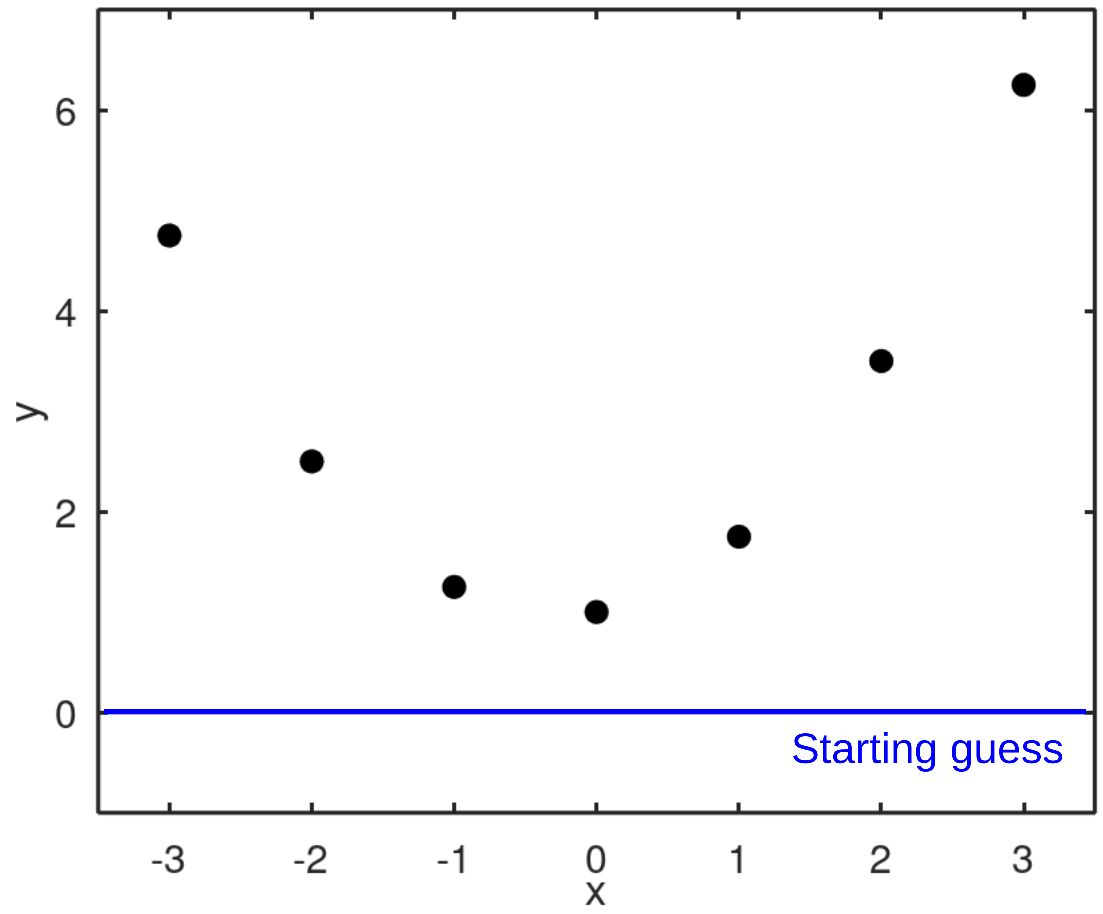

- Change of loss in dependence of each parameter a, b, c:

$$\frac{\partial \mathcal{L}_2}{\partial a} = \sum_{i=1}^{N} 2\left(a x_i^2 + b x_i + c - y_i\right) \cdot x_i^2$$

$$\frac{\partial \mathcal{L}_2}{\partial b} = \sum_{i=1}^{N} 2\left(a x_i^2 + b x_i + c - y_i\right) \cdot x_i$$

$$\frac{\partial \mathcal{L}_2}{\partial c} = \sum_{i=1}^{N} 2\left(a x_i^2 + b x_i + c - y_i\right)$$

- Update a, b, c in next epoch such that loss **gets smaller:**

$$a^{(j+1)} = a^{(j)} - \beta_a \cdot \frac{\partial \mathcal{L}_2}{\partial a}$$

$$b^{(j+1)} = b^{(j)} - \beta_b \cdot \frac{\partial \mathcal{L}_2}{\partial b}$$

$$c^{(j+1)} = c^{(j)} - \beta_c \cdot \frac{\partial \mathcal{L}_2}{\partial c}$$

„Learning rate“

Revision: Data fitting

$\beta_a = 0.0012, \beta_b = \frac{\beta_a}{10}, \beta_c = \frac{\beta_a}{100}$

20 epochs

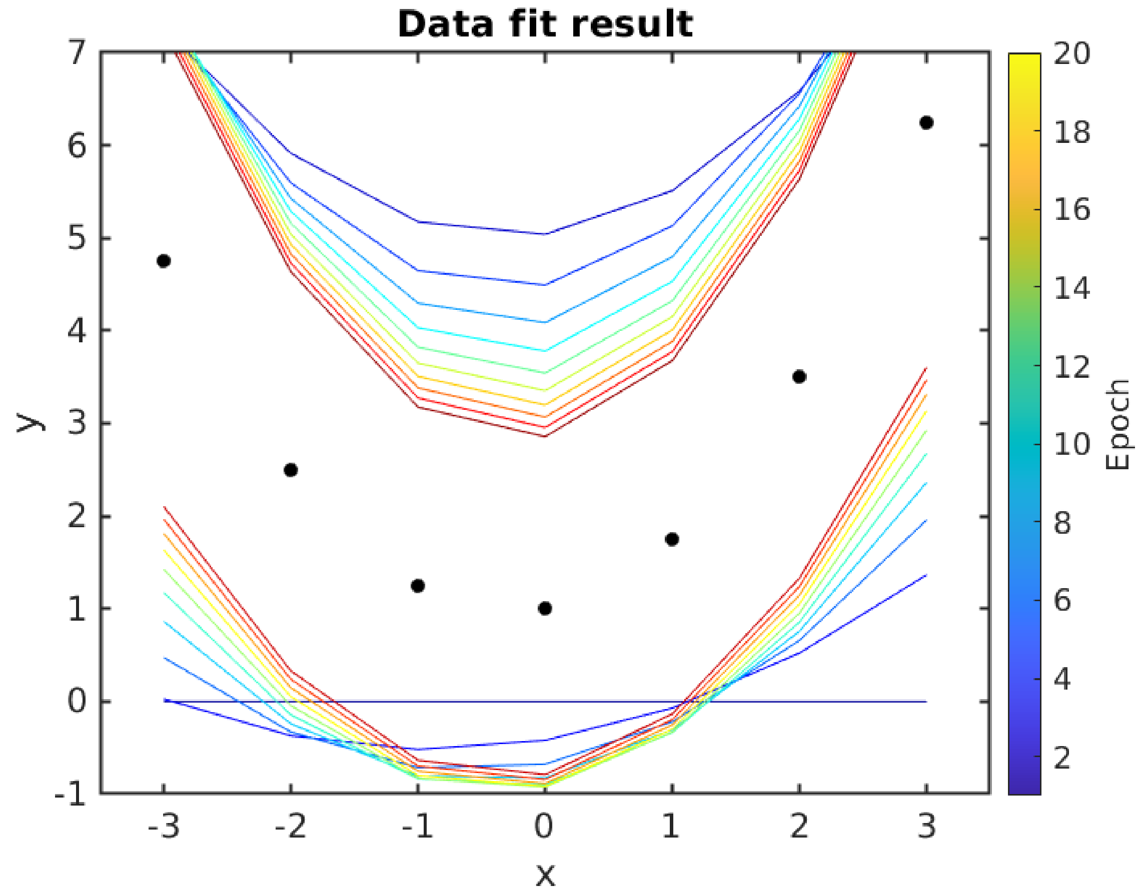

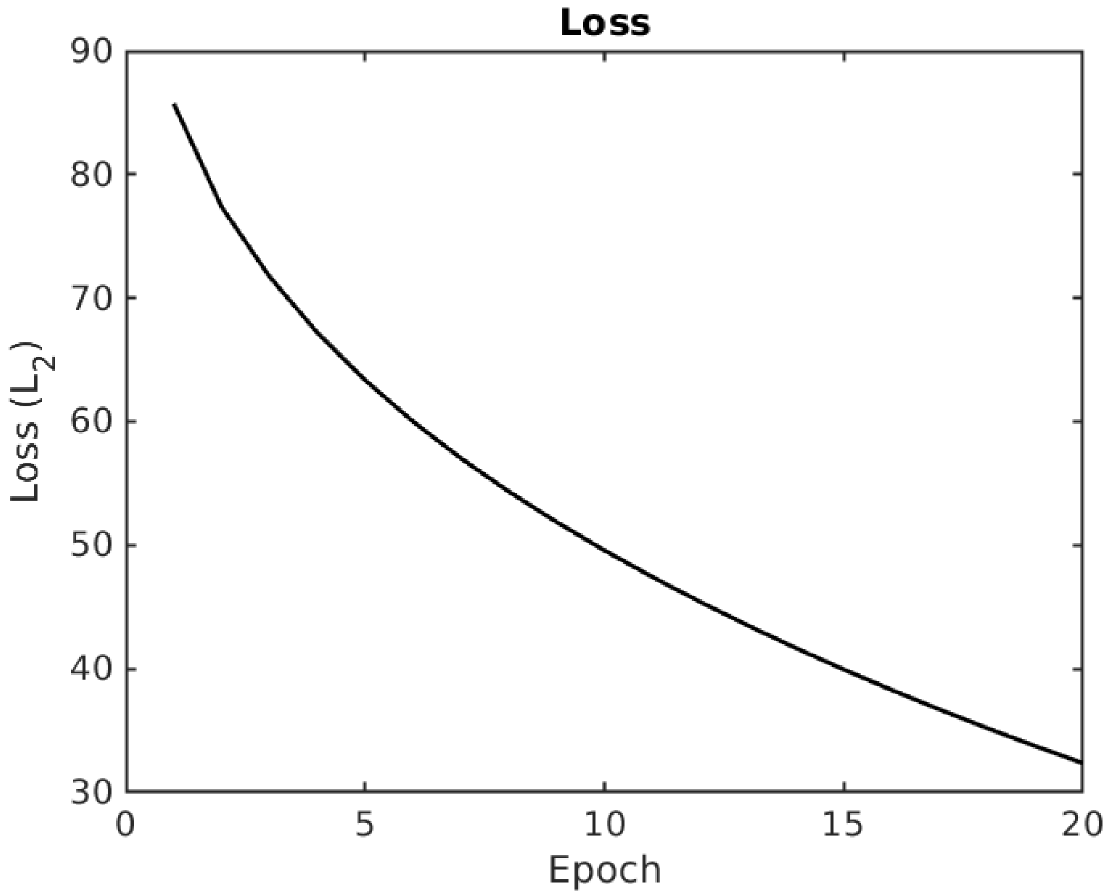

Oscillating solutions …

	$a^{(20)}$	$b^{(20)}$	$c^{(20)}$
Fit	0.4122	0.2500	−0.7319
Ground truth	0.5	0.25	1

Revision: Data fitting

$\beta_a = 0.0011, \beta_b = \frac{\beta_a}{10}, \beta_c = \frac{\beta_a}{100}$

20 epochs

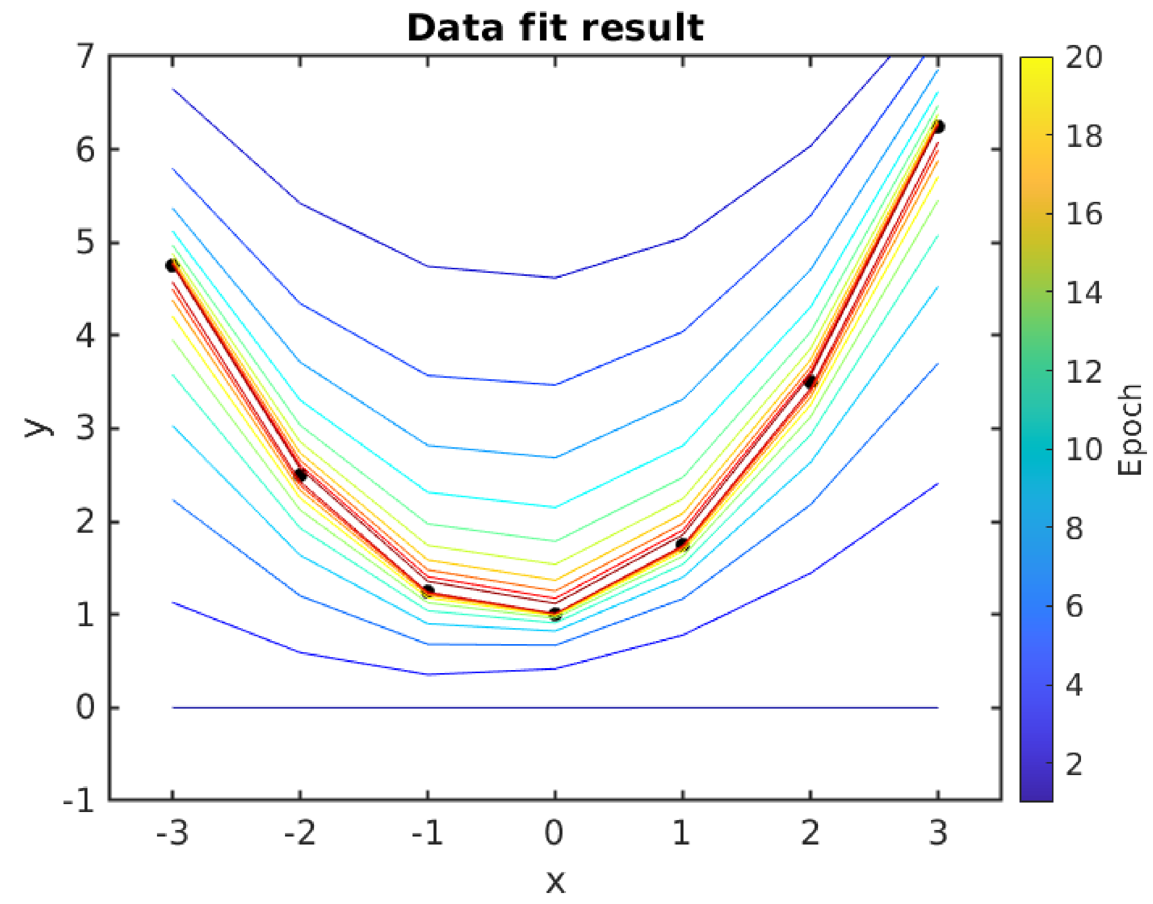

Much better fit

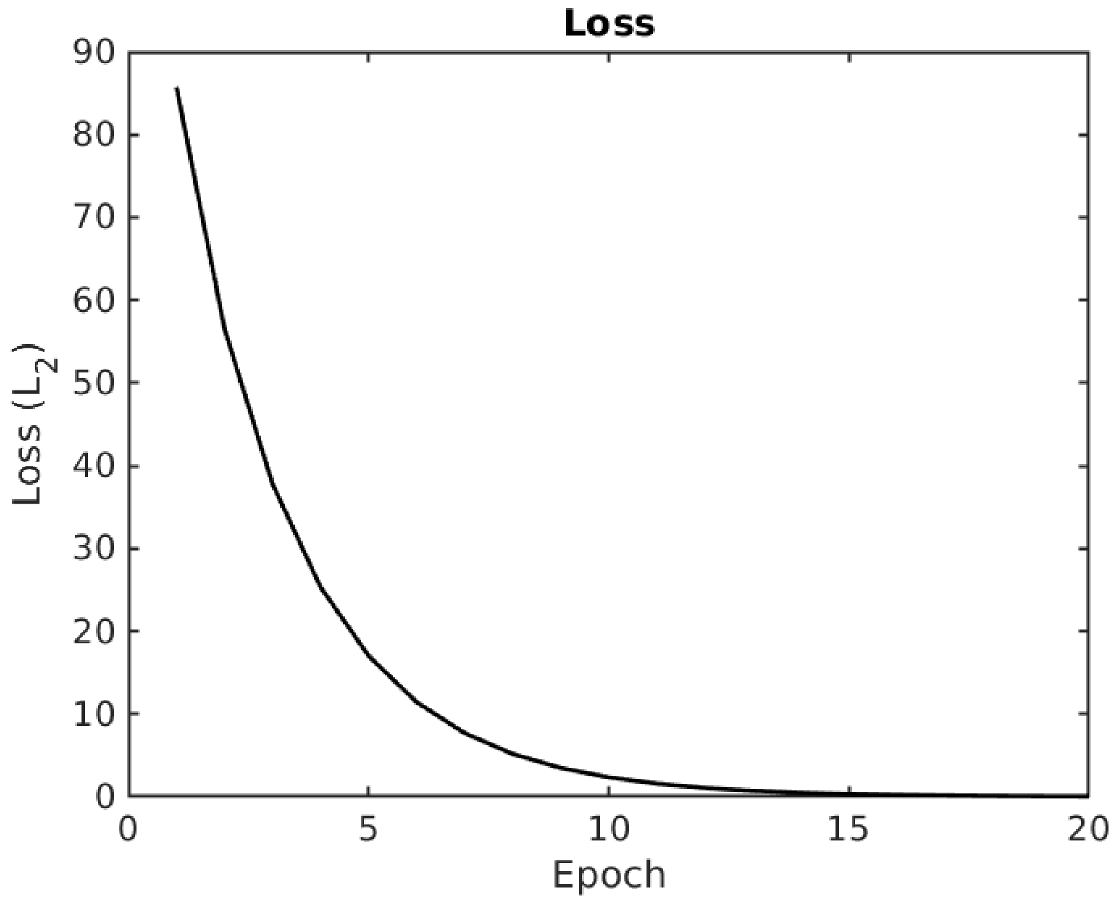

Loss asymptote

	$\boldsymbol{a}^{(20)}$	$\boldsymbol{b}^{(20)}$	$\boldsymbol{c}^{(20)}$
Fit	0.4855	0.2500	1.0115
Ground truth	0.5	0.25	1

Revision: Data fitting

$\beta_a = 0.001, \beta_b = \frac{\beta_a}{10}, \beta_c = \frac{\beta_a}{100}$

50 epochs

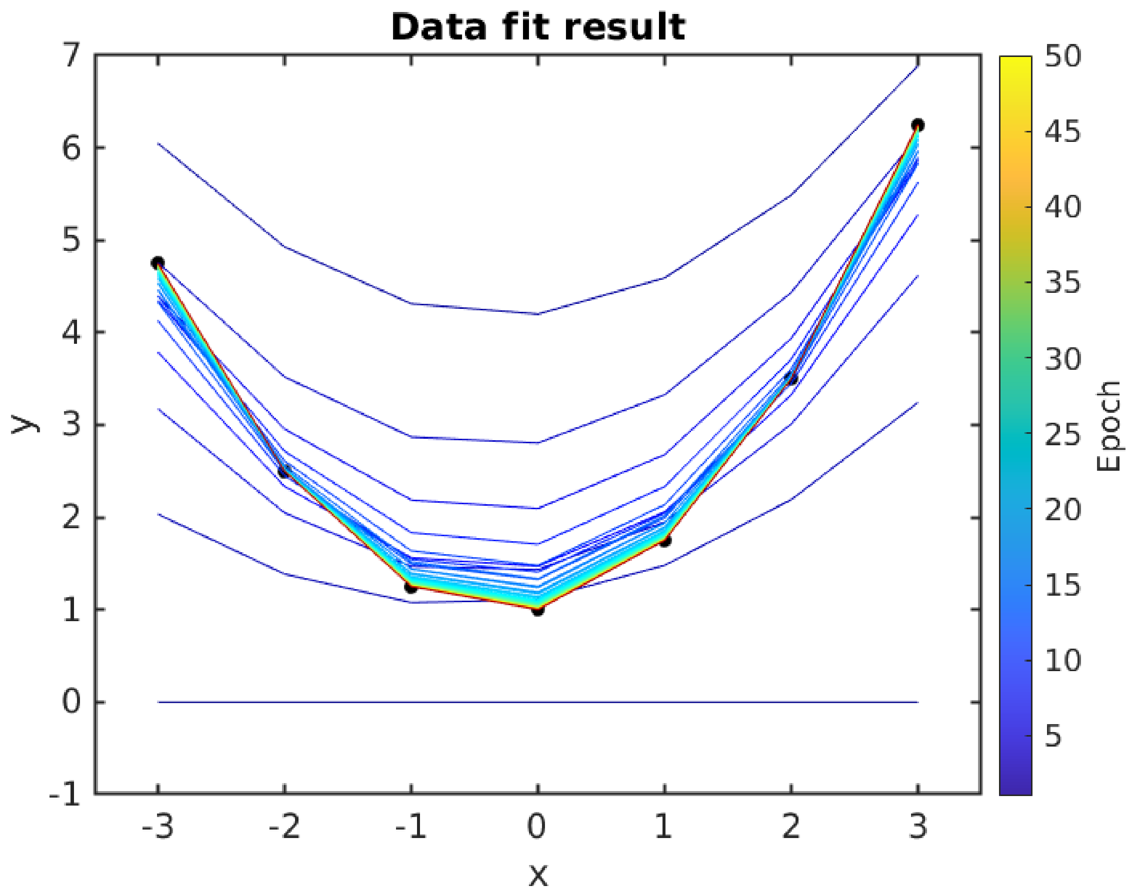

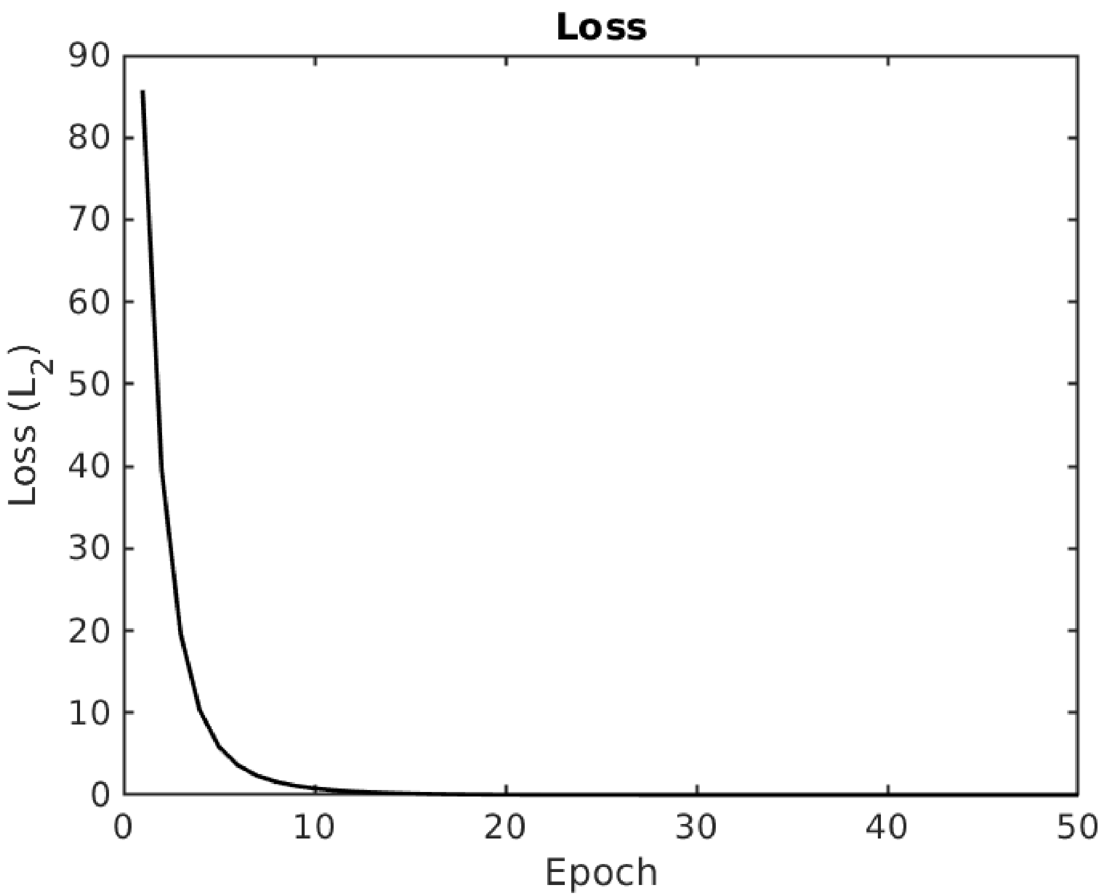

Much better fit

Loss asymptote

	$\boldsymbol{a}^{(50)}$	$\boldsymbol{b}^{(50)}$	$\boldsymbol{c}^{(50)}$
Fit	0.4998	0.2500	1.0008
Ground truth	0.5	0.25	1

Outline

STEM, DPC, COM, phases and momentum transfer

Gradient – based (single & multislice) ptychography

Electric fields in thin specimen: Ehrenfest theorem

Introduction to the inverse problem

Approaches for polarisation-induced field mapping

Minimizing the loss function: a single-scattering example

Practice hint 1 – 5, focus, coherence

Inverse multislice: concept, coherence, TDS, parametrisation

Single-scattering Ptychography

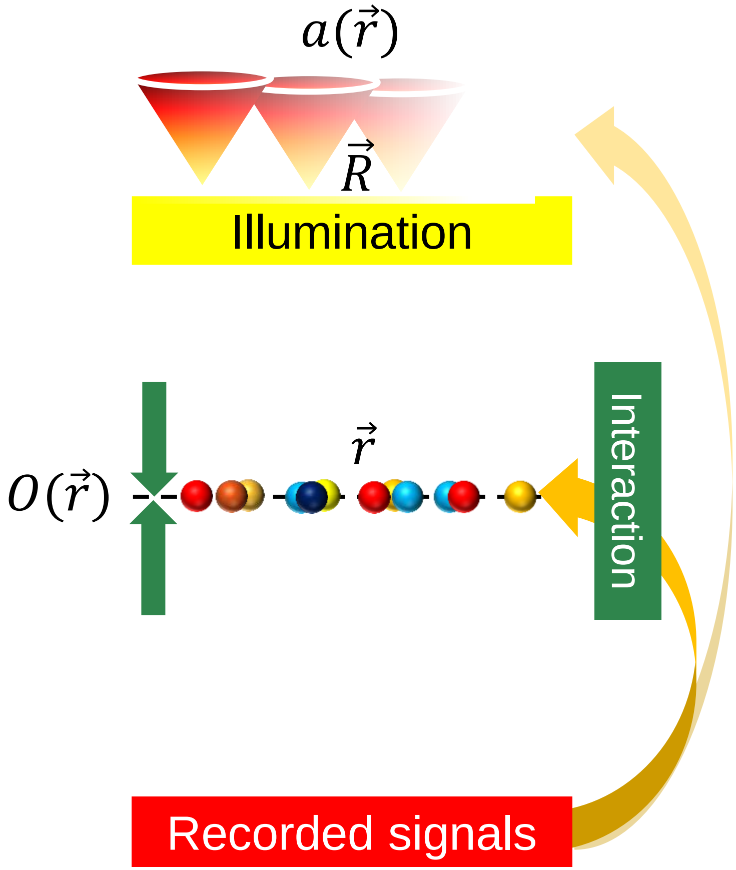

$$I(\vec{q},\vec{R}) = \left|\psi(\vec{q},\vec{R})\right|^2$$

Scattering model: (Complex) multiplicative object

$$\psi(\vec{r},\vec{R}) = \left[a(\vec{r}) \otimes \delta(\vec{r}-\vec{R})\right] \cdot O(\vec{r})$$

Object Transmission function

Model to describe observations

$$\boldsymbol{I(\vec{q},\vec{R}) = \left|\mathcal{F}_{\vec{r}}\left[\psi(\vec{r},\vec{R})\right]\right|^2}$$

$I(\vec{q},\vec{R})$

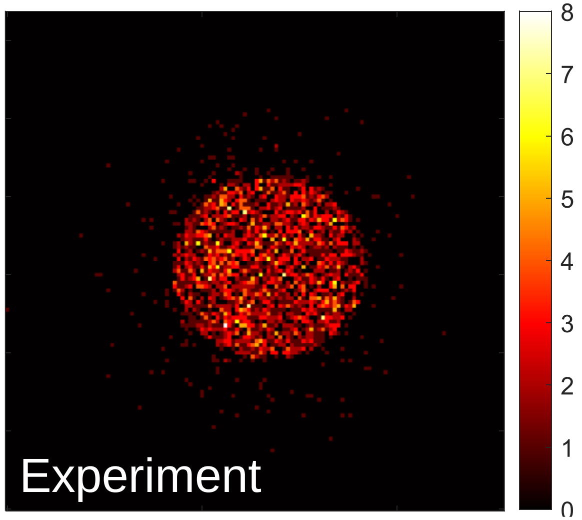

$\hat{I}(\vec{q},\vec{R})$

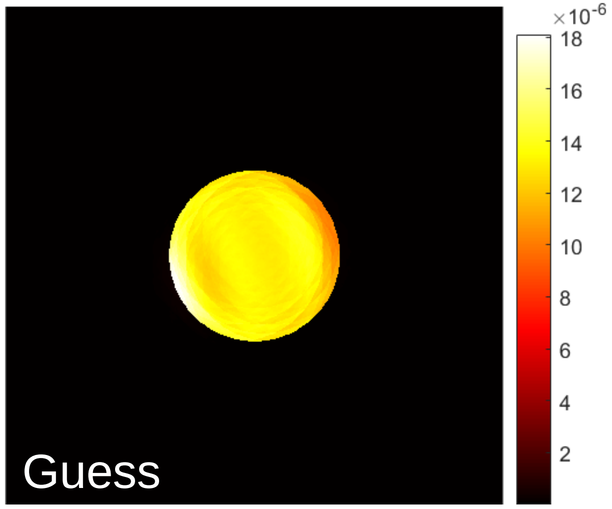

Single-scattering Ptychography

Candes et al., Phase retrieval via Wirtinger flow: Theory and algorithms, IEEE Trans. Inform. Theory **61** 1985 (2015)

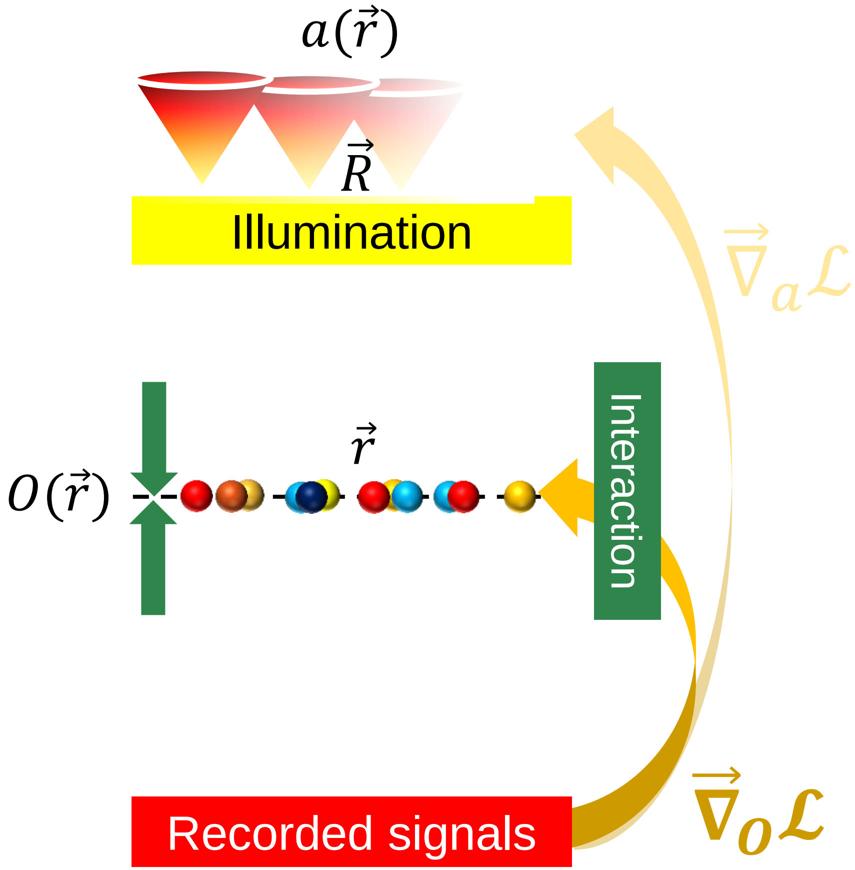

$$I(\vec{q},\vec{R}) = \left|\psi(\vec{q},\vec{R})\right|^2$$

„Wirtinger Flow“

$$\hat{O}^{t+1}(\vec{r}) = \hat{O}^{t}(\vec{r}) - \beta \cdot \boxed{\vec{\nabla}_{\hat{O}^*}\mathcal{L}}\left(\hat{I}(\vec{q},\vec{R}), I(\vec{q},\vec{R})\right) \quad \text{Object}$$

$$\hat{a}^{t+1}(\vec{r}) = \hat{a}^{t}(\vec{r}) - \beta \cdot \boxed{\vec{\nabla}_{\hat{a}^*}\mathcal{L}}\left(\hat{I}(\vec{q},\vec{R}), I(\vec{q},\vec{R})\right) \quad \text{Probe}$$

Wirtinger gradient/derivative

$I(\vec{q},\vec{R})$ $\qquad\qquad$ $\hat{I}(\vec{q},\vec{R})$

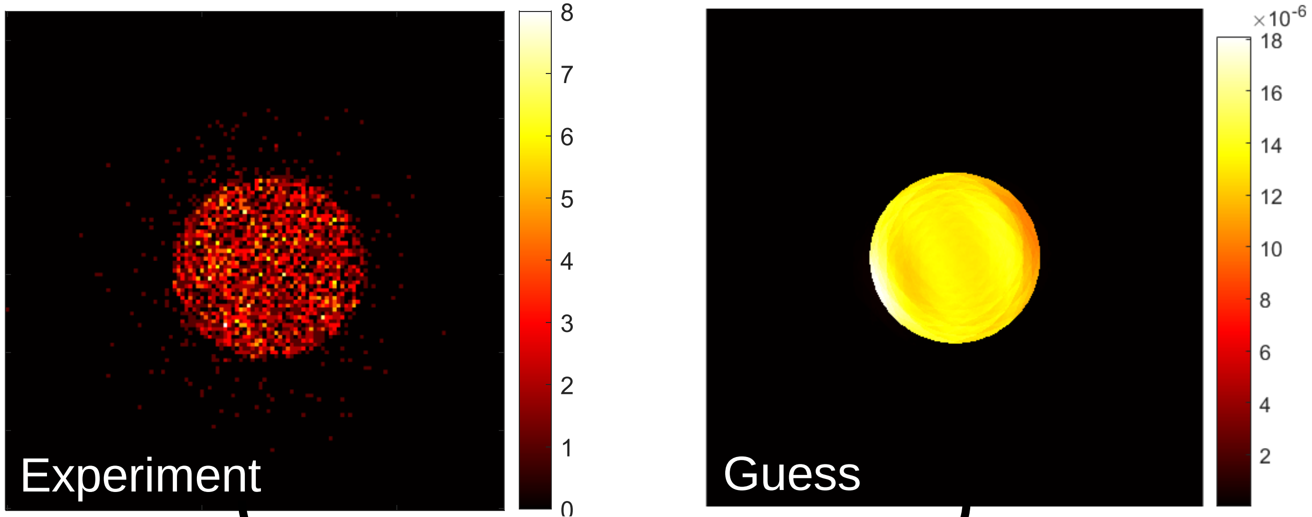

$$\mathcal{L}\left[\hat{I}(\vec{q},\vec{R}), I(\vec{q},\vec{R})\ \right] \quad \text{Loss}$$

→ Wirtinger derivatives

Complex differentiatiability of complex function

$$f(x+iy)=u(x,y)+iv(x,y)$$

→ Fulfil **Cauchy-Riemann** differential equations:

$$\frac{\partial u}{\partial x}=\frac{\partial v}{\partial y}$$
$$\frac{\partial u}{\partial y}=-\frac{\partial v}{\partial x}$$

Let $z \coloneqq x+iy$ then

$$\frac{\partial f}{\partial z}=\frac{1}{2}\left(\frac{\partial f}{\partial x}-i\frac{\partial f}{\partial y}\right)$$
$$\frac{\partial f}{\partial z^*}=\frac{1}{2}\left(\frac{\partial f}{\partial x}+i\frac{\partial f}{\partial y}\right)$$

Are the **Wirtinger derivatives**.

Example:

$$f(z)=zz^*=(x+iy)(x-iy)=x^2+y^2$$
$$\frac{\partial f}{\partial z}=\frac{1}{2}(2x-2iy)$$
$$\frac{\partial f}{\partial z^*}=\frac{1}{2}(2x+2iy)$$

Single-scattering Ptychography

MoS_2 Monolayer

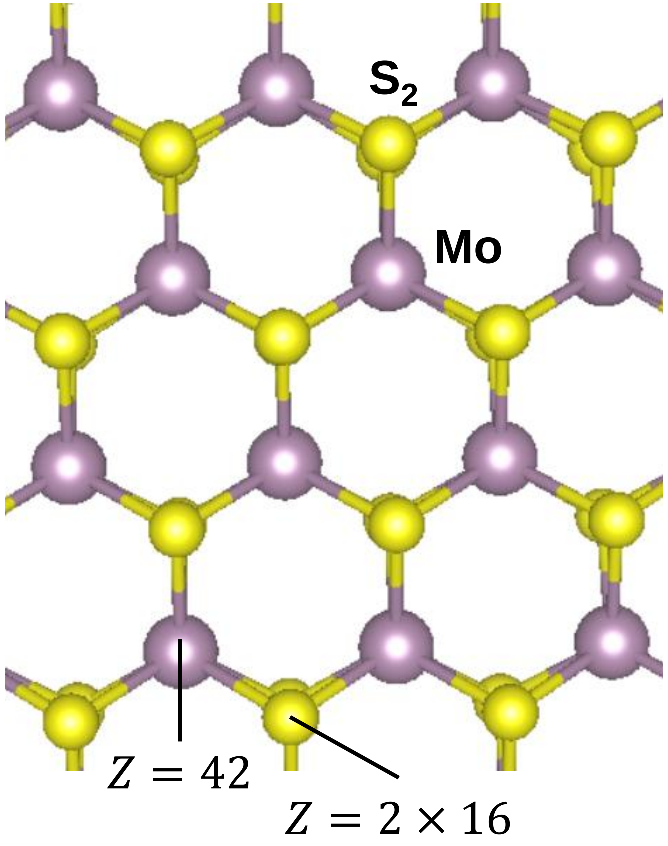

Diffraction patterns

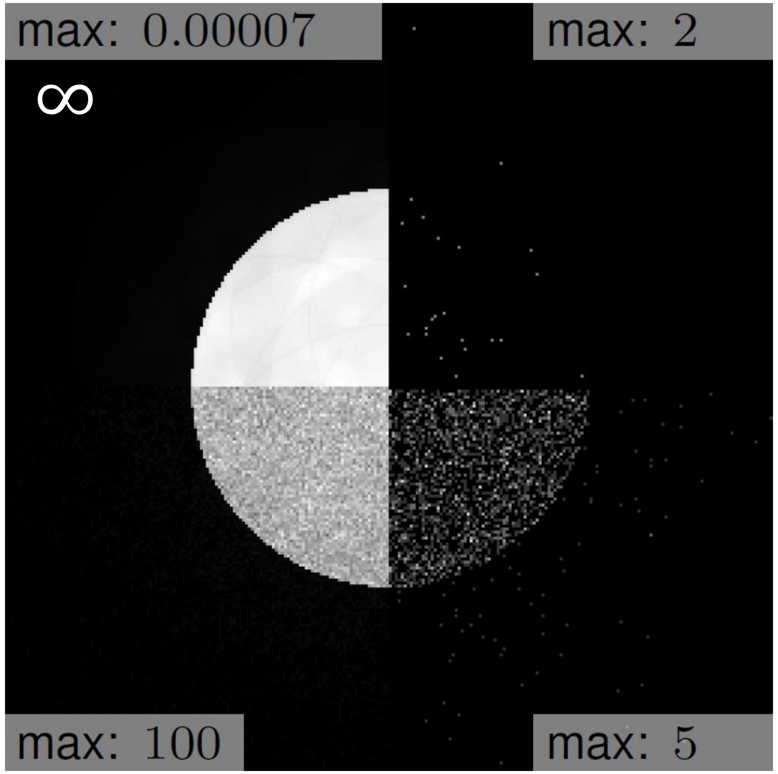

Max Leo Leidl

Leidl et al., Micron **185** 103688 (2024)

L1 loss

$$\mathcal{L}_1 = \sum_k |\hat{I}_k - I_k|$$

Mean squared error

$$\mathcal{L}_{MSE} = \sum_k (\hat{I}_k - I_k)^2$$

Amplitude loss

$$\mathcal{L}_A = \sum_k \left[\sqrt{\hat{I}_k} - \sqrt{I_k}\right]^2$$

Poisson loss

$$\mathcal{L}_P = \sum_k [\hat{I}_k - I_k \ln(\hat{I}_k + \varepsilon)]$$

Single-scattering Ptychography

MoS_2 Monolayer

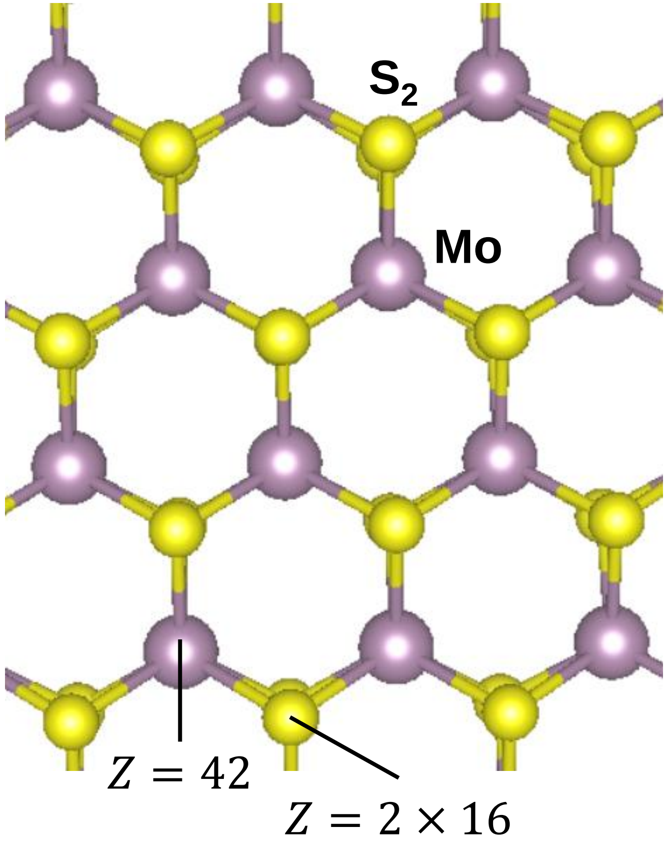

Diffraction patterns

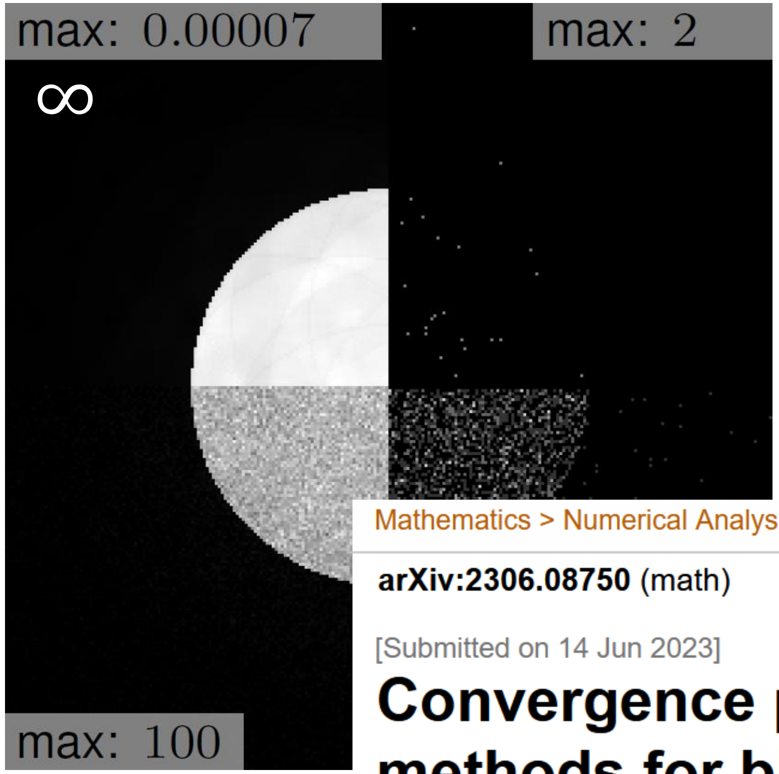

Max Leo Leidl

Mathematics > Numerical Analysis

arXiv:2306.08750 (math)

[Submitted on 14 Jun 2023]

Convergence properties of gradient methods for blind ptychography

Oleh Melnyk

L1 loss

$$\mathcal{L}_1 = \sum_k \left|\hat{I}_k - I_k\right|$$

Mean squared error

$$\mathcal{L}_{MSE} = \sum_k \left(\hat{I}_k - I_k\right)^2$$

Amplitude loss

$$\mathcal{L}_A = \sum_k \left[\sqrt{\hat{I}_k} - \sqrt{I_k}\right]^2$$

Poisson loss

$$\mathcal{L}_P = \sum_k \left[\hat{I}_k - I_k \ln(\hat{I}_k + \varepsilon)\right]$$

Single-scattering Ptychography

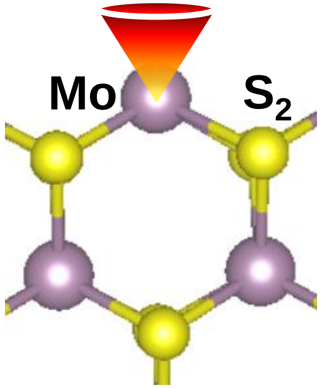

Epoch:
$t = 10$

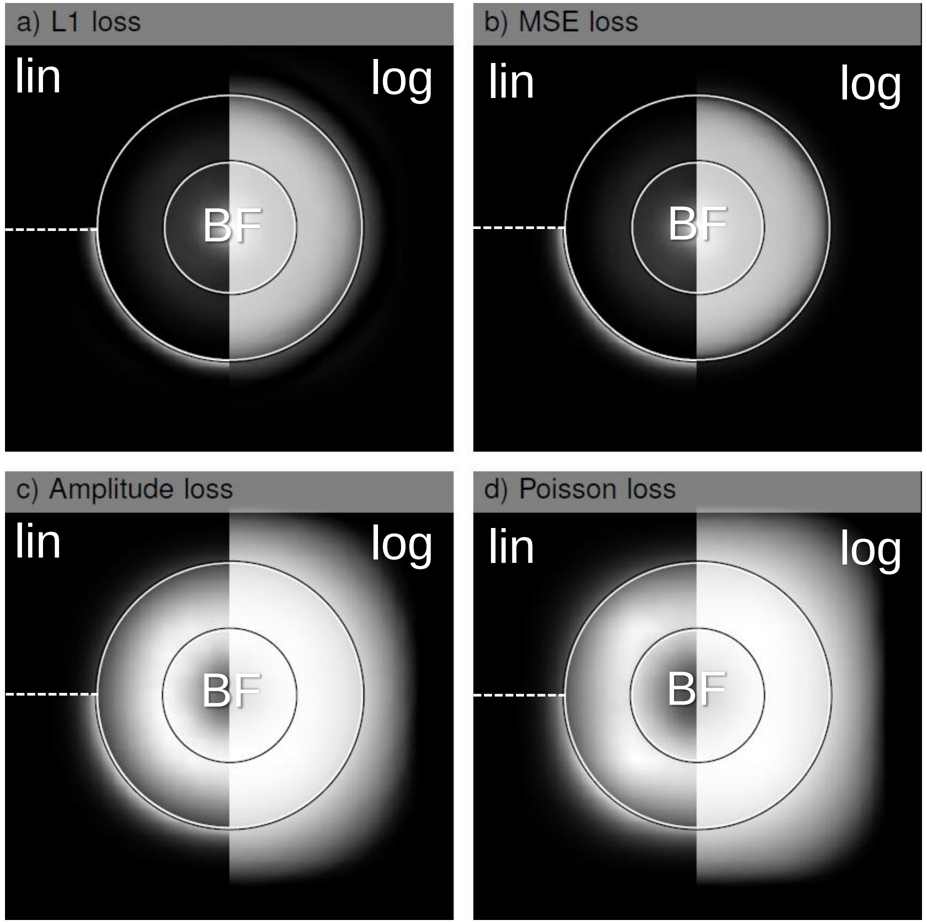

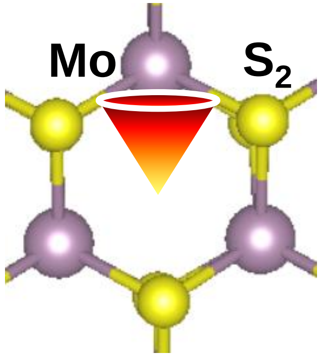

Epoch:
$t = 10$

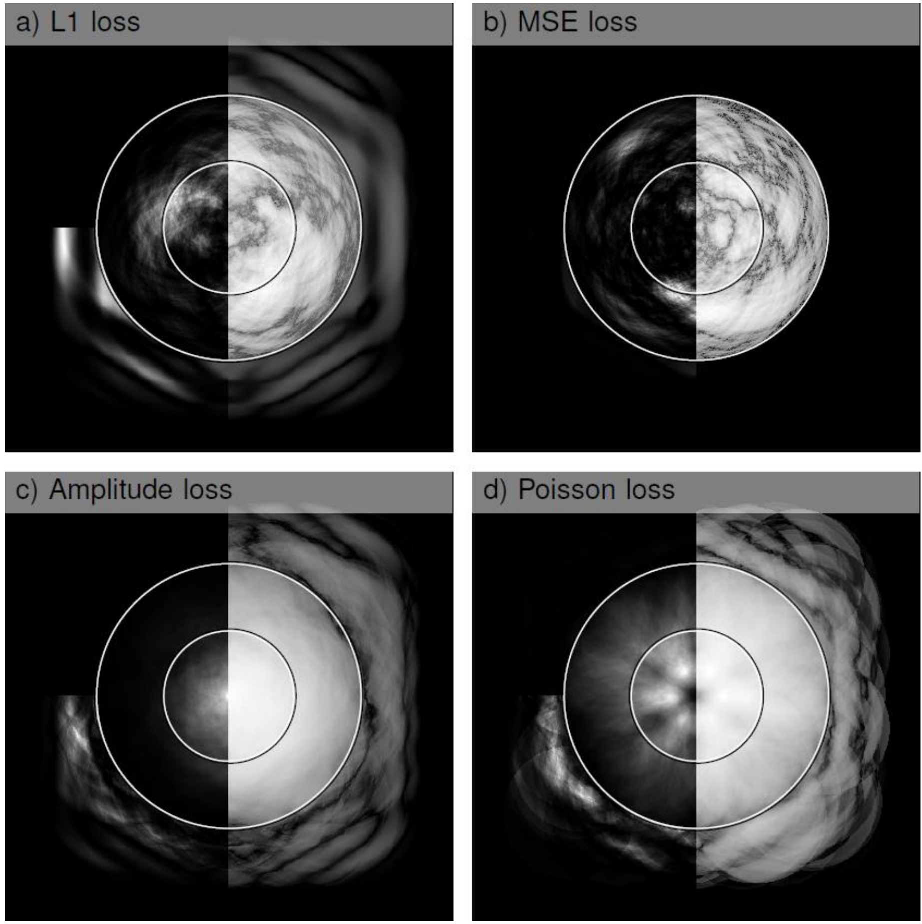

Gradient-based update spectrum: $\mathcal{F}_{\vec{r}}\left[\hat{O}^{t+1}\right] = \mathcal{F}_{\vec{r}}\left[\hat{O}^{t}\right] - \mu \cdot \mathcal{F}_{\vec{r}}\left[\vec{\nabla}_{\hat{O}^*}\mathcal{L}\left(\hat{I}(\vec{q},\vec{R}), I(\vec{q},\vec{R})\right)\right]$

L_1 loss

$$\mathcal{L}_1 = \sum_k \left|\hat{I}_k - I_k\right|$$

Mean squared error

$$\mathcal{L}_{MSE} = \sum_k \left(\hat{I}_k - I_k\right)^2$$

Amplitude loss

$$\mathcal{L}_A = \sum_k \left[\sqrt{\hat{I}_k} - \sqrt{I_k}\right]^2$$

Poisson loss

$$\mathcal{L}_P = \sum_k \left[\hat{I}_k - I_k \ln(\hat{I}_k + \varepsilon)\right]$$

Single-scattering Ptychography

High dose (10^6 $el.$/pattern)

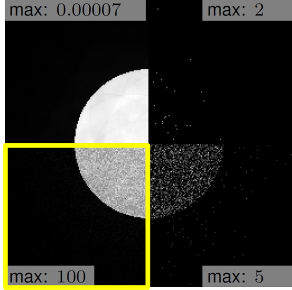

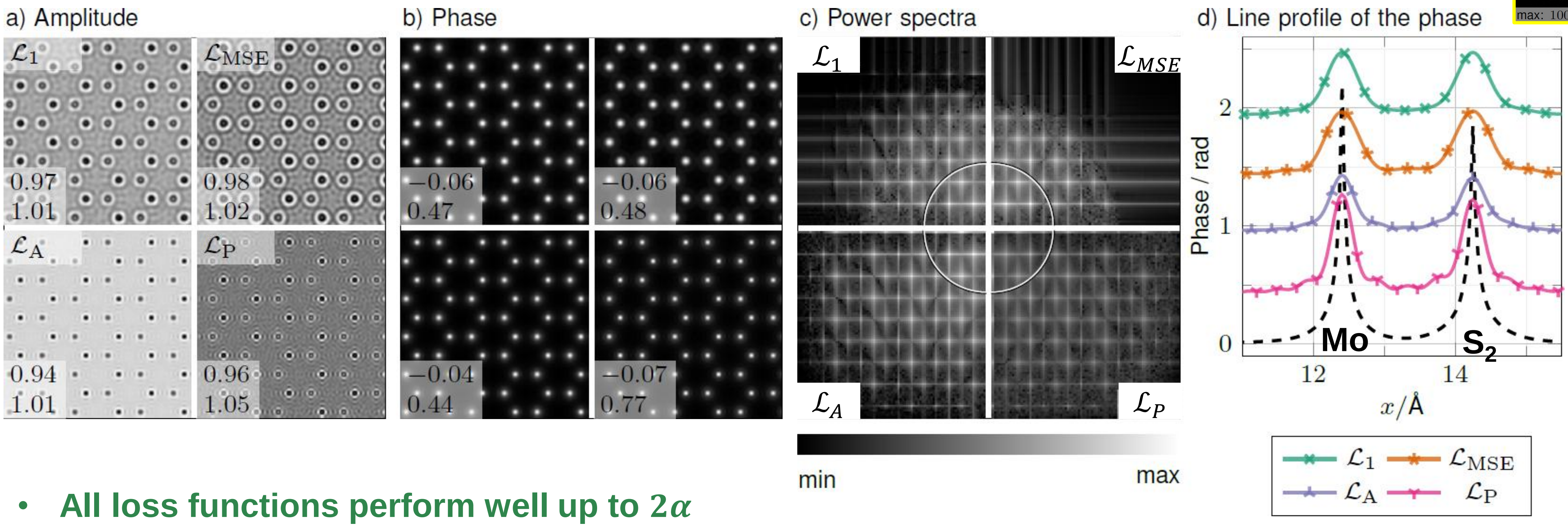

- All loss functions perform well up to 2α
- Amplitude and Poisson loss yield highest spatial frequencies

→ *Origin of differences: low DF counts*

Leidl et al., Micron **185** 103688 (2024)

L$_1$ loss

$$\mathcal{L}_1 = \sum_k \left|\hat{I}_k - I_k\right|$$

Mean squared error

$$\mathcal{L}_{MSE} = \sum_k \left(\hat{I}_k - I_k\right)^2$$

Amplitude loss

$$\mathcal{L}_A = \sum_k \left[\sqrt{\hat{I}_k} - \sqrt{I_k}\right]^2$$

Poisson loss

$$\mathcal{L}_P = \sum_k \left[\hat{I}_k - I_k \ln(\hat{I}_k + \varepsilon)\right]$$

Single-scattering Ptychography

Medium dose (10^4 $el./$pattern)

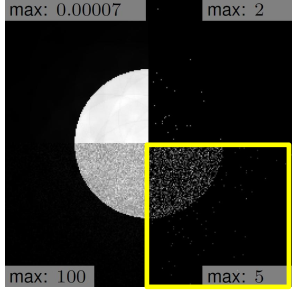

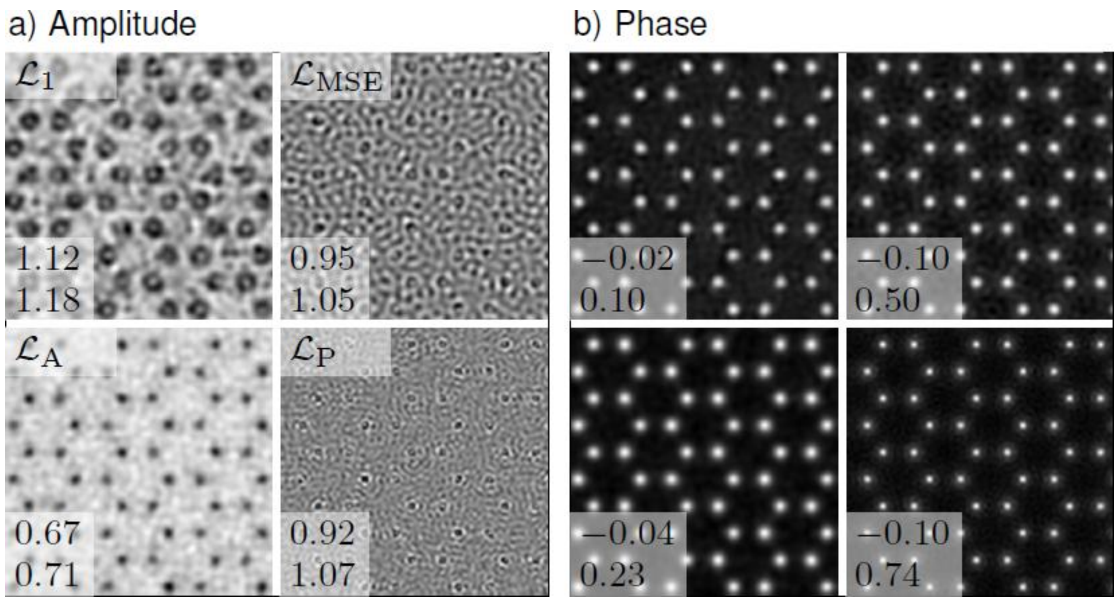

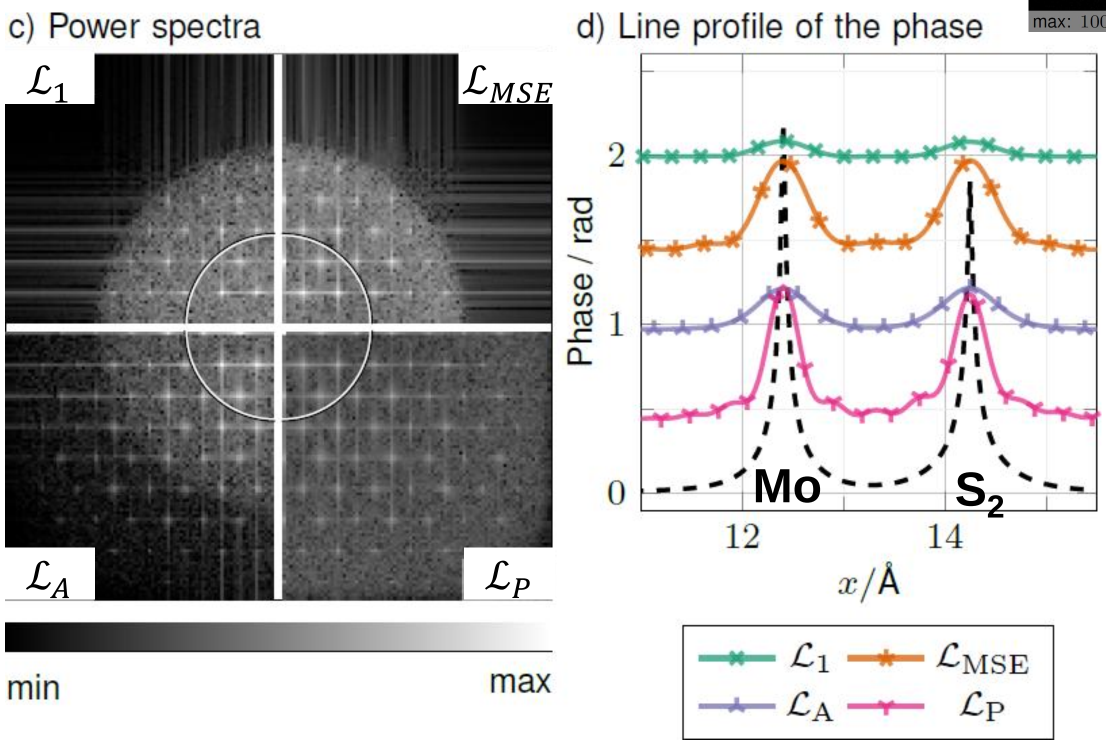

- **Amplitude and Poisson loss**

  > 1.5 ***higher spatial frequencies reconstructed***

- ***Poisson: Continuous signal & noise transfer***

Leidl et al., Micron **185** 103688 (2024)

L_1 loss

$$\mathcal{L}_1 = \sum_k \left|\hat{I}_k - I_k\right|$$

Mean squared error

$$\mathcal{L}_{MSE} = \sum_k \left(\hat{I}_k - I_k\right)^2$$

Amplitude loss

$$\mathcal{L}_A = \sum_k \left[\sqrt{\hat{I}_k} - \sqrt{I_k}\right]^2$$

Poisson loss

$$\mathcal{L}_P = \sum_k \left[\hat{I}_k - I_k \ln(\hat{I}_k + \varepsilon)\right]$$

Single-scattering Ptychography

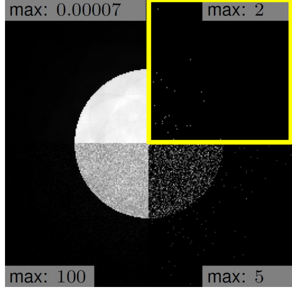

Low dose (10^2 $el./$pattern)

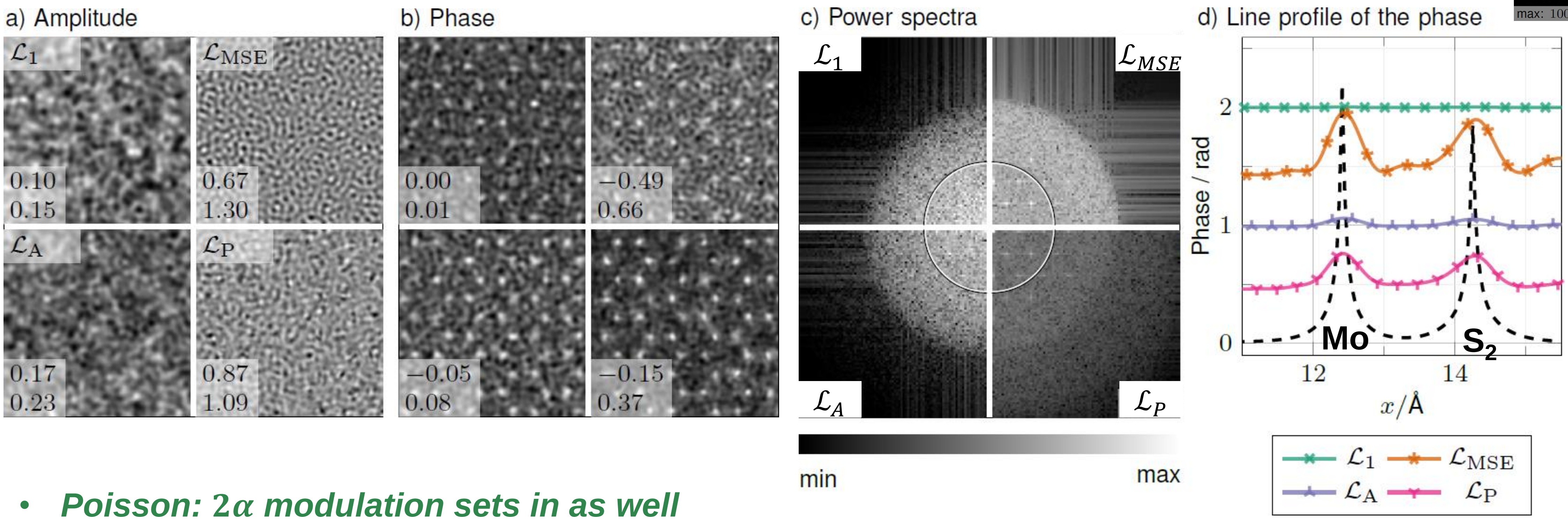

- ***Poisson: 2α modulation sets in as well***
- ***However: Best SNR in phase***

Leidl et al., Micron **185** 103688 (2024)

L$_1$ loss

$$\mathcal{L}_1 = \sum_k \left|\hat{I}_k - I_k\right|$$

Mean squared error

$$\mathcal{L}_{MSE} = \sum_k \left(\hat{I}_k - I_k\right)^2$$

Amplitude loss

$$\mathcal{L}_A = \sum_k \left[\sqrt{\hat{I}_k} - \sqrt{I_k}\right]^2$$

Poisson loss

$$\mathcal{L}_P = \sum_k \left[\hat{I}_k - I_k \ln(\hat{I}_k + \varepsilon)\right]$$

Foretaste of the practical: reconstruct atomic structure of SnS_2

Probe

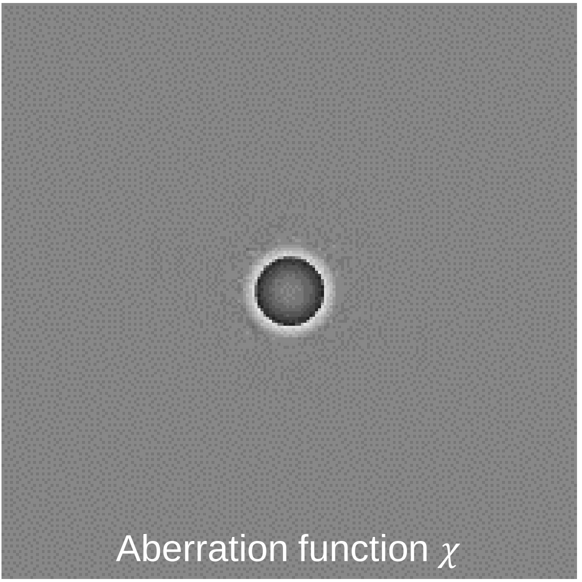
Aberration function χ

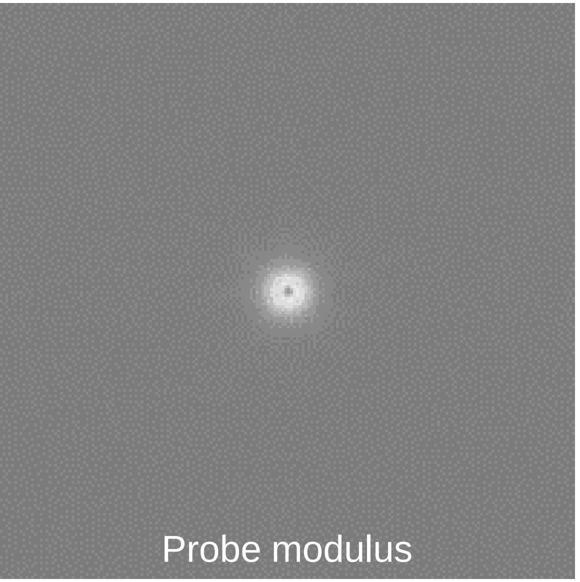
Probe modulus

Specimen

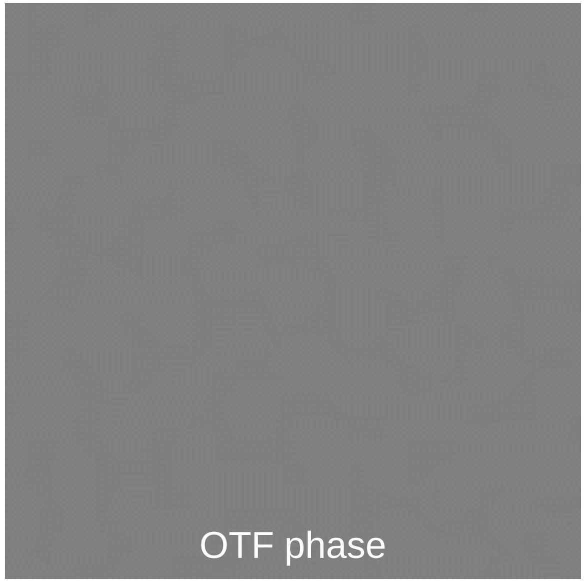
OTF phase

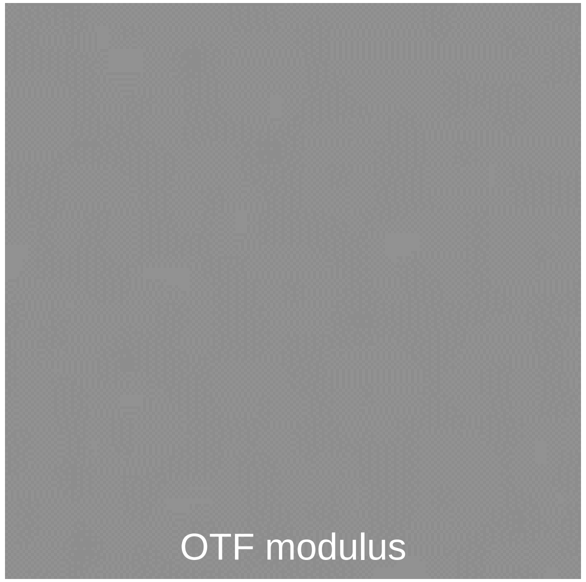
OTF modulus

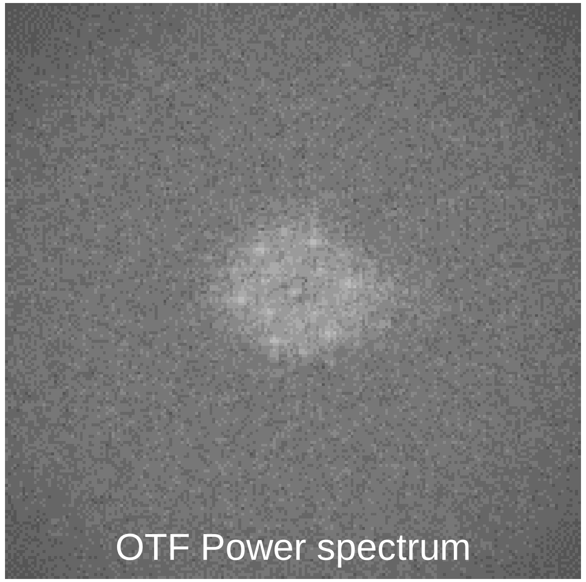
OTF Power spectrum

Selected CBEDs

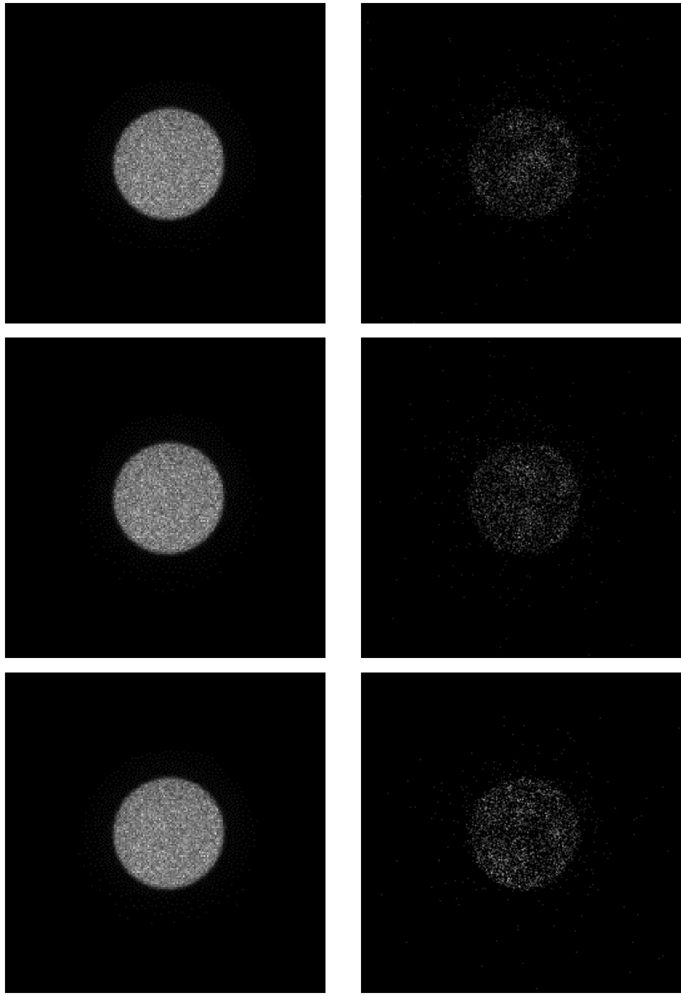

Outline

STEM, DPC, COM, phases and momentum transfer

Gradient – based (single & multislice) ptychography

Electric fields in thin specimen: Ehrenfest theorem

Introduction to the inverse problem

Approaches for polarisation-induced field mapping

Minimizing the loss function: a single-scattering example

Practice hint 1 – 5, focus, coherence

Inverse multislice: concept, coherence, TDS, parametrisation

Inversion of multislice

Science **372**, 826–831 (2021)

Benchmark study: Chen et al (Group David Muller)

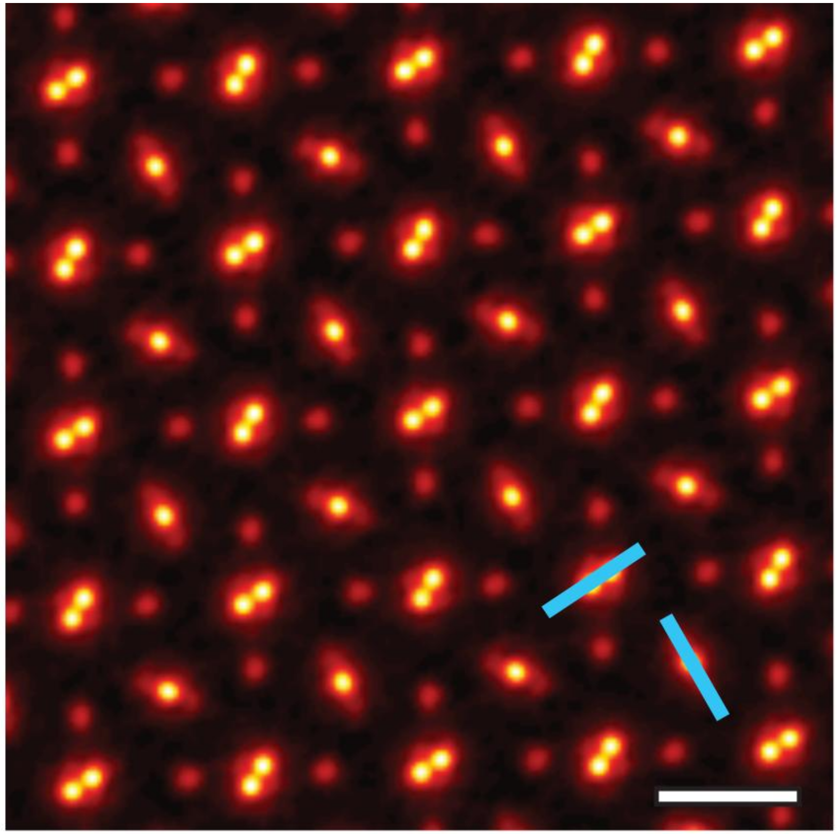

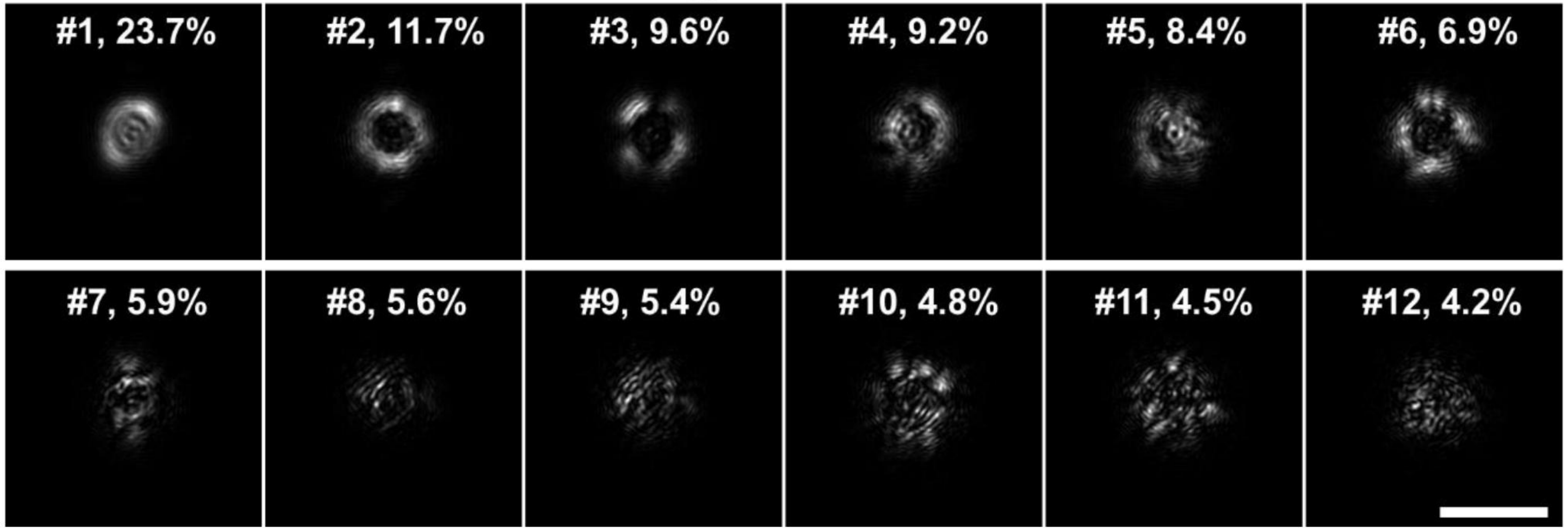

{P} multimodal probes pixel wise reconstructed

→ Order of N_{probes} x 1K x 1K = N_{probes} x 10^6 complex parameters

{S} pixel- & slice wise reconstructed

→ Order of N_{Slice} x 1K x 1K = N_{Slice} x 10^6 complex parameters

→ **Reconstruction of 10^7 complex parameters**

→ **No physics constraints to potentials and wave functions**

→ **Handcrafted regularisation concepts**

Inversion of multislice

... But multislice inversion is for thick specimens
... in which TDS is omnipresent

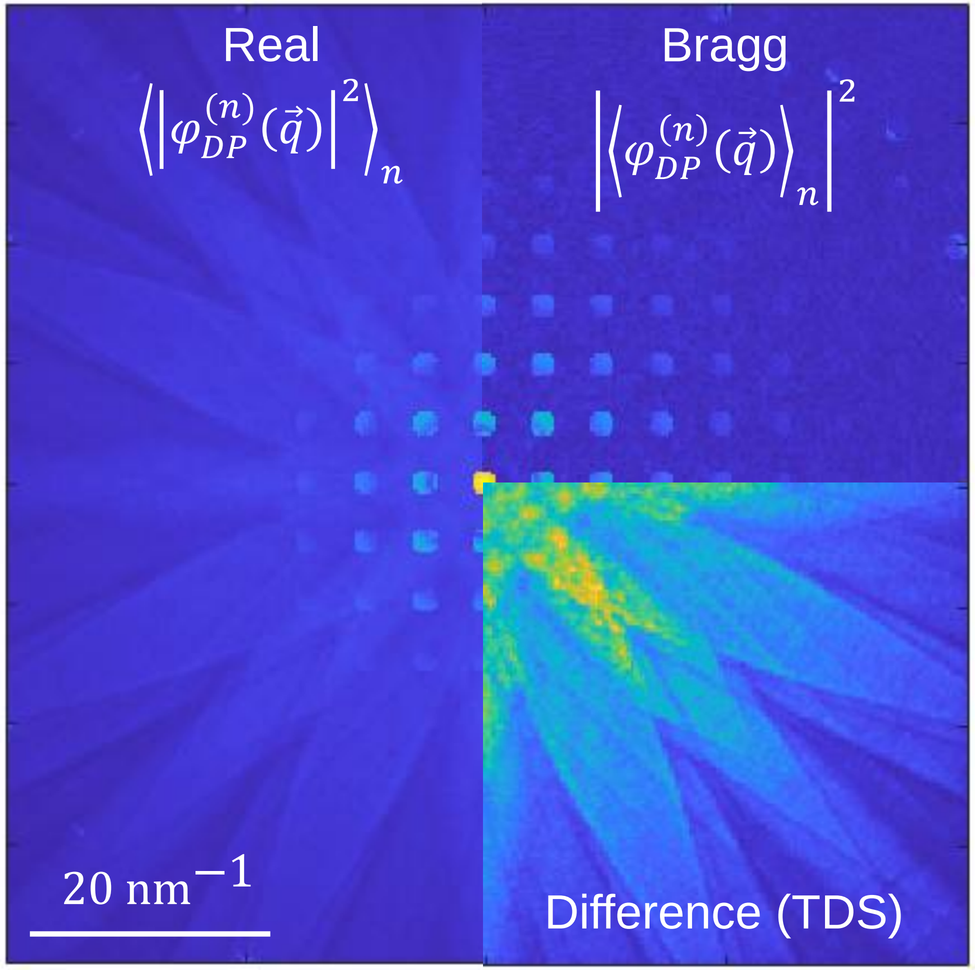

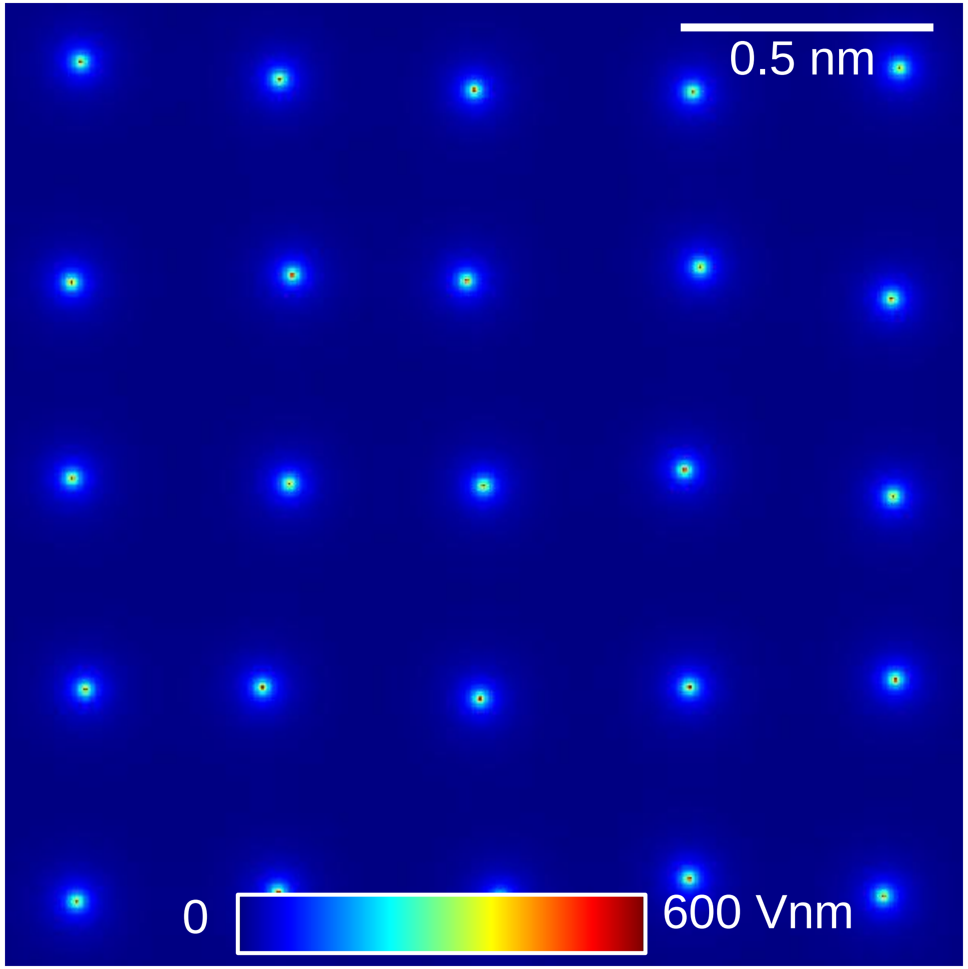

TDS: Model violations in pixelwise reconstructions (STO)

$$\mathcal{L} \longrightarrow \mathcal{L} + \mu R$$

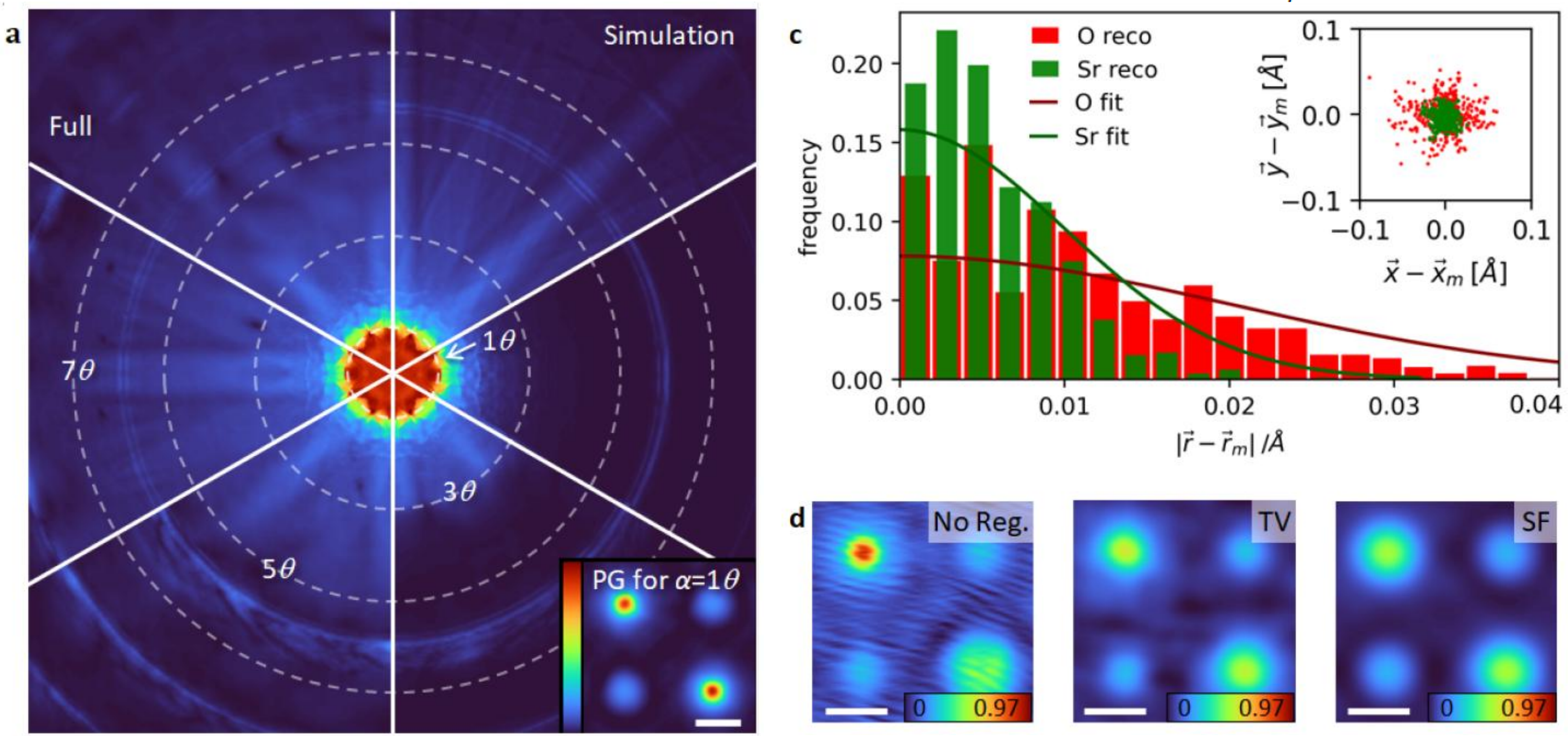

Z.Herdegen et al., Phys. Rev. B 110, 064102 (2024)

Inversion of multislice

Gradient calculation: Multislice as a Neural Network

Van den Broek, Phys Rev Lett **109**, 245502 (2012)

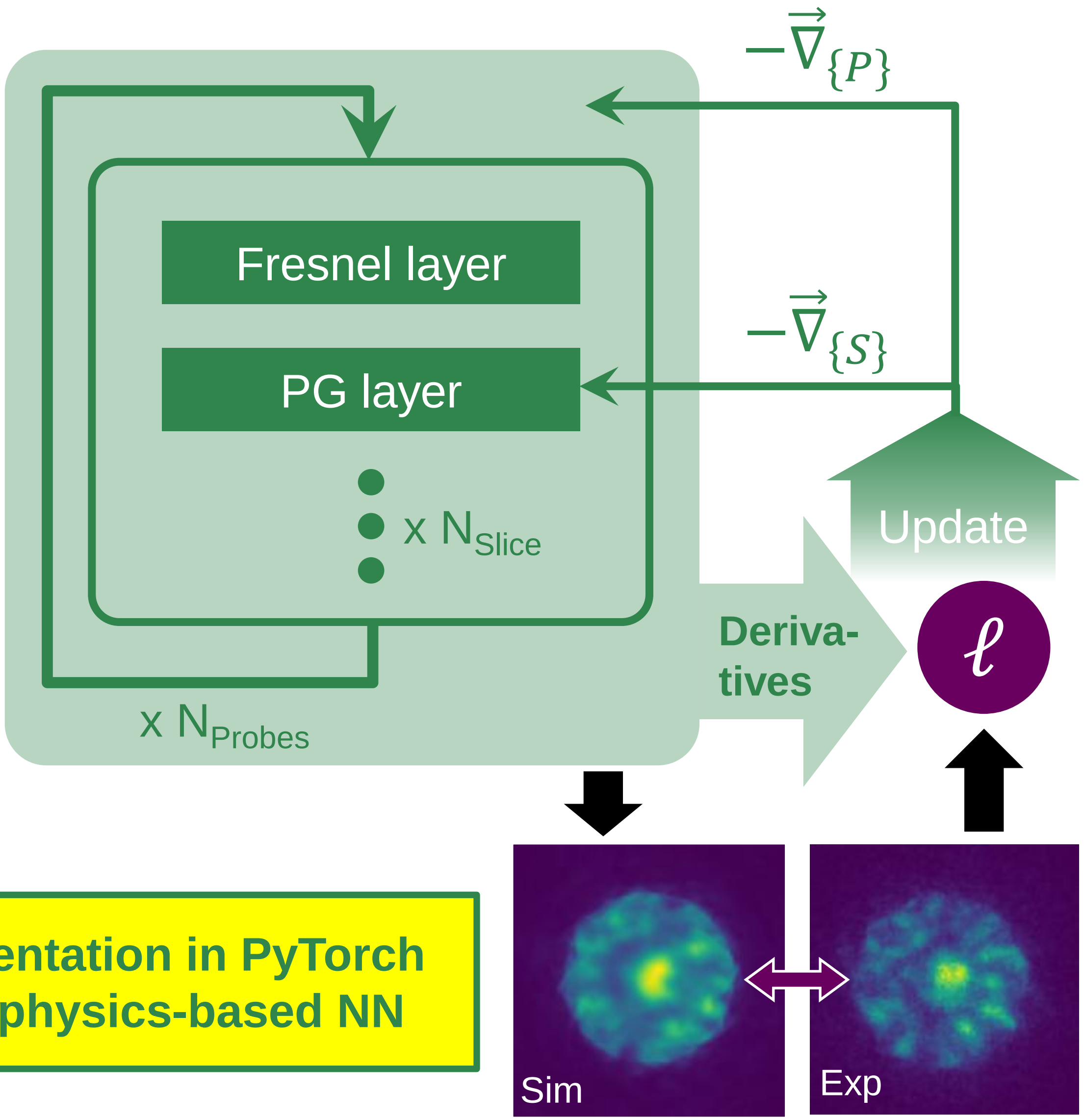

- **Implementation in PyTorch**
- **Strictly physics-based NN**

Pixel-wise (unimodal)

Science **372**, 826–831 (2021)

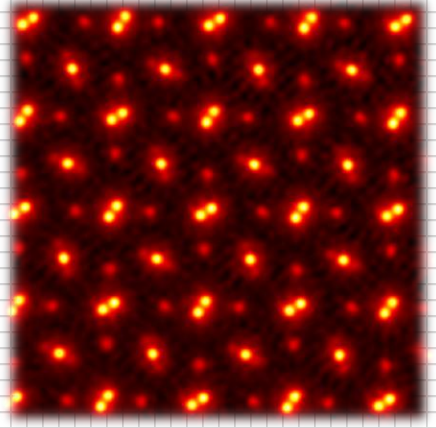

N_{Slice} x 1K x 1K = N_{Slice} x 10^6

N_{probes} x 1K x 1K = N_{probes} x 10^6

„Multimodal objects“: Thibault et al., Nature **494**, 68 (2013)

Inversion of multislice

Parametrised inversion of partially coherent dynamical scattering

- **Partially coherent probe formation known**
  Probe expressed by:

Semi-angle, aberrations

Scan position

$$\psi_k = \alpha_k \cdot \phi_{in}^{\{P\}}(\vec{r} - \vec{s} - \vec{\eta}_k, \delta_k)$$

Probability for $\vec{\eta}_k, \delta_k$

Partial spacial coherence

Focus fluctuations

→ Order of N_{probes} x 10 **real** parameters

→ Bounded to **physical solutions**

- **Specimen potential known**
  Built by *N* atoms:

Debye-Waller Factor

$$V_{DW}(\vec{r}) = \sum_{n=1}^{N} w_n \cdot D_n \otimes v_{Z_n}(\vec{r} - \vec{r}_n)$$

Weight to adjust type

Atomic potential (from Hartree-Fock)

Single **Frozen Phonon** configuration τ in slice j:

$$V_{FP}^{(j)}(\vec{r}, \tau) = \sum_{n=1}^{N} w_n \cdot v_{Z_n}\left(\vec{r} - \vec{r}_n - \sqrt{\langle u_n^2 \rangle} \cdot \vec{g}_{n,\tau}\right)$$

Random Gaussian displacements

Inversion of multislice

Gradient calculation: Multislice as a Neural Network

Van den Broek, Phys Rev Lett **109**, 245502 (2012)

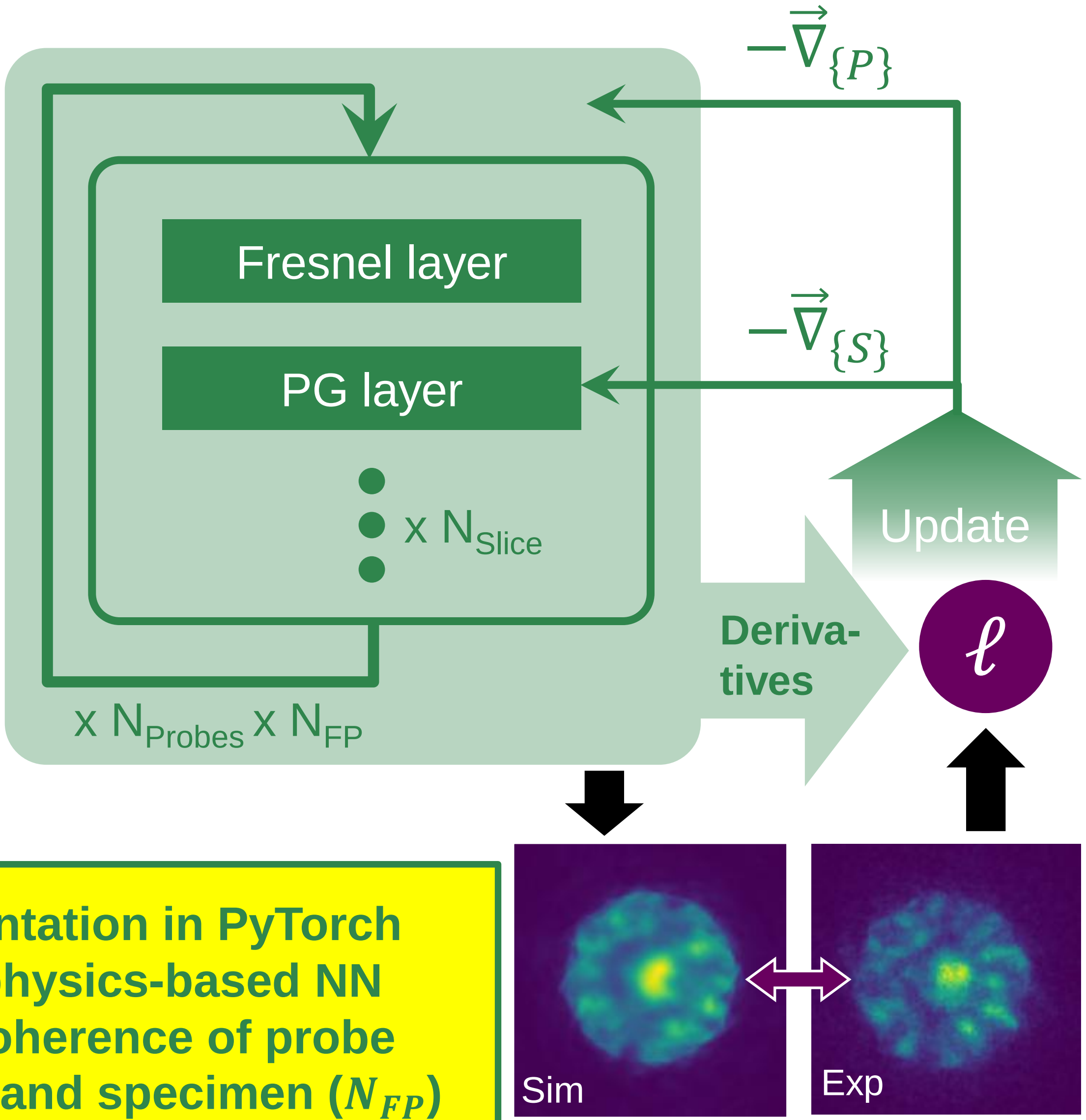

- Implementation in PyTorch
- Strictly physics-based NN
- Partial coherence of probe (N_{probes}) and specimen (N_{FP})

Pixel-wise (unimodal)

Science **372**, 826–831 (2021)

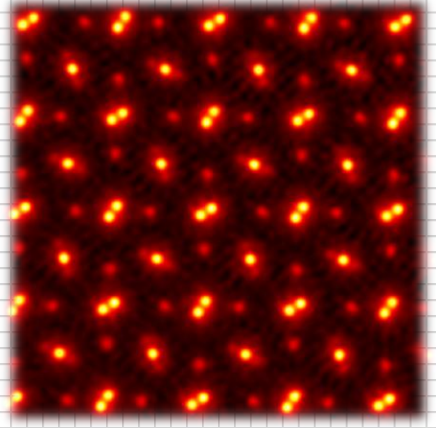

N_{Slice} x 1K x 1K = N_{Slice} x 10^6

N_{probes} x 1K x 1K = N_{probes} x 10^6

Parameterised

Nat. Comm. **15**, 101 (2024)

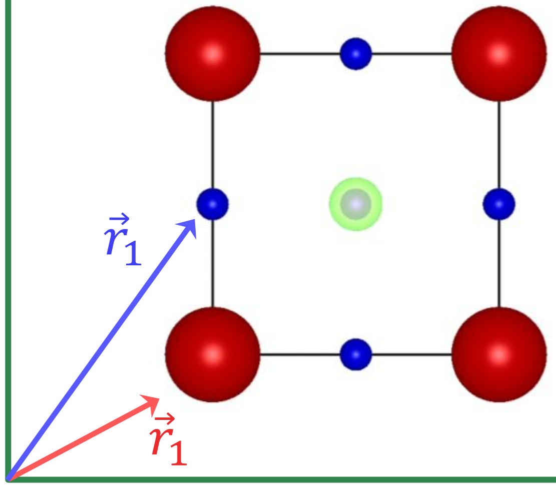

Inversion of multislice: Multimodal probe & specimen

Multi-modal reconstruction to enable TDS

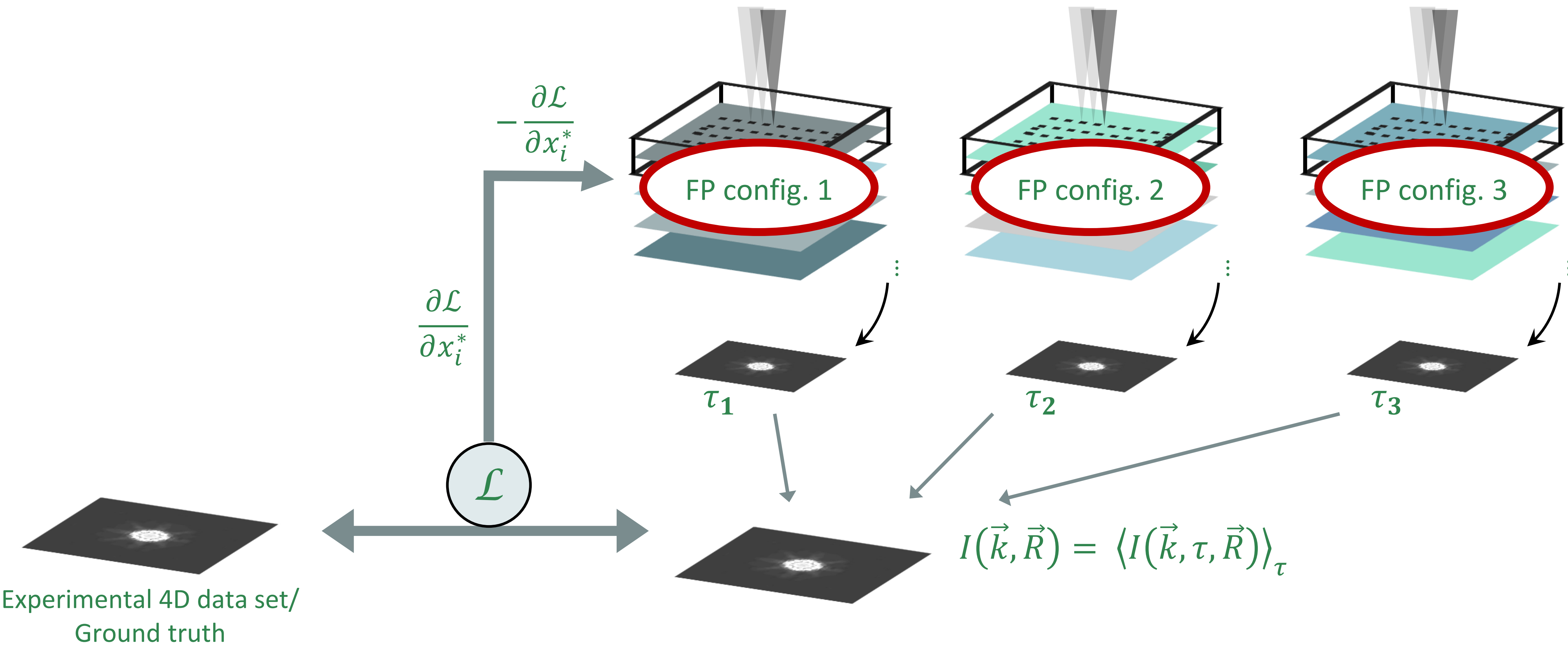

Z.Herdegen et al., Phys. Rev. B 110, 064102 (2024)

Hybrid parameterised/pixellated model

Decontamination of specimen surfaces

Hybrid model

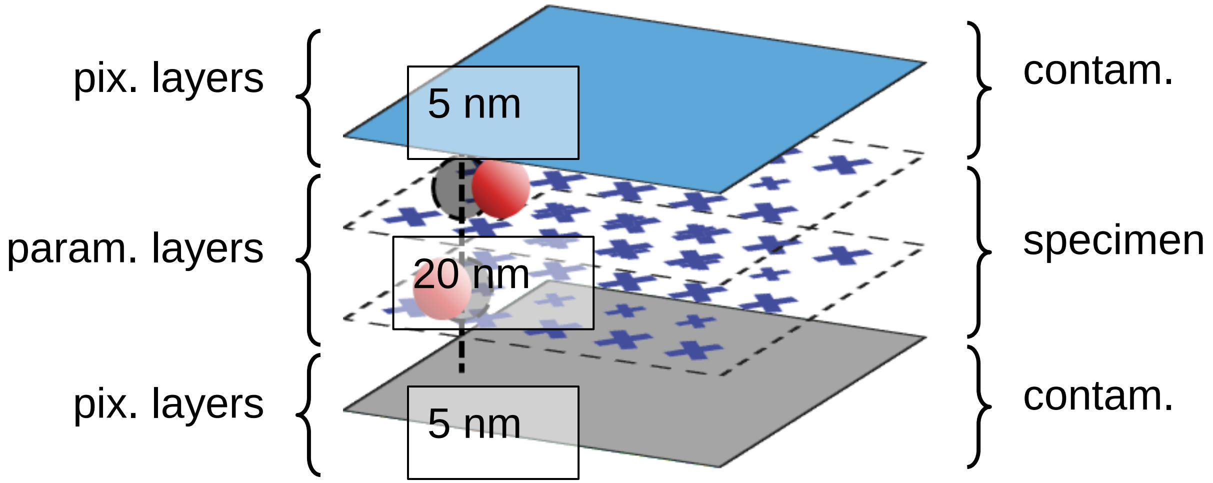

Reconstructed amorphous carbon layers (simulation study)

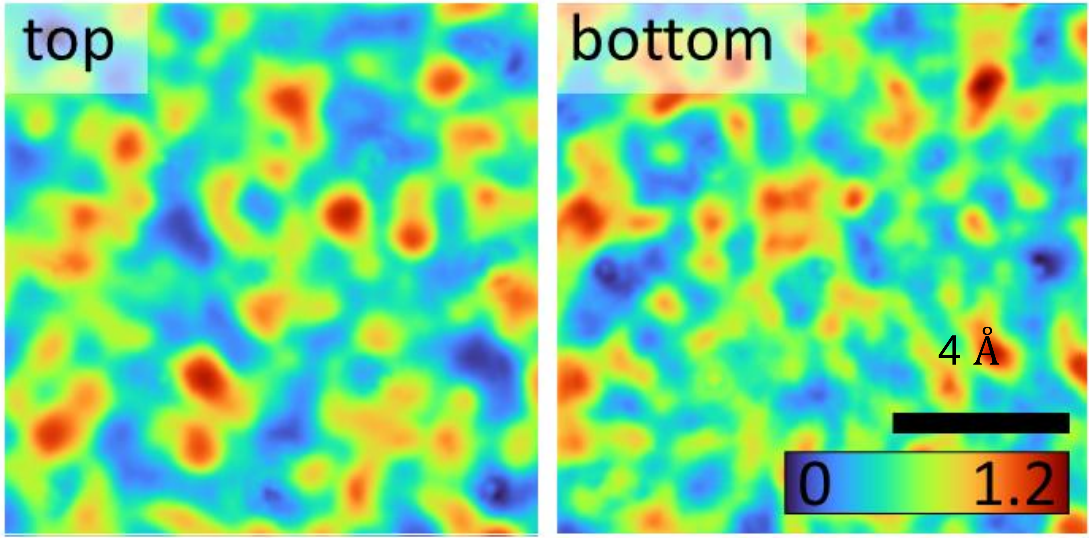

Z.Herdegen et al., Phys. Rev. B 110, 064102 (2024)

Inverse multislice in PZT ferroelectrics

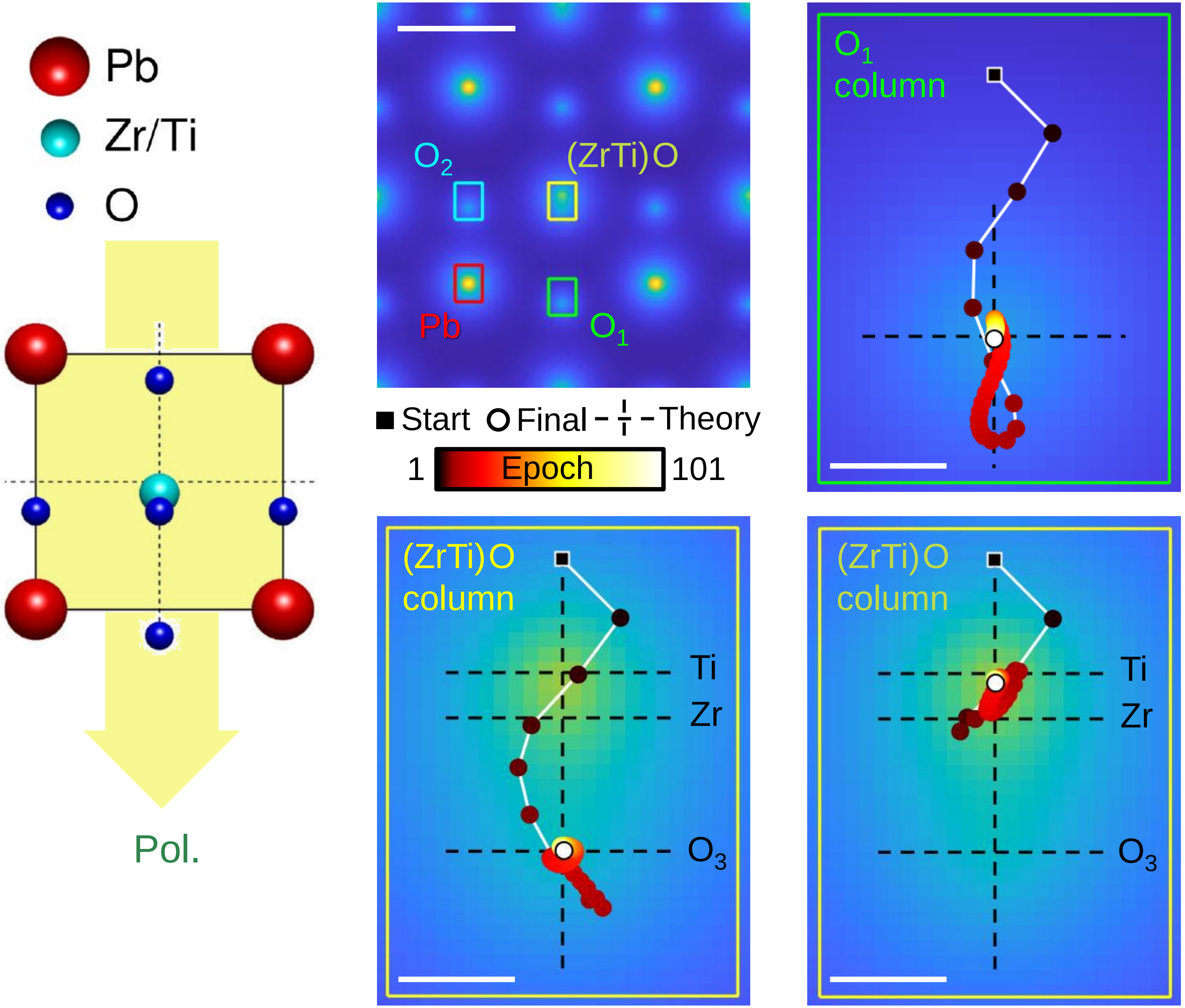

- **Polarisation detected without prior**
- **Accurate atom positions**
- **Different species in same column distinguished**
- **Virtual atom approximation valid**

Diederichs et al., Nature Communications **15**, 101 (2024)

Inverse multislice of PZT ferroelectrics

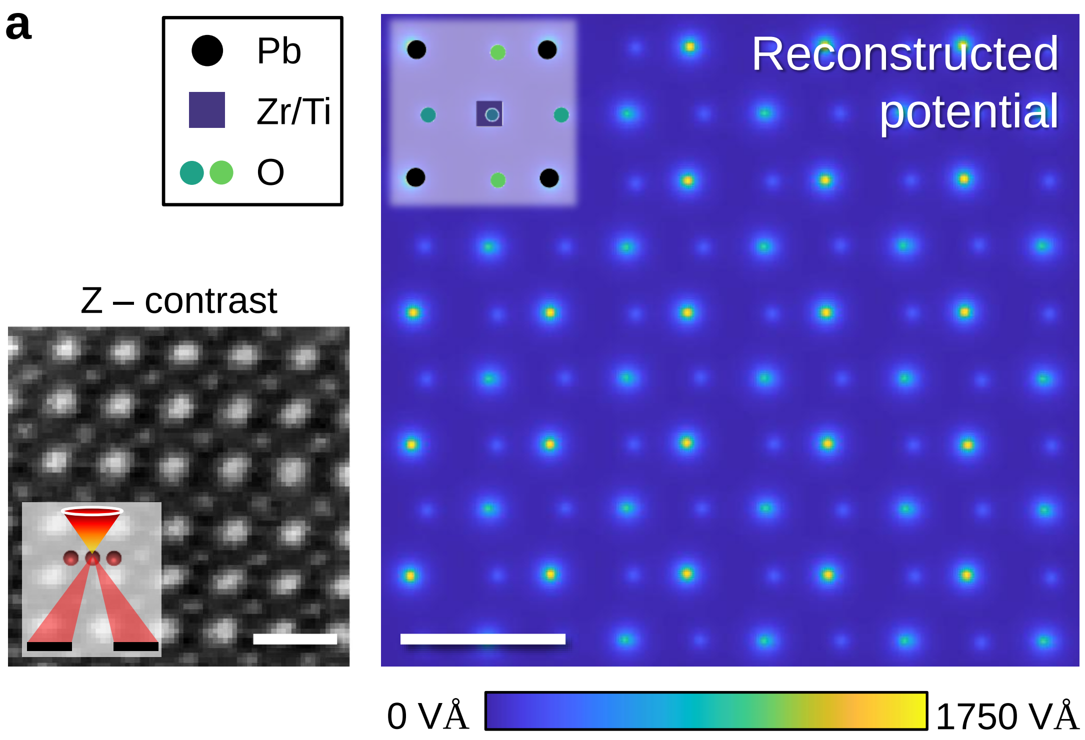

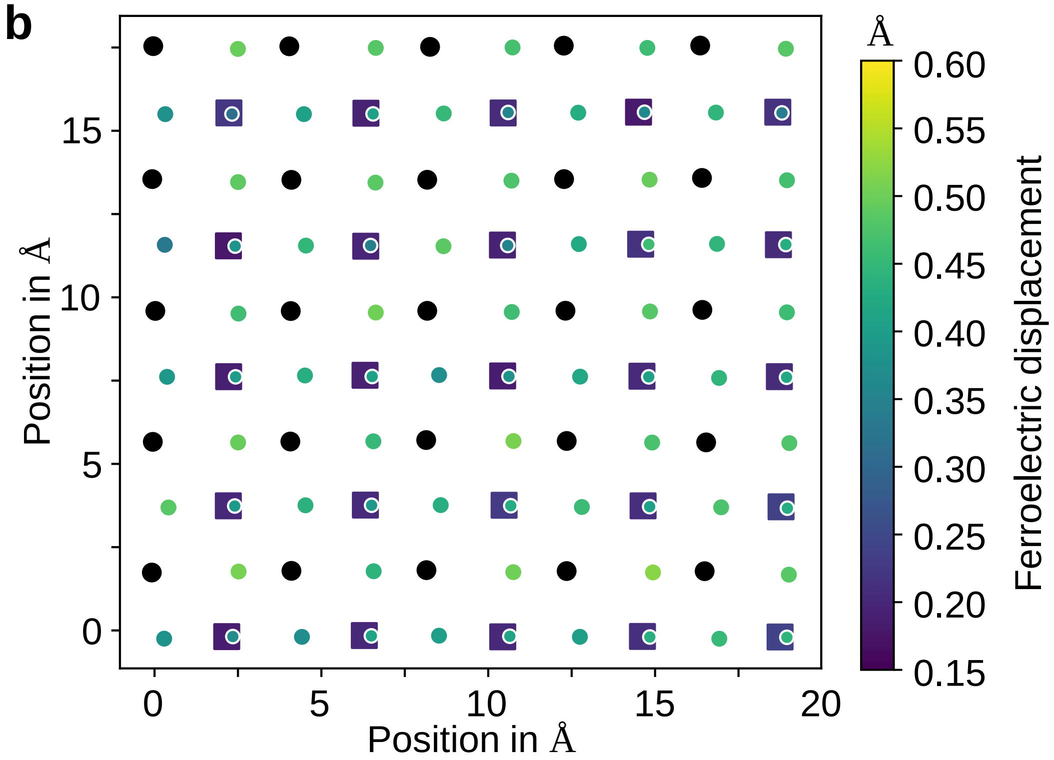

→ **Incorporates TDS in inverse model**

→ **Measured atom positions:**

Precise to a few picometers

Separated in mixed column

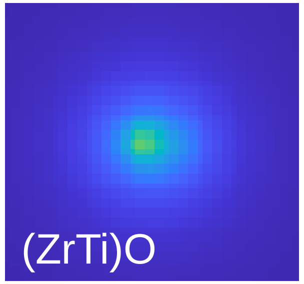

Site	c direction Exp. [pm]	c direction Lit. [pm]	a direction Exp. [pm]	a direction Lit. [pm]
Ti/Zr	20 (2)	17/26	0 (2)	0
O_1	42 (4)	43	2 (3)	
O_2	48 (2)	48	5 (3)	
O_3	39 (4)	48	1 (2)	

Diederichs et al., Nature Communications **15**, 101 (2024)

Inverse multislice of PZT ferroelectrics

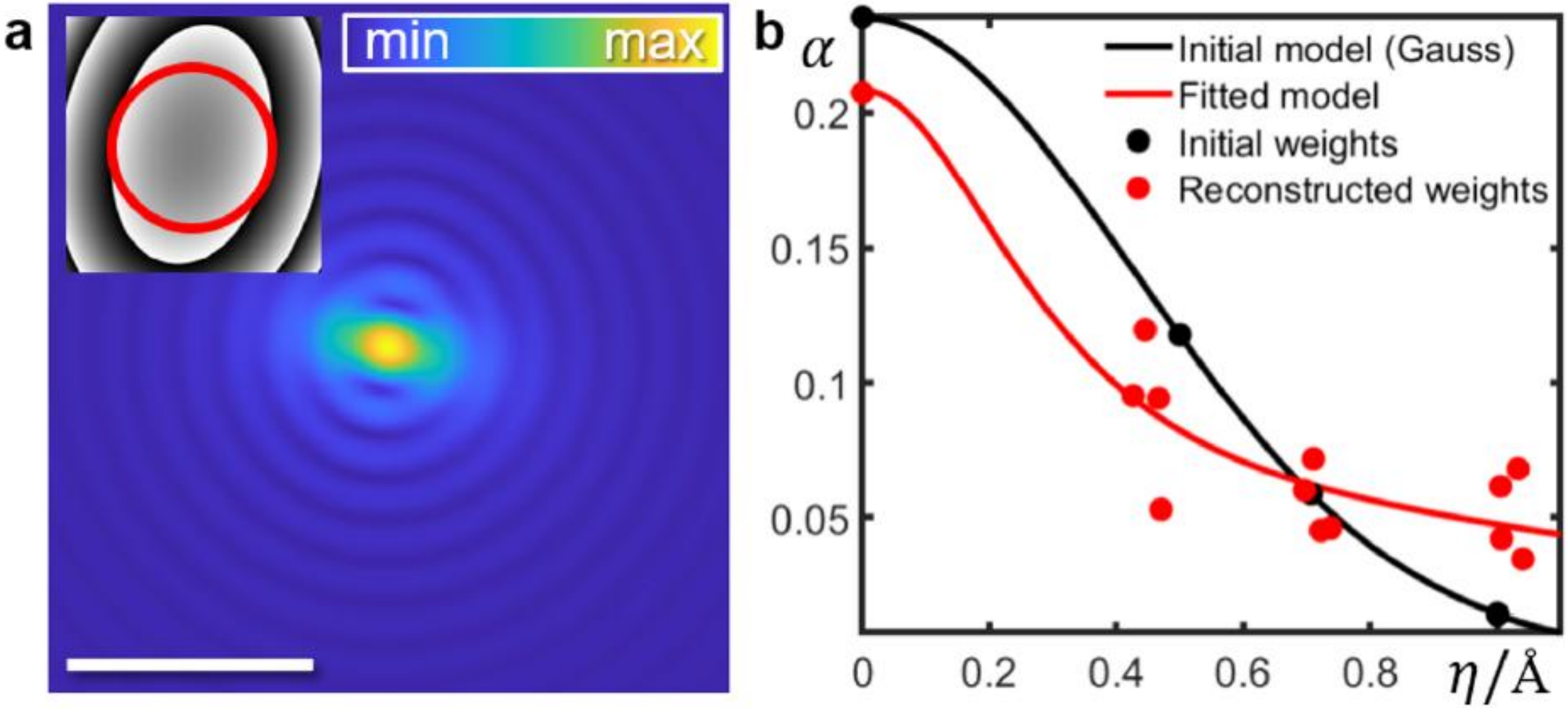

$A_1 = 13.58$ Å (204.12°), $A_2 = 9.51$ Å (128.41°), $B_2 = 8.67$ Å (126.7°)

Importance of TDS

Loss characteristics

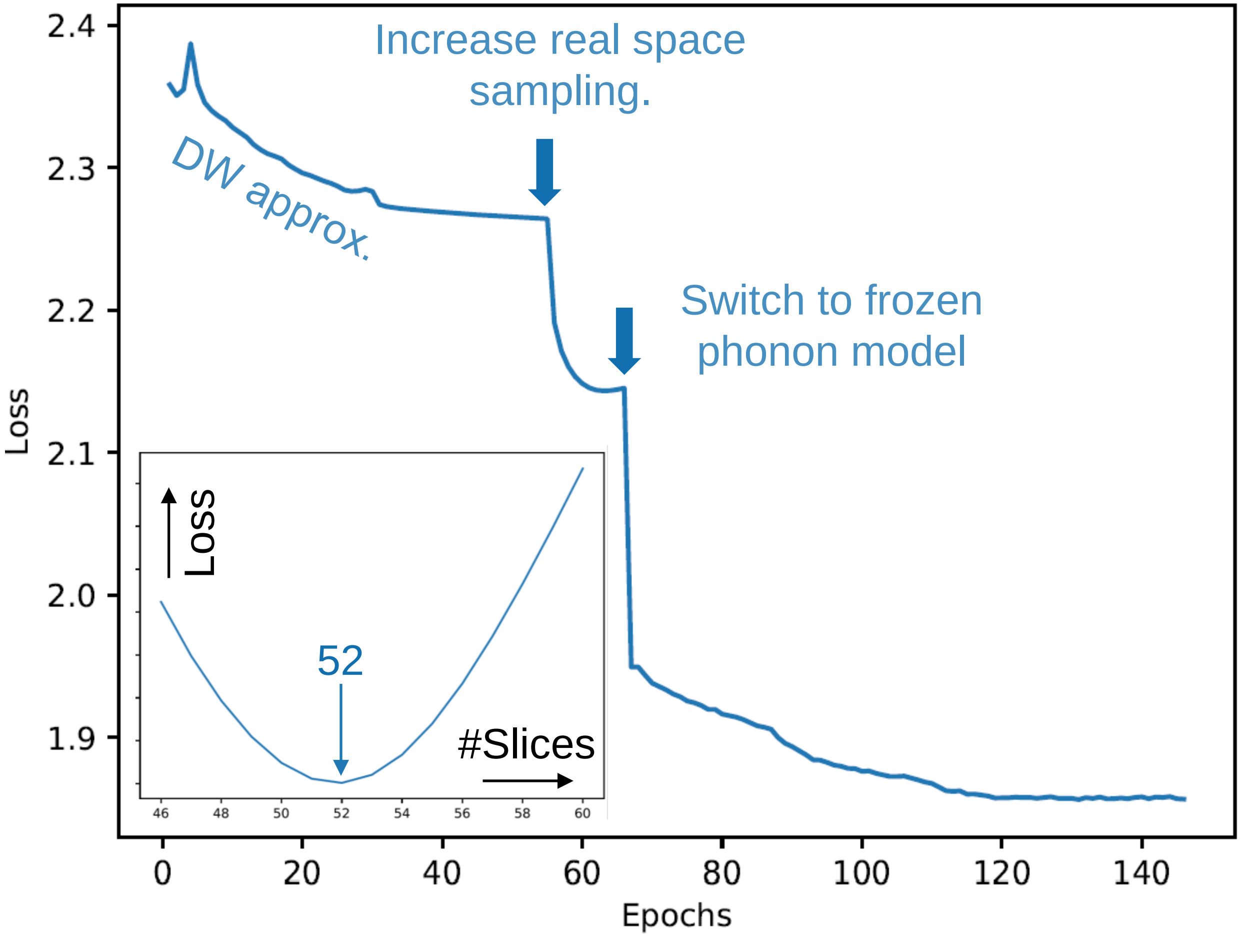

Single-state DW result for displacements

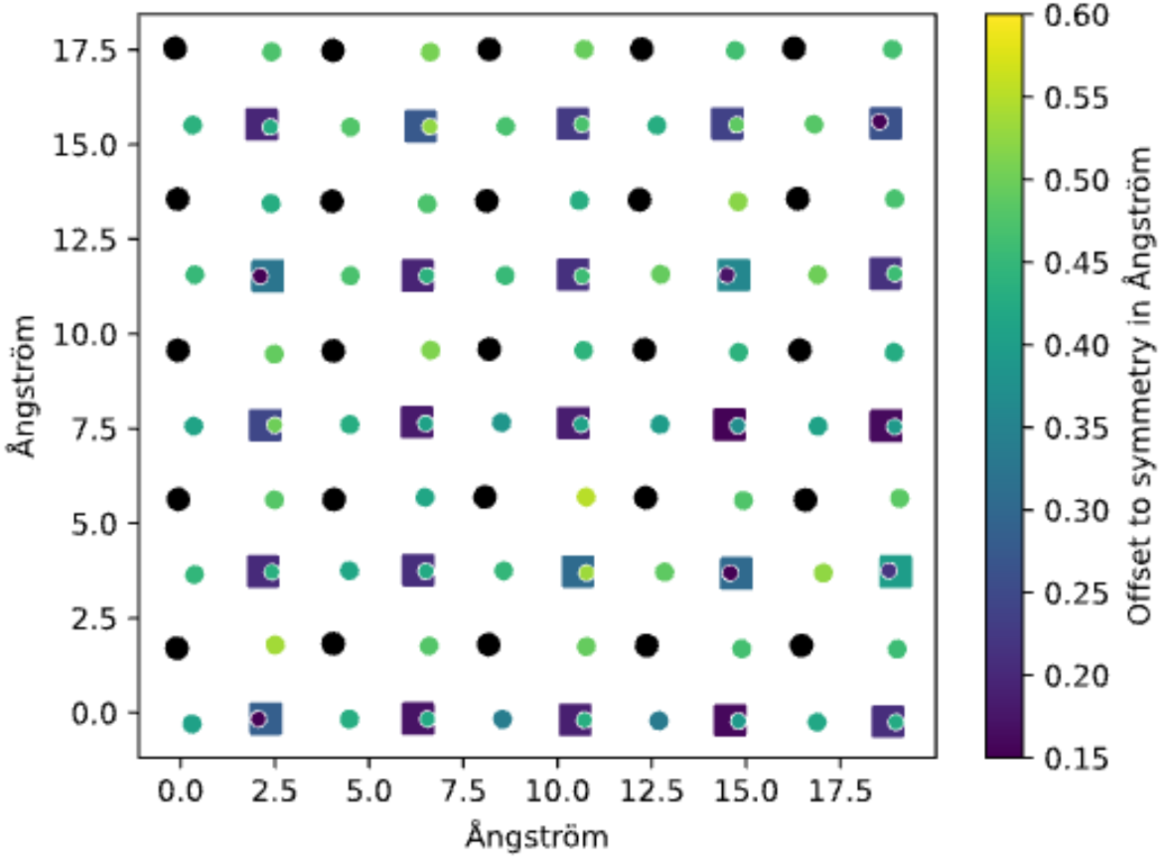

- Unique minimum in thickness scan
- Drastic improvement of $\mathcal{L}_1$ loss upon switch to FP

- Precision significantly worse compared to FP
- Polarisation direction (partly) wrong for O

Diederichs et al., Nature Communications **15**, 101 (2024)

Importance of TDS

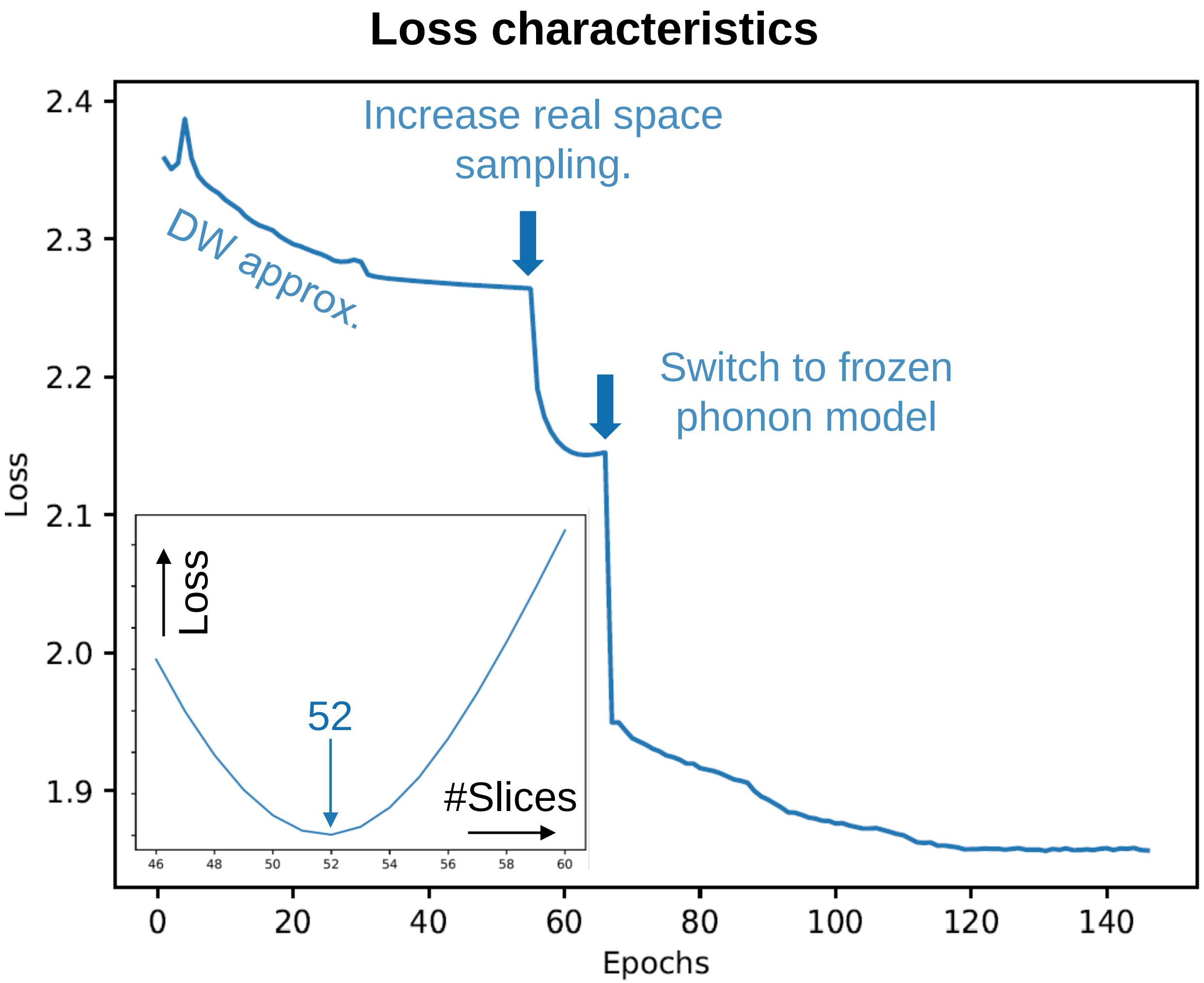

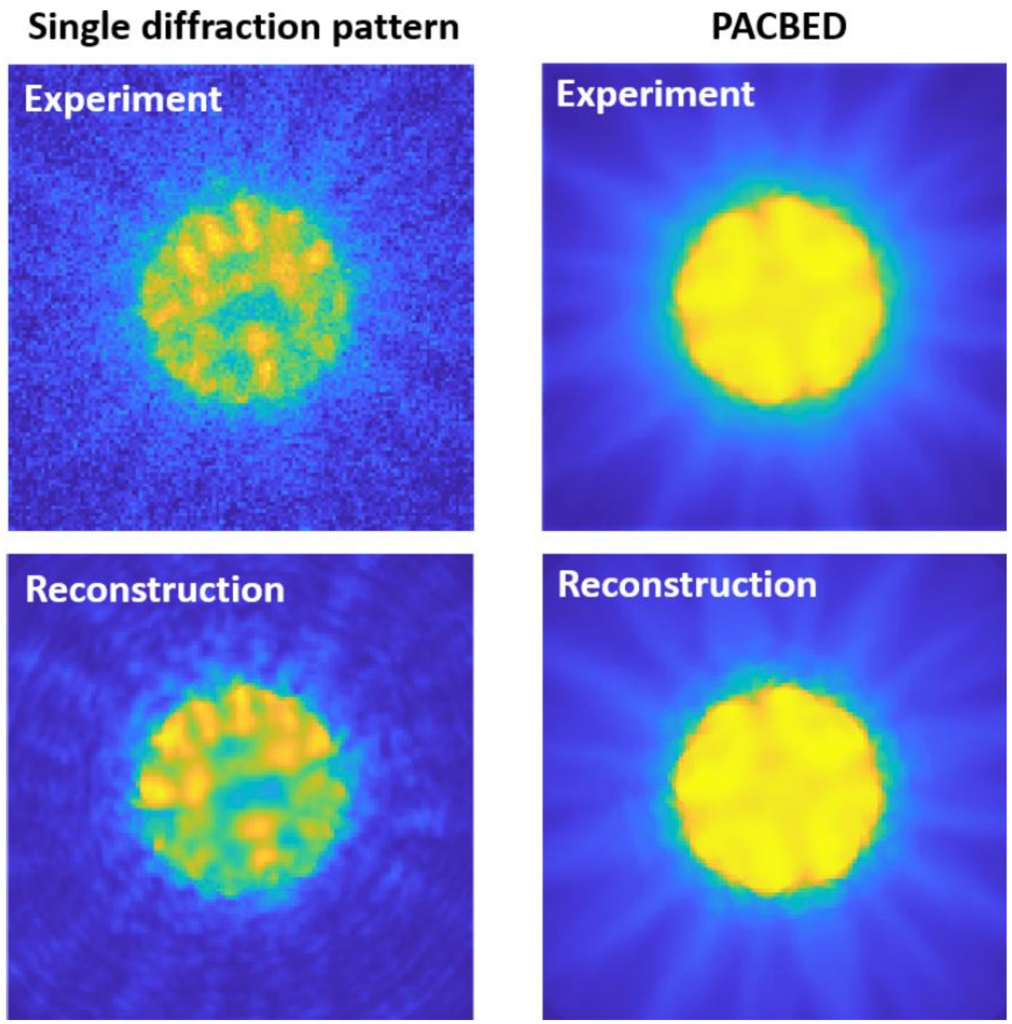

- Unique minimum in thickness scan
- Drastic improvement of $\mathcal{L}_1$ loss upon switch to FP

- TDS reproduced reliably with frozen phonon model (Einstein)

Diederichs et al., Nature Communications **15**, 101 (2024)

Summary ferroelectric case study

Parametrized inverse multislice:

- Inverse model with Frozen Phonons
- Thermal diffuse scattering included
- Z-contrast
- Mistilt-eliminated structural imaging

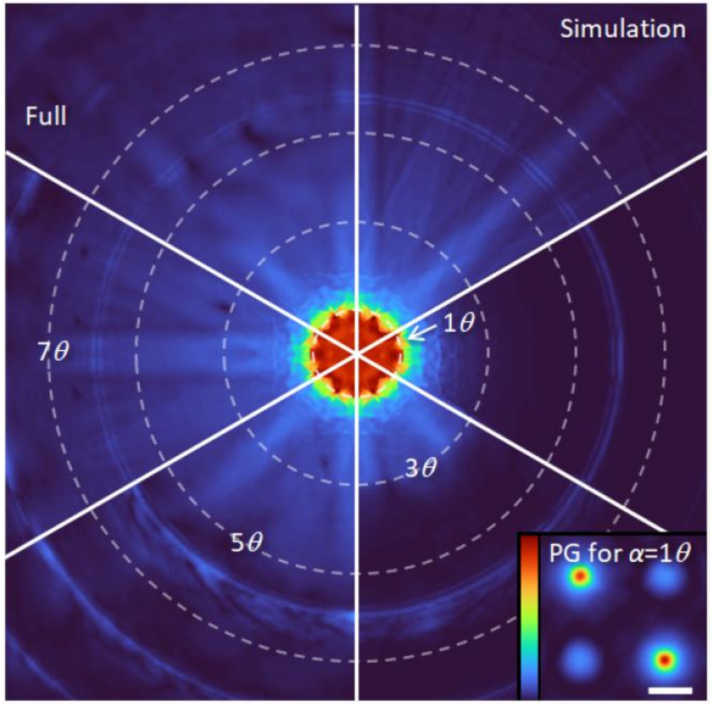

Ziria Herdegen et al.,
Physical Review B **110**, 064102 (2024)

See also: A. Gladyshev arXiv:2309.12017

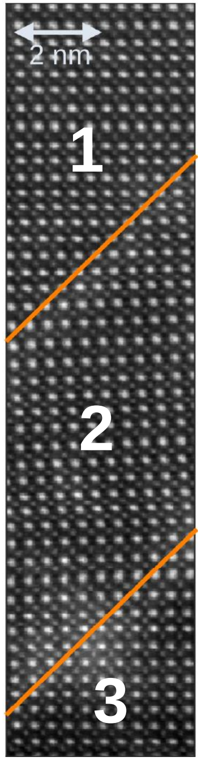

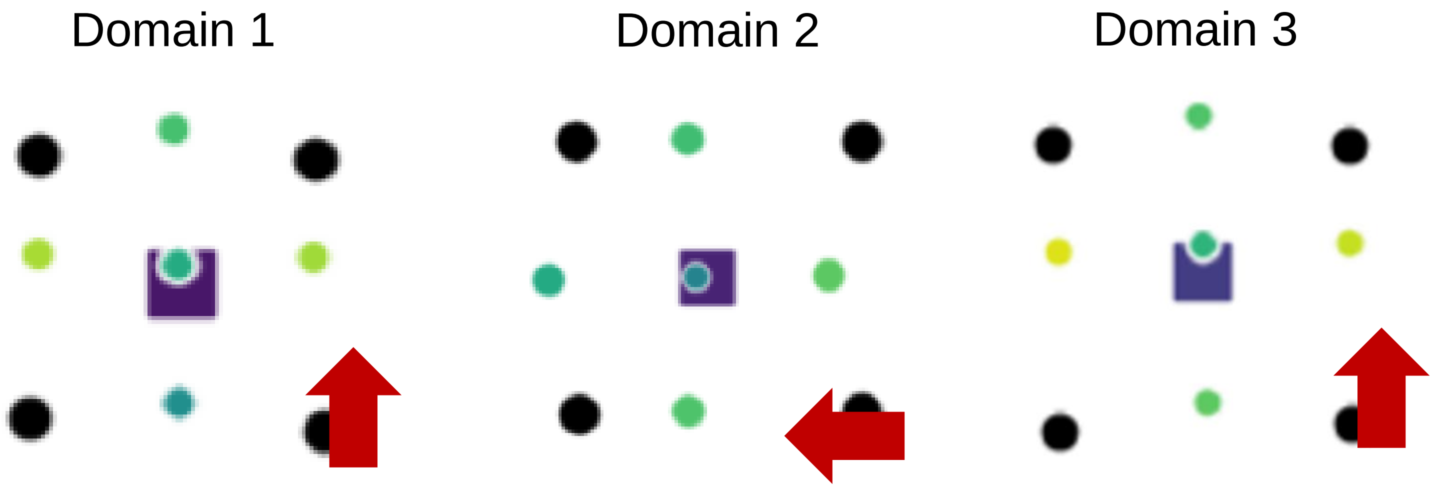

Nat. Commun. **15**, 101 (2024), PhD thesis Strauch

Merci beaucoup!

STEM, DPC, COM, phases and momentum transfer

Gradient – based (single & multislice) ptychography

Electric fields in thin specimen: Ehrenfest theorem

Introduction to the inverse problem

Approaches for polarisation-induced field mapping

Minimizing the loss function: a single-scattering example

Practice hint 1 – 5, focus, coherence

Inverse multislice: concept, coherence, TDS, parametrisation

TorchSlice software in practicals